



Inflation Factors

**Danilo Leiva-León, Viacheslav Sheremirov, Jenny Tang, and
Egon Zakrajšek**

Abstract:

This paper develops an econometric framework for identifying latent factors that provide real-time estimates of supply and demand conditions shaping goods- and services-related price pressures in the U.S. economy. The factors are estimated using category-specific personal consumption expenditures (PCE) data on prices and quantities, using a sign-restricted dynamic factor model that imposes theoretical predictions of the effects of fluctuations in supply and demand on prices and associated quantities through factor loadings. The resulting estimates are used to decompose total PCE inflation into contributions from common factors—goods demand, goods supply, services demand, services supply, and inflation expectations—and category-specific idiosyncratic components. Validation exercises demonstrate that the estimated factors provide an informative and coherent narrative of inflation dynamics over time and can be effectively used for forecasting and policy analysis.

JEL Classifications: C11, C32, E31

Keywords: Inflation, goods, services, supply, demand, expectations, dynamic factor models, sign restrictions, factor loadings

Danilo Leiva-León (danilo.leiva-leon@bos.frb.org) and Viacheslav Sheremirov (viacheslav.sheremirov@bos.frb.org) are principal economists and policy advisors in the Federal Reserve Bank of Boston Research Department. Jenny Tang (jenny.tang@bos.frb.org) is a vice president and economist in the Federal Reserve Bank of Boston Research Department. Egon Zakrajšek (egon.zakrajsek@bos.frb.org) is an executive vice president and the director of research at the Federal Reserve Bank of Boston.

The authors thank Philippe Andrade, Gabriel Chodorow-Reich, Daniel Cooper, Giovanni Olivei, Vivian Yue, Tao Zha, and participants in the Harvard Economics Michael Chae Seminar on Macroeconomic Policy, the Emory University Macroeconomics Seminar, the Bentley Applied Macroeconomics Workshop, and the 2025 CEBRA Annual Meeting for helpful comments. Ara Patvakanian provided outstanding research assistance.

Federal Reserve Bank of Boston Research Department Working Papers disseminate staff members' empirical and theoretical research with the aim of advancing knowledge of economic matters. The papers present research-in-progress and often include conclusions that are preliminary. They are published to stimulate discussion and invite critical comments. The views expressed herein are solely those of the author(s) and should not be reported as representing the views of the Federal Reserve Bank of Boston, the principals of the Board of Governors, or the Federal Reserve System.

This paper, which may be revised, is available on the website of the Federal Reserve Bank of Boston at <https://www.bostonfed.org/publications/research-department-working-paper.aspx>.

1 Introduction

The inflation surge that rattled the United States, along with economies around the world in 2021, took most observers by surprise. Undoubtedly, the COVID-19 pandemic threatened a severe and prolonged economic downturn, unleashing an enormous monetary and fiscal policy stimulus, which proved difficult to calibrate. At the same time, consumers, wary of contracting the virus, switched en masse from spending on in-person services to purchasing goods from online retailers. So, while aggregate demand remained strong on balance, its composition changed dramatically, helping to boost total inflation (see [Ferrante et al., 2023](#)).

The pandemic also severely disrupted the supply side of the U.S. economy (see [Bernanke and Blanchard, 2023](#)). The emergence of the Omicron variant of COVID-19 in late 2021 led to a steep decline in imports, as many countries crucial to global production chains struggled to vaccinate their populations quickly. The ensuing shortage of imported inputs—especially of raw materials and intermediate goods—spilled into domestic production, leading to severe bottlenecks and inventory shortages in many sectors. Labor shortages also contributed to a contraction in supply, as an unusually large number of U.S. workers quit their jobs or retired early (see [Amanor-Boadu, 2022](#); [Montes et al., 2022](#)). A decline in the inflow of foreign workers, due in part to pandemic-related travel restrictions, compounded this contraction in labor supply, hitting certain service sectors especially hard. If that were not enough, Russia’s invasion of Ukraine in early 2022 sent global food and energy prices sharply higher.

While it may be tempting to attribute the recent global inflation surge entirely to unforeseen shocks—of which there were plenty—it is fair to say that the analytical frameworks used to track the myriad complex forces at work and forecast inflation did not prove suitable. Arguably, the prevailing models were too aggregated and failed to discern the implications of the pandemic-induced shifts in demand on price dynamics. Moreover, with their emphasis on the relationship between inflation and economic slack, the workhorse models—by and large estimated or calibrated over a period of quiescent inflation—saw the inflation surge as largely transitory, failing to anticipate both its vigor and persistence. Such forecasting “mishaps” can have important consequences for monetary policy because accurately identifying the source(s) of inflationary pressures in real time is critical for formulating the appropriate policy response.¹

To help address these shortcomings, we propose a novel econometric framework for estimating factors corresponding to underlying supply and demand forces. These factors shape the real-time cyclical dynamics of inflation as measured by the personal consumption expenditures (PCE) price index, the Federal Reserve’s preferred measure of the general price level. In our framework, the factors are estimated by exploiting the co-movement embedded in the PCE data on prices and corresponding quantities across different consumption categories and by relying on the theoretical

¹In fact, a number of major central banks launched internal and external reviews of their pandemic responses, including extensive evaluations of their inflation forecasting methodologies; see, for example, [Bernanke \(2024\)](#) for the Bank of England, [Hernández de Cos et al. \(2024\)](#) for the Bank of Canada, and [Chahad et al. \(2022, 2023\)](#) for the European Central Bank.

predictions of the effects of fluctuations in supply and demand on prices and associated quantities. In particular, our identification of changes in supply and demand conditions is based on an intuitive observation that lies at the heart of economic theory: When demand increases, both quantities and prices of products consumed increase, but when supply increases, quantities rise and prices fall.

To account for these theoretical predictions, we introduce a so-called sign-restricted dynamic factor model (SiR-DFM), which allows us to quantify the sources and dynamics of various price pressures as they arise. Importantly, the model distinguishes between supply- and demand-based price pressures arising in the goods versus services sectors, a distinction that played an important role during the pandemic-era inflation surge and the subsequent—and still ongoing—disinflation process.² It accounts for features typically observed in data at high levels of disaggregation, such as time-varying volatility and outliers, thus enabling a more precise quantification of incipient price pressures. In addition, the model incorporates information about inflation expectations, which capture lower-frequency inflation dynamics, thereby helping to isolate cyclical fluctuations in the underlying supply and demand conditions, a key input into monetary policy decisionmaking.

We use the SiR-DFM framework to decompose total PCE inflation into six underlying components: (1) common demand for goods, (2) common demand for services, (3) common supply of goods, (4) common supply of services, (5) inflation expectations, and (6) idiosyncratic or category-specific supply and demand contributions. When applied to the recent inflation episode, the decomposition shows that over the first few months of the pandemic, as widespread business closures went into effect, both common demand and common supply components collapsed. These two developments had opposite effects on inflation and roughly offset each other. By mid-2020, demand-driven inflation—supported by significant monetary and fiscal stimulus—started to surge. Total inflation, however, remained subdued initially because, as the economy reopened, the easing of supply-side pressures offset the snapback in demand.

This dynamic shifted in the later stages of the pandemic. The ongoing strength in demand for goods was compounded by a significant and persistent increase in demand for services, sparking a sharp rise in inflation in early 2021. By the end of the year, the surging demand-driven inflation collided with the supply-side constraints caused by disruptions in global production chains and pandemic-related labor shortages, further boosting inflation. Crucially, throughout this entire period, the contribution of inflation expectations remained constant, helping to prevent the emergence of destabilizing inflation dynamics, even as the economy was buffeted by a complex interplay

²For earlier work on how changing expenditure shares can influence the behavior of inflation, see [Wolman and Ding \(2005\)](#). In addition, [Ruge-Murcia and Wolman \(2022\)](#) estimate a multisector New Keynesian model using U.S. data from 1995 through 2019 and find that sectoral shocks were major contributors to the inflation deviations from the Federal Reserve’s target during the 2012–2019 period. For the more recent period, [Ferrante et al. \(2023\)](#) document that the rotation of demand from services to goods during the pandemic significantly boosted total inflation due to the constraints faced by producers in expanding production. On the theoretical side, [Guerrieri et al. \(2022\)](#) present a model in which an adverse supply shock in one sector can lead to a reduction in product demand from other sectors. Using a calibrated multisector model of the U.S. economy, [Luo and Villar \(2023\)](#) find that the inflationary effect of sectoral supply shocks was amplified by input–output linkages across sectors, and [Amiti et al. \(2023\)](#) show how a confluence of labor disutility and input price shocks impeded substitution across input types, amplifying the inflationary effect of pandemic-era sectoral shocks. At the international level, [di Giovanni et al. \(2023\)](#) estimate a model in which this effect can occur across countries.

of demand- and supply-side shocks.

Next, we provide a series of validation exercises involving sample periods outside the recent inflation episode to ensure that our estimated inflation factors can be labeled as either supply or demand driven. First, we compare our inflation factors with standard supply- and demand-related macroeconomic variables, such as labor productivity and measures of economic slack, a simple exercise that yields expected correlations. Second, we evaluate the response of our inflation factors to demand-side shocks, such as the ones associated with monetary policy decisions, and supply-side shocks, such as those originating in the global oil market. These formal exercises indicate clearly that our supply and demand inflation factors respond—as expected—to well-identified external supply and demand shocks, respectively, validating the way we interpret them.

Lastly, we evaluate the predictive content of the estimated inflation factors for future inflation. We compare two versions of an econometric time-series model used typically to forecast either total or core PCE inflation. The first version contains (real-time) information about our inflation factors, while the second version does not. The results show that including the estimated inflation factors in the standard model leads to substantial improvements in the accuracy of inflation forecasts. Moreover, forecasts of the inflation factors themselves can be used to learn about the outlook for demand- and supply-driven inflationary pressures.

Broadly speaking, our paper contributes to the large literature that uses theoretical restrictions—more specifically, sign restrictions—to infer “structural” economic shocks.³ In their seminal contribution, [Blanchard and Quah \(1989\)](#) use theoretical predictions to identify aggregate demand and aggregate supply shocks in a standard vector autoregression (VAR) framework. More recently, [Giannone and Primiceri \(2024\)](#) employ a VAR framework with sign restrictions to parse the role of supply- and demand-side disturbances during the pandemic-era inflation surge in the euro area. While sign-restricted VARs, along with their variants or extensions, provide useful information about the structural shocks driving inflation, the associated estimation uncertainty is typically large due to the set-identifying procedure that underlies this general approach.⁴ By contrast, we estimate our measures of common supply and demand conditions with considerable precision by exploiting information embedded in the co-movement of prices and their corresponding quantities across a large number of disaggregated PCE categories.

More recently, [Shapiro \(2024\)](#) and [Sheremirov \(2022\)](#) apply a sign-restriction approach to disaggregated PCE data by separately estimating category-specific VAR models. Our approach differs from those of [Shapiro \(2024\)](#) and [Sheremirov \(2022\)](#) in three important ways. First, we impose sign restrictions on a single dynamic factor model, which allows us to simultaneously and efficiently process all the information about prices and quantities from the different PCE categories. Second, we separate common demand and common supply components from idiosyncratic (that is, category-specific) demand and supply fluctuations. Third, our method allows us to examine the

³[Arias et al. \(2018\)](#) and [Antolín-Díaz and Rubio-Ramírez \(2018\)](#) have broadened this approach by developing algorithms to infer structural shocks based on not only sign but also exclusion and narrative restrictions, respectively.

⁴See [Fry and Pagan \(2011\)](#) for a comprehensive review and critique of the literature that uses various sign-restriction strategies in VAR settings to identify structural aggregate demand and supply disturbances.

gross contributions of all underlying demand and supply forces—common sector-level factors and idiosyncratic category-specific disturbances—to total PCE inflation. This provides us with a better understanding of how these individual forces shape inflation dynamics in real time, which can be especially useful when these forces are having offsetting effects on inflation.

Relevant to our approach is the recent work by [Eickmeier and Hofmann \(2025\)](#), who exploit factor rotation in principal component analysis applied to a large data set of standard real activity and price-related macroeconomic variables to estimate one common supply and one common demand factor. Their data, unlike our PCE categories, do not exhibit a direct correspondence between prices and quantities, which complicates the interpretation of the estimated factors. Our framework, by contrast, exploits the direct price and quantity correspondence in disaggregated PCE categories, allowing us to straightforwardly decompose not only total PCE inflation but also category-specific idiosyncratic price changes into their respective demand and supply components.

The remainder of the paper is structured as follows. Section 2 introduces our empirical framework, discusses the identification strategy, and describes the data. Section 3 presents the estimated common supply and demand factors and the associated decomposition of total PCE inflation, with a focus on the pandemic-era inflation dynamics. Section 4 presents the analysis that uses external information to validate the interpretation of the estimated supply and demand factors. Section 5 shows how our factors can be used to improve real-time inflation forecasts, and Section 6 concludes.

2 Methodology

In this section, we outline our econometric methodology. We begin with a simple demand-and-supply system that connects prices and corresponding quantities within a consumption category and features—in addition to category-specific supply and demand shocks—common demand and supply shifters. We use this framework to derive the sign restrictions that we impose on the factor loadings in a set of measurement equations in a dynamic factor model in which the transition equations govern the dynamics of the latent common demand and supply factors.

2.1 A Conceptual Framework

Let $\Delta q_{i,t}$ and $\Delta p_{i,t}$ denote changes in (real) quantities and prices associated with consumption category $i = 1, 2, \dots, N$ at time t , respectively, where N denotes the number of categories comprising the consumption basket. We define category-specific supply and demand structural equations that account for common supply and demand shifters—denoted by s_t and d_t , respectively—as follows:

$$\Delta q_{i,t} = \phi_i^s \Delta p_{i,t} + \kappa_i^s s_t + u_{i,t}^s; \quad (1)$$

$$\Delta p_{i,t} = -\phi_i^d \Delta q_{i,t} + \kappa_i^d d_t + u_{i,t}^d, \quad (2)$$

with $\phi_i^d, \kappa_i^d, \phi_i^s, \kappa_i^s > 0$ for all i . In this system, ϕ_i^s is the price elasticity of supply, ϕ_i^d is the inverse price elasticity of demand, and κ_i^s and κ_i^d denote category i 's sensitivities (that is, factor loadings) to

common supply and demand shifters, s_t and d_t , respectively; the category-specific, or idiosyncratic, supply and demand shifters are denoted by $u_{i,t}^s$ and $u_{i,t}^d$, respectively.

Rearranging equations (1) and (2) enables changes in prices and quantities associated with category i to be expressed as a function of contemporaneous information on both common and idiosyncratic shifters according to the following reduced form:

$$\Delta q_{i,t} = \lambda_i^d d_t + \lambda_i^s s_t + \xi_{i,t}; \quad (3)$$

$$\Delta p_{i,t} = \theta_i^d d_t + \theta_i^s s_t + \eta_{i,t}. \quad (4)$$

The mapping between the parameters associated with the structural and reduced-form representations of the system provides information about the restrictions needed to identify common supply and demand factors from disaggregated data on prices and quantities. These identifying restrictions are:

$$\lambda_i^d = (1 + \phi_i^s \phi_i^d)^{-1} \phi_i^s \kappa_i^d > 0; \quad (5)$$

$$\lambda_i^s = (1 + \phi_i^s \phi_i^d)^{-1} \kappa_i^s > 0; \quad (6)$$

$$\theta_i^d = (1 + \phi_i^s \phi_i^d)^{-1} \kappa_i^d > 0; \quad (7)$$

$$\theta_i^s = -(1 + \phi_i^s \phi_i^d)^{-1} \phi_i^d \kappa_i^s < 0. \quad (8)$$

The reduced-form idiosyncratic innovations $\xi_{i,t}$ and $\eta_{i,t}$ become a function of both the structural category-specific supply and demand shifters and structural parameters:

$$\xi_{i,t} = (1 + \phi_i^s \phi_i^d)^{-1} (u_{i,t}^s + \phi_i^s u_{i,t}^d); \quad (9)$$

$$\eta_{i,t} = (1 + \phi_i^s \phi_i^d)^{-1} (u_{i,t}^d - \phi_i^d u_{i,t}^s). \quad (10)$$

In accordance with standard economic theory, our identifying restrictions assume that shifts in common demand move prices and quantities in the same direction—that is, a broad-based increase in demand would induce a rise in the prices and quantities across all the categories in the consumption basket. Shifts in common supply, on the other hand, are assumed to move prices and quantities in the opposite direction: A broad-based increase in supply would lead to a rise in the quantities but a decline in the prices associated with all the consumption categories.

2.2 Empirical Implementation

To incorporate the relationships between common factors and disaggregated prices and quantities described in the preceding subsection into a unified empirical framework, we propose a sign-restricted dynamic factor model (SiR-DFM), which enables us to disentangle common and idiosyncratic dynamics while accounting for the aforementioned identifying restrictions.⁵ According to equations (3)

⁵In a similar vein, [Matthes and Schwartzman \(2025\)](#) propose a sign-restricted VAR model that uses sector-specific information about PCE prices and quantities with aggregate variables to measure the impact of household consumption shocks on aggregate fluctuations.

and (4), changes in category-specific prices and quantities are assumed to be influenced by three distinct types of dynamics: common supply, common demand, and idiosyncratic. Common supply and common demand sources of fluctuations can both be thought of as latent common factors extracted from disaggregated price and quantity data, according to the theory-based restrictions on the factor loadings given by equations (5) through (8). Given the changing and complex interplay between supply and demand forces in driving goods- and services-related inflation, especially during the recent inflation episode, our SiR-DFM is designed to extract four common latent factors from disaggregated PCE data. This set of factors is intended to summarize the evolving conditions of supply of goods ($s_t^{(g)}$), supply of services ($s_t^{(v)}$), demand of goods ($d_t^{(g)}$), and demand of services ($d_t^{(v)}$).

Specifically, let $\Delta q_{j,t}$ and $\Delta p_{j,t}$ denote the monthly log-differences of quantities and prices associated with a *goods* category j in month t , respectively, for $j = 1, 2, \dots, N_g$, where N_g is the number of distinct goods-related categories in the Personal Income and Outlays report (that is, the PCE report) published monthly by the U.S. Department of Commerce's Bureau of Economic Analysis. Analogously, let $\Delta q_{k,t}$ and $\Delta p_{k,t}$ denote the monthly log-differences of quantities and prices associated with a *services* category k in month t , respectively, for $k = 1, 2, \dots, N_v$, where N_v is the number of distinct services-related categories in the PCE report. Then, the system of measurement equations describing changes in prices and quantities across the different categories of consumption goods and services is given by:

$$\Delta q_{j,t} = \lambda_j^d d_t^{(g)} + \lambda_j^s s_t^{(g)} + \xi_{j,t}^{(g)}, \quad j = 1, 2, \dots, N_g; \quad (11)$$

$$\Delta p_{j,t} = \theta_j^d d_t^{(g)} + \theta_j^s s_t^{(g)} + \eta_{j,t}^{(g)}, \quad j = 1, 2, \dots, N_g; \quad (12)$$

$$\Delta q_{k,t} = \gamma_k^d d_t^{(v)} + \gamma_k^s s_t^{(v)} + \xi_{k,t}^{(v)}, \quad k = 1, 2, \dots, N_v; \quad (13)$$

$$\Delta p_{k,t} = \delta_k^d d_t^{(v)} + \delta_k^s s_t^{(v)} + \eta_{k,t}^{(v)}, \quad k = 1, 2, \dots, N_v. \quad (14)$$

The identifying restrictions on the factor loadings used to infer the latent common supply and demand factors are implied by the relation between reduced-form and structural parameters given by equations (5) through (8). In particular, we impose the following sign restrictions on the factor loadings in the system of measurement equations (11) through (14):

$$\lambda_j^d > 0 \text{ and } \lambda_j^s > 0, \quad j = 1, 2, \dots, N_g; \quad (15)$$

$$\theta_j^d > 0 \text{ and } \theta_j^s < 0, \quad j = 1, 2, \dots, N_g; \quad (16)$$

$$\gamma_k^d > 0 \text{ and } \gamma_k^s > 0, \quad k = 1, 2, \dots, N_v; \quad (17)$$

$$\delta_k^d > 0 \text{ and } \delta_k^s < 0, \quad k = 1, 2, \dots, N_v. \quad (18)$$

The latent demand factors associated with goods and services are assumed to evolve according to a vector-autoregressive process of order m (VAR(m)), allowing for potential feedback between demand developments across the two broad consumption categories; the latent goods and services supply factors are also assumed to follow a similar VAR(m) process. To account for the time-

varying trend inherent in total PCE inflation, we include an observed variable in both VAR specifications to absorb this source of low-frequency variation. From a theoretical perspective, inflation expectations—the rate at which economic agents expect prices to rise in the future—should be a key determinant of this time-varying trend, with fluctuations around the trend capturing cyclical supply and demand price pressures.

We capture this notion by including data on inflation expectations as an exogenous variable in the VAR(m) specifications governing the evolution of the latent factors, which yields the following VAR-X(m) transition equations:

$$\begin{bmatrix} d_t^{(g)} \\ d_t^{(v)} \end{bmatrix} = \Phi_{d,0} + \beta_d \pi_{t-1}^E + \Phi_{d,1} \begin{bmatrix} d_{t-1}^{(g)} \\ d_{t-1}^{(v)} \end{bmatrix} + \cdots + \Phi_{d,m} \begin{bmatrix} d_{t-m}^{(g)} \\ d_{t-m}^{(v)} \end{bmatrix} + \begin{bmatrix} \epsilon_t^{(g)} \\ \epsilon_t^{(v)} \end{bmatrix}; \quad (19)$$

and

$$\begin{bmatrix} s_t^{(g)} \\ s_t^{(v)} \end{bmatrix} = \Phi_{s,0} + \beta_s \pi_{t-1}^E + \Phi_{s,1} \begin{bmatrix} s_{t-1}^{(g)} \\ s_{t-1}^{(v)} \end{bmatrix} + \cdots + \Phi_{s,m} \begin{bmatrix} s_{t-m}^{(g)} \\ s_{t-m}^{(v)} \end{bmatrix} + \begin{bmatrix} \nu_t^{(g)} \\ \nu_t^{(v)} \end{bmatrix}, \quad (20)$$

where the scalar π_{t-1}^E denotes expectations of future inflation based on information available as of month $t-1$, with the associated vectors of coefficients $\beta_d = [\beta_d^{(g)} \ \beta_d^{(v)}]'$ and $\beta_s = [\beta_s^{(g)} \ \beta_s^{(v)}]'$. The VAR-X vectors of innovations $\epsilon_t = [\epsilon_t^{(g)} \ \epsilon_t^{(v)}]'$ and $\nu_t = [\nu_t^{(g)} \ \nu_t^{(v)}]'$ associated with the demand and supply processes are assumed to be independent and normally distributed as $\epsilon_t \sim \mathcal{N}(\mathbf{0}, \Omega_d)$ and $\nu_t \sim \mathcal{N}(\mathbf{0}, \Omega_s)$.

The idiosyncratic terms in the measurement equations (11) through (14) are intended to capture dynamics that are unrelated to changes in common supply or demand conditions and instead reflect supply and/or demand developments affecting prices or quantities in a specific consumption category. These terms are assumed to follow independent autoregressive processes of order n (AR(n)) and are given by:

$$\rho_j^g(L) \zeta_{j,t}^{(g)} = \zeta_{j,t}^{(g)}, \quad j = 1, 2, \dots, N_g; \quad (21)$$

$$\psi_j^g(L) \eta_{j,t}^{(g)} = \omega_{j,t}^{(g)}, \quad j = 1, 2, \dots, N_g; \quad (22)$$

$$\rho_k^v(L) \zeta_{k,t}^{(v)} = \zeta_{k,t}^{(v)}, \quad k = 1, 2, \dots, N_v; \quad (23)$$

$$\psi_k^v(L) \eta_{k,t}^{(v)} = \omega_{k,t}^{(v)}, \quad k = 1, 2, \dots, N_v, \quad (24)$$

where $\rho_j^g(L)$, $\psi_j^g(L)$, $\rho_k^v(L)$, and $\psi_k^v(L)$ denote lag polynomials of order n , and the idiosyncratic innovations $\zeta_{j,t}^{(g)}$, $\omega_{j,t}^{(g)}$, $\zeta_{k,t}^{(v)}$, and $\omega_{k,t}^{(v)}$ are assumed to be normally distributed, with flexible volatility processes that account for features typically observed in disaggregated data on prices and quantities. Specifically, by denoting a generic idiosyncratic innovation by $z_{i,t}$, $i \in \{\zeta^{(g)}, \omega^{(g)}, \zeta^{(v)}, \omega^{(v)}\}$, we allow for stochastic volatility with outlier adjustment, according to

$$z_{i,t} \sim \mathcal{N}(0, o_{i,t}^2 \times e^{h_{i,t}}), \quad (25)$$

where the log-volatility process follows a random walk

$$h_{i,t} = h_{i,t-1} + \varsigma_{i,t}, \quad (26)$$

with $\varsigma_{i,t} \sim \mathcal{N}(0, \sigma_i^2)$ for $i \in \{\zeta^{(g)}, \omega^{(g)}, \zeta^{(v)}, \omega^{(k)}\}$; the outlier component $o_{i,t}$ is defined as in [Stock and Watson \(2016\)](#):

$$o_{i,t} = \begin{cases} 1 & \text{with probability } (1 - \chi_i); \\ \mathcal{U}_{[a,b]} & \text{with probability } \chi_i, \end{cases} \quad (27)$$

where $\mathcal{U}_{[a,b]}$ denotes the uniform distribution with support interval $[a, b]$.

To achieve statistical identification of the common latent supply and demand factors, we apply the parameter restrictions suggested by [Bai and Wang \(2015\)](#). First, this implies setting the covariance matrices of VAR-X innovations $\mathbf{\Omega}_d = \mathbf{\Omega}_s = \mathbf{I}$, thus allowing for only noncontemporaneous feedback between factors. In addition, we impose restrictions on certain elements of the matrix of factor loadings in the system of measurement equations in the state-space representation of the model to fix the rotation of the latent factors. Specifically, the $[1, 1]$ element of the matrix of factor loadings corresponding to the goods categories must be positive, and the $[1, 2]$ element must equal zero; the same restrictions apply to the $[1, 1]$ element and the $[1, 2]$ element of the matrix of factor loadings associated with the services categories.

This requires us to select a “first” (that is, $j = 1$) goods category and a “first” (that is, $k = 1$) services category. To minimize the effects of these assumptions on our results, we select categories with very small (average) weights in the overall consumption basket—that is, $j = 1 = \text{Tobacco}$ in the case of goods and $k = 1 = \text{Gambling}$ in the case of services.⁶ The restrictions on the $[1, 1]$ elements are easily satisfied by our theoretically motivated sign restrictions, which imply that $\lambda_1^d > 0$ and $\gamma_1^d > 0$. The restrictions on the $[1, 2]$ elements imply that $\lambda_1^s = 0$ and $\gamma_1^s = 0$. The former thus imposes a zero restriction on the factor loading relating the **Tobacco** quantity index to the goods supply common factor $s_t^{(g)}$, whereas the latter imposes a zero restriction on the factor loading relating the **Gambling** quantity index to the services supply common factor $s_t^{(v)}$.⁷

The resulting model is estimated with Bayesian methods. Specifically, we use the Gibbs sampler to simulate the posterior distribution of parameters and latent variables of the model, following the procedures proposed by [Kim and Nelson \(1999\)](#) and [Stock and Watson \(2016\)](#) for sampling common factors and stochastic volatility processes, respectively. The identifying restrictions on the factor loadings, given by equations (15) through (18), are verified at every iteration of the sampler. We set the lag order of all common factors (m) and idiosyncratic processes (n) as $m = n = 2$. We use 10,000 iterations for the Gibbs sampler and discard the first 2,000 iterations to allow for “burn-in.” Additional details on the estimation algorithm are provided in [Appendix A](#).

⁶Between April 1968 and April 2025, our sample period, **Tobacco** accounted for 1.07 percent of the overall consumption basket, on average, whereas **Gambling** accounted for 0.76 percent on average.

⁷In effect, we are assuming that in these two categories, supply-side fluctuations are due entirely to idiosyncratic—that is, category-specific—supply shifters. As a robustness check, we first-ordered other “small” consumption categories, and all the results (available upon request from the authors) were quantitatively and qualitatively very similar to our baseline results reported in the paper.

2.2.1 Inflation Decomposition

The preceding framework allows us to decompose price changes in each category of the PCE report into four underlying components: expected inflation, cyclical sectoral (that is, goods and services) supply developments, cyclical sectoral demand developments, and idiosyncratic dynamics. In doing so, we derive the following historical decomposition of disaggregated price changes:

$$\Delta p_{j,t} = \alpha_j^{(g)} \pi_{t-1}^E + \theta_j^d d_t^{(g*)} + \theta_j^s s_t^{(g*)} + \eta_{j,t}^{(g)}, \quad j = 1, 2, \dots, N_g; \quad (28)$$

$$\Delta p_{k,t} = \alpha_k^{(v)} \pi_{t-1}^E + \delta_k^d d_t^{(v*)} + \delta_k^s s_t^{(v*)} + \eta_{k,t}^{(v)}, \quad k = 1, 2, \dots, N_v, \quad (29)$$

where the coefficients $\alpha_j^{(g)} = \theta_j^d \beta_d^{(g)} + \theta_j^s \beta_s^{(g)}$ and $\alpha_k^{(v)} = \delta_k^d \beta_d^{(v)} + \delta_k^s \beta_s^{(v)}$ measure the respective sensitivity of goods- and services-related log-price changes from month $t-1$ to month t to expected future inflation as of month $t-1$, that is, π_{t-1}^E .

The cyclical sector-specific demand- and supply-related factors, denoted by $d_t^{(g*)}$, $d_t^{(v*)}$, $s_t^{(g*)}$, and $s_t^{(v*)}$, are then defined as

$$\begin{aligned} d_t^{(g*)} &= d_t^{(g)} - \beta_d^{(g)} \pi_{t-1}^E, \\ d_t^{(v*)} &= d_t^{(v)} - \beta_d^{(v)} \pi_{t-1}^E, \\ s_t^{(g*)} &= s_t^{(g)} - \beta_s^{(g)} \pi_{t-1}^E, \\ s_t^{(v*)} &= s_t^{(v)} - \beta_s^{(v)} \pi_{t-1}^E. \end{aligned}$$

The decomposition in equations (28) and (29) is obtained by substituting equations (19) and (20) into equations (11) through (14) and rearranging terms. Then, total monthly PCE inflation, denoted by π_t , can be defined as the weighted sum of disaggregated price changes,

$$\pi_t = \sum_{j=1}^{N_g} \tilde{w}_{j,t} \Delta p_{j,t} + \sum_{k=1}^{N_v} \tilde{w}_{k,t} \Delta p_{k,t}, \quad (30)$$

where $\tilde{w}_{j,t}$, $j = 1, 2, \dots, N_g$ and $\tilde{w}_{k,t}$, $k = 1, 2, \dots, N_v$ are the expenditure weights associated with the different goods- and services-related categories in the PCE report.⁸ By substituting equations (28) and (29) into equation (30) and rearranging terms, we can break down total PCE inflation into common components associated with inflation expectations, cyclical supply- and demand-driven inflation in the goods and services sectors, and idiosyncratic inflation. It is worth noting that the same approach can be used to break down the growth in real PCE into the same set of demand, supply, and idiosyncratic components.

⁸The category-specific weights in month t correspond to the geometric average of the expenditure shares in month $t-1$ and month t .

2.2.2 Data and Model Selection

In the estimation, we use monthly data on prices and quantities for 51 PCE categories that are split into 30 goods-related and 21 services-related categories.⁹ All category-specific price and quantity series are seasonally adjusted, and monthly log-differences of both prices and quantities are scaled by their corresponding (in-sample) standard deviation prior to estimation. Using these data, we estimate several variants of our SiR-DFM framework that consider modeling choices such as (1) using near-term versus long-term expected inflation to capture fluctuations in trend inflation, (2) excluding information about inflation expectations altogether, and (3) extracting only one common demand and one common supply factor, as opposed to supply and demand factors that differentiate between goods and services.

In these model-selection exercises, our measure of near-term expected inflation corresponds to expected inflation over the next 12 months, as reported in the University of Michigan’s Survey of Consumers. We construct this measure by splicing the monthly median expectation of year-ahead inflation—the data for which start in January 1978—with the quarterly average expectation of year-ahead inflation, the data for which go back to the early 1960s. Our measure of long-term expected inflation is also based on the University of Michigan’s Survey of Consumers and gauges expected inflation over the next five to 10 years. This series, however, is available at a monthly frequency only from April 1990 onward. For the earlier time period, we use the quarterly long-term expected inflation series from the Federal Reserve Board’s FRB/US database (see [Brayton and Tinsley, 1996](#)).¹⁰ Combining our measure of near- and long-term inflation expectations with the disaggregated PCE data then determines our sample period, which runs from January 1968 through April 2025.

For each estimated model, we compute the deviance information criterion (DIC), a hierarchical modeling generalization of the Akaike information criterion (AIC) employed in frequentist inference. Table 1 reports this “goodness-of-fit” criterion (smaller is better) for the various specifications we consider. The first three rows of the table consider SiR-DFM specifications with only one common supply and one common demand factor—that is, these specifications do not allow for potentially different aggregate dynamics between goods- and services-related PCE categories. Within this class, the specification with the smallest DIC corresponds to the specification that includes near-term expected inflation in the transition equations (19) and (20).¹¹

The next three rows of the table consider SiR-DFM specifications that allow for differential aggregate supply and demand dynamics between goods- and services-related PCE categories. Note

⁹The 51 PCE categories used in the estimation correspond to the so-called Level 4 disaggregation, which includes a total of 53 categories. As is typical, our analysis excludes the two Level 4 categories with occasionally negative expenditure weights, namely **Net Expenditures Abroad by US Residents** and **Net Foreign Travel** (see [Sheremirov, 2022](#); [Shapiro, 2024](#)). The expenditure weights of the remaining 51 categories are then re-normalized to sum to one. Table B-1 in Appendix B lists the PCE categories used in the analysis.

¹⁰When converting quarterly expectations series to monthly frequency, we assign the quarterly value to all three months of the quarter. Figure B-1 in Appendix B shows the near- and long-term inflation expectations series used in the estimation.

¹¹In this case, the transition equations (19) and (20) follow univariate—as opposed to bivariate—autoregressive processes.

TABLE 1: Model Selection

SiR-DFM Specification			
Supply Factors	Demand Factors	Inflation Expectations	DIC
1	1	none	181482.999
1	1	near term	181345.321
1	1	long term	181491.132
2	2	none	179122.839
2	2	near term	178575.863
2	2	long term	178280.699*

NOTE: Estimation period: monthly data from January 1968 through April 2025. The entries in the table list the deviance information criteria (DIC) implied by the different SiR-DFM specifications. Specifications with two factors (rows 1 through 3) estimate only a single common supply and a single common demand inflation factor. Specifications with four factors (rows 4 through 6) estimate two common supply (goods and services) and two common demand (goods and services) inflation factors. * denotes the model specification with the smallest DIC.

first that regardless of whether the transition equations of these specifications include near-term, long-term, or no inflation expectations, the resulting DICs are uniformly smaller compared with specifications in which common factors are not distinguished as goods- versus services-related; this indicates that the goods-versus-services distinction is an important feature of our data that needs to be accounted for in the estimation. Second, a SiR-DFM specification that incorporates long-term inflation expectations into transition equations (19) and (20) yields the smallest DIC overall, providing the best description of the data, according to this metric.¹²

3 Main Results

This section presents our main results, starting with the estimates of the common supply and demand factors associated with goods and services. We then present a historical decomposition of PCE inflation based on our estimated factors followed by a closer examination of inflation dynamics during and following the pandemic-era inflation surge.

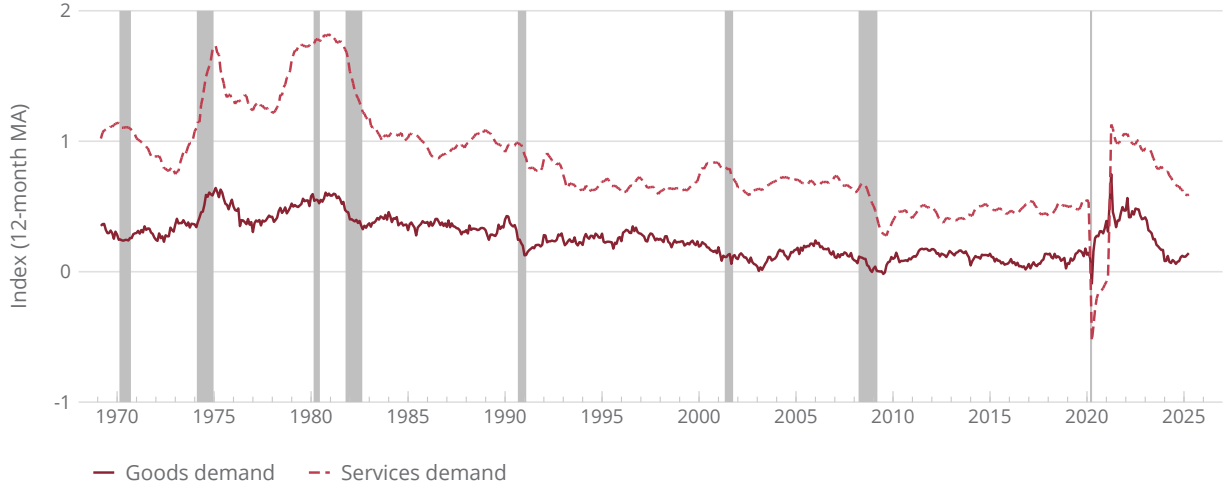
3.1 Inflation Factors and Historical Decomposition of PCE Inflation

Figure 1 shows our estimates of the inflation factors, with Panel A focusing on the two demand factors and Panel B on the two supply factors; for ease of visual representation, we plot the estimated monthly factors as 12-month moving averages.¹³ As shown in Panel A, the inflation factors

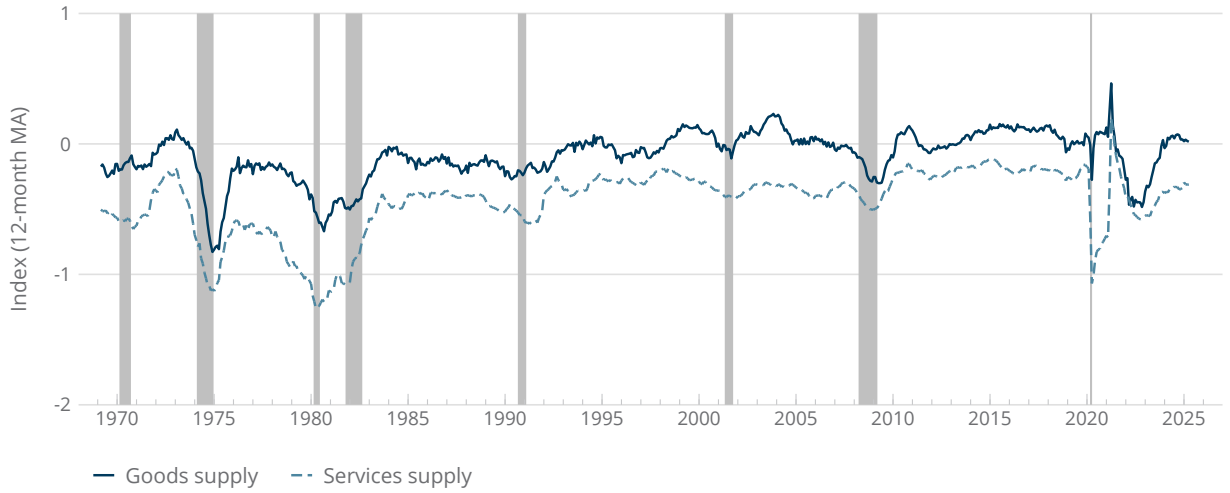
¹²Notably, as a matter of theory, the near-term inflation expectations should factor in households' wage negotiations and firms' pricing decisions. Estimating how fluctuations in near-term inflation expectations affect trend inflation, however, has proven to be difficult, in large part because survey-based measures of near-term inflation expectations are highly correlated with past inflation, which blurs their direct impact on inflation dynamics (see Hajdini, 2023). At the same time, other research has found that survey-based measures of long-term inflation expectations can significantly sharpen estimates of trend inflation compared with other popular alternatives (see Chan et al., 2018).

¹³Figures C-1 and C-2 in Appendix C show the estimates of the four monthly common factors along with their [P10, P90] credible intervals, which indicate that they are estimated with a considerable degree of precision. Figures C-3 through C-6 show the estimates of the corresponding factor loadings, and Figures C-7 and C-8 show the estimated

FIGURE 1: Inflation Factors



A. Common demand factors



B. Common supply factors

NOTE: Monthly data from March 1969 through April 2025. The lines in Panel A show the 12-month moving average of the medians of the posterior distribution of the common goods demand ($d_t^{(g)}$) and the common services demand ($d_t^{(s)}$) factors; the lines in Panel B depict the 12-month moving average of the medians of the posterior distribution of the common goods supply ($s_t^{(g)}$) and the common services supply ($s_t^{(s)}$) factors. The shaded vertical bars depict recessions as determined by the National Bureau of Economic Research.

SOURCE: Authors' calculations using data from the Bureau of Economic Analysis, the Federal Reserve Board, and the University of Michigan.

associated with demand for goods and with demand for services display two key features. First, the estimates of the two demand factors are almost always positive, an indication of the upward pressure that rising demand exerts on inflation and a pattern implied by equations (4) and (6).

time-varying (log) variances and the estimated occurrence and size of the outliers in the innovations associated with the category-specific idiosyncratic AR(2) processes in equations (21) through (24).

Second, the services demand factor is notably more persistent than the goods demand factor—even when the two factors are smoothed using a moving-average filter—a reflection, in part, of the higher labor intensity of services.

The inflation factors associated with the supply of goods and the supply of services are shown in Panel B. Unlike their demand counterparts, the supply factors tend to exhibit mostly negative values. This pattern is consistent with the upward pressure that contracting supply is expected to exert on inflation, according to equations (4) and (8). As with the demand factor, the services supply factor exhibits a notably greater persistence than the goods supply factor.

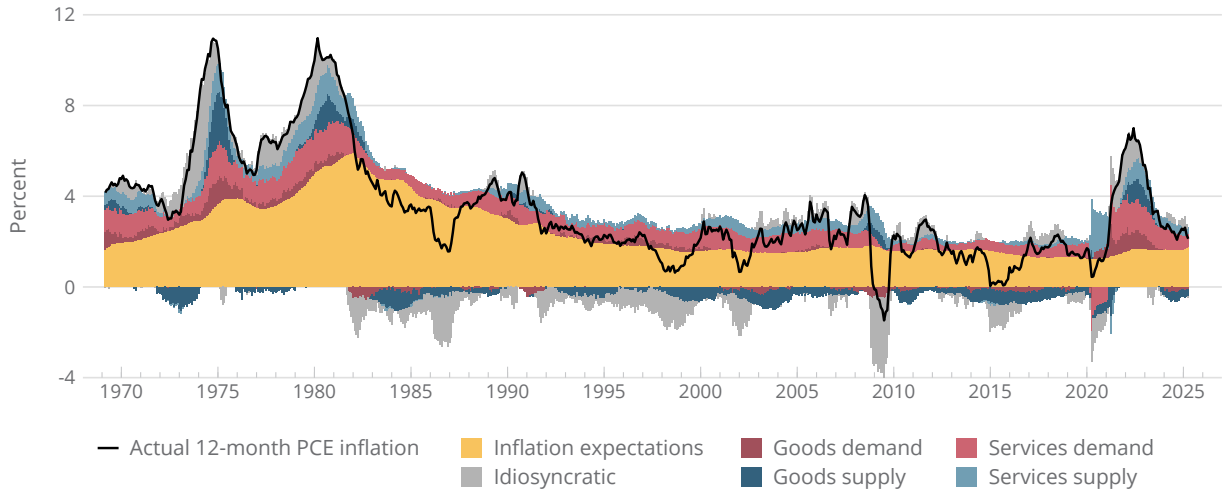
Common to all four inflation factors is a time-varying trend: downward in the case of demand factors and upward in the case of supply factors. This low-frequency variation in the estimated factors can be captured in part by the evolution of long-term inflation expectations over our sample period (see Figure B-1 in Appendix B). According to our estimation results (see Figure C-9 in Appendix C), the posterior median of the coefficient vector $\beta_d = [\beta_d^{(g)} \ \beta_d^{(v)}]'$ on π_{t-1}^E in equation (19) is positive, whereas the posterior median of the coefficient vector $\beta_s = [\beta_s^{(g)} \ \beta_s^{(v)}]'$ on π_{t-1}^E in equation (20) is negative. The former result implies that a decline in long-term expected inflation in month $t - 1$ is associated with a decrease in common goods and services demand factors during the subsequent month, while the same decline in long-term expected inflation is associated with a subsequent increase in common goods and services supply factors, according to the latter result. Because longer-term inflation expectations are a critical factor in determining the average inflation rate over time, the difference between the estimated factors and the inflation-expectations component captures cyclical fluctuations in the underlying supply and demand conditions for goods and services.¹⁴

Understanding these cyclical sources of inflation dynamics in a regime of well-anchored inflation expectations is paramount to the effective conduct of monetary policy because inflation caused by receding aggregate supply creates tradeoffs that do not exist when inflation is caused by rising aggregate demand. Specifically, when inflation results from rising demand, monetary policy can stabilize the economy by bringing demand back down to its sustainable level, thereby simultaneously making progress toward both stable prices and full employment. However, when inflation is due to a contraction in supply, monetary policy can stabilize prices only by pushing employment below full employment. Using the estimated factors, we separate persistent *common* inflation components from idiosyncratic category-specific inflation fluctuations, given that the former are especially relevant for the conduct of monetary policy (see Borio et al., 2021).

Figure 2 shows the historical decomposition of 12-month total PCE inflation from March 1969

¹⁴Figure C-10 in Appendix C shows the estimates of the coefficients $\alpha_j^{(g)} = \theta_j^d \beta_d^{(g)} + \theta_j^s \beta_s^{(g)}$, $j = 1, 2, \dots, N_g$, and $\alpha_k^{(v)} = \delta_k^d \beta_d^{(v)} + \delta_k^s \beta_s^{(v)}$, $k = 1, 2, \dots, N_v$, which measure the sensitivity of category-specific standardized log price changes from month $t - 1$ to month t to π_{t-1}^E , expectations of inflation over the next five to 10 years based on information available as of month $t - 1$. While these estimates exhibit considerable heterogeneity across categories, especially within a broad services category, the weighted median of the posterior medians across the 30 goods categories (Panel A) is quite similar to the weighted median of the posterior medians across the 21 services categories (Panel B). According to these estimates, an increase in long-term expected inflation of 1 standard deviation (about 1.5 percentage points) in month t is associated with an increase of roughly one-tenth of a standard deviation, on balance, in monthly inflation rates in both broad consumption categories during the subsequent month.

FIGURE 2: Historical Decomposition of Inflation



NOTE: Monthly data from March 1969 through April 2025. The black line shows the 12-month total PCE inflation, and the colored areas show the estimated contributions of inflation expectations, the different supply- and demand-side components, and the idiosyncratic component.

SOURCE: Authors' calculations using data from the Bureau of Economic Analysis, the Federal Reserve Board, and the University of Michigan.

through April 2025 based on the estimated factors shown in Figure 1.¹⁵ Demand-driven contributions to inflation, shown by the dark red and light red areas, tend to be positive and sizable. This is particularly the case for the demand of services. However, the magnitude of demand contributions has evolved over time; they were more prominent from the 1970s to the Great Recession and somewhat smaller from 2010 to 2020.

Increases in supply-driven contributions to inflation, shown by the dark blue and light blue areas in Figure 2, often follow increases in commodity prices. This was the case not only in the 1970s and early 1980s, a period that includes two oil-price shocks, but also during the Great Recession, when supply-driven inflation offset demand-driven deflation. Indeed, a surge in oil prices can explain the so-called missing disinflation during this period.¹⁶ Our decomposition indicates that, starting in the mid-1980s, inflation driven by goods supply was low—often below zero—a period that coincided with a notable pickup in productivity growth. The expansion of international trade in the 2000s and 2010s likely played a role in further dampening supply-driven goods inflation.

Note that the estimated contribution of the inflation expectations component, the yellow area, has been essentially constant—at about 2 percent—since the mid-1990s and barely budged during

¹⁵The sum of our estimated contributions does not exactly equal the actual PCE inflation at each point in time, though it is extremely close. The tiny discrepancy primarily reflects the fact that our sample omits two PCE categories (that is, *Net Expenditures Abroad by U.S. Residents* and *Net Foreign Travel*) with occasionally negative expenditure weights.

¹⁶For example, [Coibion and Gorodnichenko \(2015\)](#) argue that an increase in oil prices resulted in a material increase in short-term inflation expectations, as consumers tend to be particularly attentive to salient prices such as gasoline prices.

the recent spike in inflation. This pattern stands in sharp contrast to the one that prevailed during the Great Inflation of the 1970s and early 1980s, when inflation expectations’ contribution to total inflation was much more significant.¹⁷ The difference between the two periods reflects the Federal Reserve’s credible commitment to price stability following the so-called Volcker disinflation and underscores the macroeconomic benefits of stable long-term inflation expectations (see [Bernanke, 2007](#)).

3.2 Pandemic-era Inflation Dynamics

Our methodology provides novel and nuanced insights into the highly unusual and complex pandemic-era inflation dynamics by sharply delineating when and the extent to which inflation during this period was driven by either supply or demand factors. Figure 3 zooms in on the recent period through April 2025, with Panel A focusing on three-month (annualized) inflation rates to better illustrate the various phases, and with Panel B depicting the associated decomposition of the three-month (annualized) growth in real consumption.

Over the first few months of the pandemic—as widespread business closures and mobility restrictions went into effect—common demand and common supply both collapsed. As shown in Panel A, these two developments had roughly opposite effects on inflation, resulting, on net, in a deflation of about 2 percent on the three-month annualized basis by the late spring of 2020. The deflationary impact of the pandemic-induced collapse in common demand and supply is also evident in a massive contraction in real PCE over the same period, as shown in Panel B. Not surprisingly, the sharp contraction in consumer spending was primarily due to a substantial pullback in the demand for services and the corresponding reduction in services supply, as fear of the virus kept people at home and businesses shut down.¹⁸

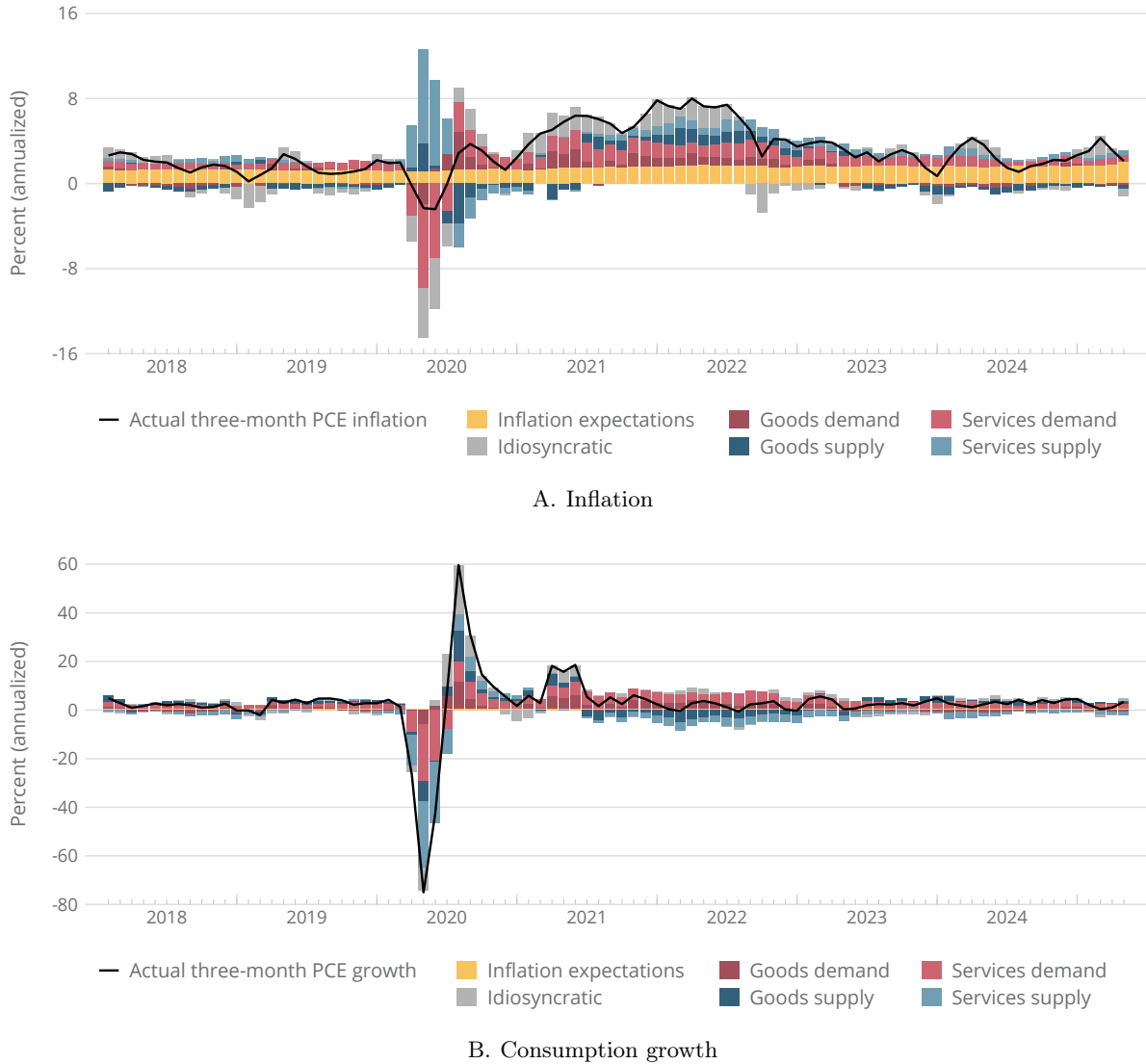
The recovery and relief legislation enacted in March and April 2020, along with the relaxation in May of some restrictions on economic activity, led to a sharp rebound in consumer demand—for both goods and services—over the summer and early autumn (Panel B), boosting inflation to about 4 percent (Panel A).¹⁹ This pent-up demand, however, subsided quickly, while the continued improvement in the supply of both goods and services helped restrain the initial inflationary impulse. In fact, by the end of 2020, inflation on a three-month annualized basis was essentially back to the Federal Reserve’s 2 percent target, and consumption growth was at its pre-pandemic pace.

¹⁷This finding is consistent with research that has found that the “unanchoring” of inflation expectation during this period—together with adverse supply shocks—boosted inflation expectations, allowing high inflation to persist and become embedded in the economy vis-à-vis wage- and price-setting behavior (see [Ireland, 2007](#); [Ball and Mazumder, 2011](#)).

¹⁸Note that the goods demand was much less affected—and only briefly so—during this period, according to our estimates. While most consumers followed the orders that restricted them from leaving their homes—other than to purchase essential items from grocery stores or pharmacies—significant “panic buying” nevertheless took hold, in some cases forcing retailers to limit the number of purchases of high-demand goods. Demand for goods during this period was also bolstered by a significant consumer switch to online sales channels (see [Young et al., 2022](#)).

¹⁹Most important among the early fiscal measures aimed at blunting the economic damage of the pandemic was the \$2.2 trillion stimulus bill called the Coronavirus Aid, Relief, and Economic Security (CARES) Act, which the U.S. Congress passed on March 25, 2020, and President Trump signed into law two days later.

FIGURE 3: Inflation and Consumption Growth during the Pandemic



NOTE: Monthly data from January 2018 through April 2025. The black line in Panel A shows the three-month (annualized) total PCE inflation, and the colored areas show the estimated contributions of inflation expectations, the different supply- and demand-side components, and the idiosyncratic component. The black line in Panel B shows the three-month (annualized) growth of (real) PCE, and the colored areas show the estimated contribution of the same components.

SOURCE: Authors' calculations using data from the Bureau of Economic Analysis, the Federal Reserve Board, and the University of Michigan.

The Federal Reserve's massive monetary stimulus put in place in March and April of 2020—which included interest rate cuts, forward guidance, a significant expansion of its balance sheet, and regulatory changes—combined with the additional relief and recovery legislation enacted in December 2020 and early 2021 gave the recovery an added boost.²⁰ According to our estimates, demand-

²⁰See Clarida et al. (2021) for a detailed description of the Federal Reserve's policy response during the pandemic.

driven spending on both goods and services jumped notably in the spring of 2021 (Panel B), helping to push inflation above 6 percent by mid-year (Panel A). These dynamics are contrary to “Team Transitory’s” argument that the rise in inflation over this period was primarily due to supply-side factors, reflecting lingering pandemic bottlenecks and increased costs of producing and distributing goods more generally—if anything, our estimates indicate a supply-driven goods *disinflation* over this period.

Aggregate supply conditions did start to worsen over the second half of 2021, attenuating the decline in inflation resulting from the diminution of idiosyncratic price pressures and a moderation in demand-driven goods inflation (Panel A). Inflation driven by demand for services, by contrast, proved to be substantially stickier, a result consistent with the slow resolution of pandemic-induced labor shortages, which were especially severe in the services sector. The emergence of the Omicron variant of COVID-19 in late 2021 delivered another adverse shock to the already-strained aggregate supply conditions. Omicron’s high transmissibility exacerbated the preexisting labor shortages, not only in the service sector but also in manufacturing and logistics-related industries such as trucking and shipping.

With inflation clearly on the loose, the Federal Reserve’s Federal Open Market Committee (FOMC), at its December 2021 meeting, removed the word “transitory” from its post-meeting statement, accelerated the tapering of asset purchases, and signaled that the tapering pace would likely evolve in a manner that would end purchases by March 2022. In early 2022, the sharp rise in infections globally led to border closures and international travel restrictions as well as to widespread factory shutdowns, especially in China, where the government imposed a strict “zero-COVID” policy that included mass lockdowns. The ensuing production and shipping disruptions led to acute shortages of key manufacturing components and significantly extended order backlogs for electronics, cars, and other products. If that were not enough, Russia’s invasion of Ukraine in late February 2022 sent global food and energy prices soaring. These negative supply developments collided with the elevated and persistent demand for both goods and services and helped push the three-month annualized inflation above 8 percent by mid-2022, according to our estimates (Panel A).

The Federal Reserve’s response to these developments was swift and aggressive. In January 2022, the FOMC statement noted that “with inflation well above 2 percent and a strong labor market, the Committee expects it will soon be appropriate to raise the target range for the federal funds rate.” Indeed, in March, the FOMC ended net asset purchases and lifted the target range off the effective lower bound and, over the remainder of the year, raised the target range a total of 425 basis points, from a 0.0 to 0.25 percent range to a 4.25 to 4.5 percent range.

Our estimates indicate that the notable deceleration in PCE prices at the end of 2022 was entirely due to idiosyncratic factors, as common demand- and supply-side pressures remained elevated (Panel A). During the first half of 2023, with inflation still well above the Federal Reserve’s 2 percent target and with labor market conditions remaining very tight, the FOMC continued to raise the

On the fiscal side, the most significant policy response was the American Rescue Plan of 2021, a \$1.9 trillion stimulus package signed into law by President Biden on March 11, 2021.

target range for the federal funds rate, though at a slower pace than in the latter part of 2022.²¹ With time, however, the effects of the cumulative monetary tightening started to appear in the aggregate components. Demand-driven goods inflation moderated relatively quickly, followed by a more gradual slowing of demand-driven services inflation. As global supply chains started to stabilize after the severe disruptions of the previous few years, positive supply developments—especially of goods supply—also contributed to a decline in inflation over the second half of 2023 and early 2024.

We have focused thus far on disentangling common supply and demand forces that shaped the pandemic-era inflation dynamics. While these common forces explain a large portion of the variation in inflation over this period, there is also an idiosyncratic component (the gray area in Panel A of Figure 3) that at times significantly affected total PCE inflation.²² This component reflects factors specific to a particular category of goods or services and may involve category-specific demand and/or supply developments. For example, our model attributes to idiosyncratic inflation a one-time change in energy prices that is quickly reverted and that does not spill over into other categories—a so-called relative price shock.

To disentangle the impact of relative supply and demand shocks on corresponding idiosyncratic price developments, we estimate category-specific structural Bayesian VAR (BVAR) models composed of our estimated idiosyncratic fluctuations in quantities and prices and identify the associated structural supply and demand shocks via sign restrictions. Formally, we consider the following category-specific BVAR:

$$\begin{bmatrix} \tilde{\xi}_{i,t} \\ \tilde{\eta}_{i,t} \end{bmatrix} = \mathbf{B}_{i,0} + \mathbf{B}_{i,1} \begin{bmatrix} \tilde{\xi}_{i,t-1} \\ \tilde{\eta}_{i,t-1} \end{bmatrix} + \cdots + \mathbf{B}_{i,r} \begin{bmatrix} \tilde{\xi}_{i,t-r} \\ \tilde{\eta}_{i,t-r} \end{bmatrix} + \underbrace{\begin{bmatrix} + & + \\ - & + \end{bmatrix}}_{\mathbf{A}_i} \begin{bmatrix} e_{i,t}^{(s)} \\ e_{i,t}^{(d)} \end{bmatrix},$$

where $\tilde{\xi}_{i,t}$ denotes our model-implied estimate of the idiosyncratic (real) consumption one-month growth in PCE category i , $\tilde{\eta}_{i,t}$ denotes the corresponding idiosyncratic one-month inflation, and $e_{i,t}^{(s)}$ and $e_{i,t}^{(d)}$ are the category-specific (that is, relative) supply and demand shocks, respectively.²³

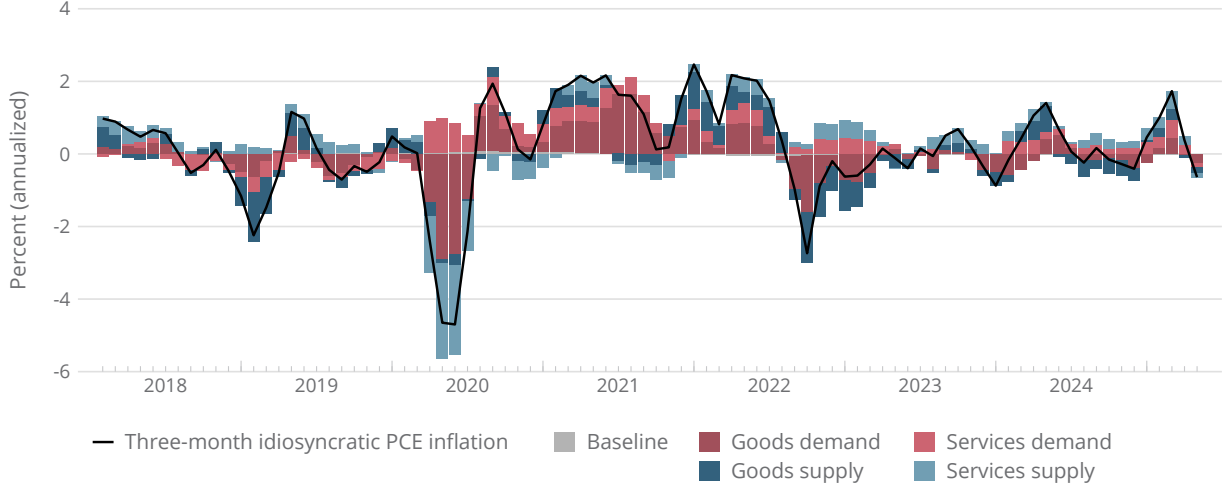
The latter two structural innovations, collected in the vector $\mathbf{e}_{i,t} = [e_{i,t}^{(s)} \ e_{i,t}^{(d)}]'$, are assumed to

²¹The slowdown in the pace of policy firming was importantly motivated by the emergence of banking-sector strains in March 2023, which led to a notable tightening of credit conditions for many businesses and households. All told, the FOMC raised the federal funds rate target range 25 basis points at its January, March, and May 2023 meetings; at its June 2023 meeting, it held the range steady at the 5.0 to 5.25 percent, where it remained until September 2024.

²²As [Borio et al. \(2023\)](#) documented extensively, the establishment of credible monetary policy frameworks, resulting in low and stable inflation, has been accompanied by a marked decrease in the co-movement of prices across finely disaggregated sectors of the economy. Consequently, idiosyncratic (or sector-specific) price changes have emerged as a more significant driver of fluctuations in aggregate price indexes under these conditions. This empirical trend is mirrored in our inflation decomposition, which shows that the estimated idiosyncratic inflation component was responsible for more than 85 percent of the variance in monthly PCE inflation from the mid-1990s to the end of 2019—a period of low and stable inflation—in contrast to roughly 45 percent in earlier years.

²³In a slight abuse of our earlier notation, we omit the distinction between goods ($j = 1, 2, \dots, N_g$) and services ($k = 1, 2, \dots, N_v$) categories (see equations 11 through 14) when specifying the category-specific BVARs because they are estimated separately for each $i = 1, 2, \dots, (N_g + N_v)$; following [Shapiro \(2024\)](#), we set the category-specific BVAR lag length $r = 12$, for all i .

FIGURE 4: Idiosyncratic Inflation during the Pandemic



NOTE: Monthly data from January 2018 through April 2025. The black line shows the three-month (annualized) total idiosyncratic PCE inflation implied by our model (the gray area in Panel A of Figure 3), and the colored areas show the estimated contributions of goods- and services-related supply and demand shocks. SOURCE: Authors' calculations using data from the Bureau of Economic Analysis, the Federal Reserve Board, and the University of Michigan.

be normally distributed, $\mathbf{e}_{i,t} \sim \mathcal{N}(\mathbf{0}, \mathbf{I})$, and the entries of the impact multiplier matrix \mathbf{A}_i are “sign-restricted,” following the approach of Giannone and Primiceri (2024). This implies that a positive supply shock specific to a consumption category leads to a decrease in a relative price in that category and an increase in the corresponding quantities; a category-specific demand shock, on the other hand, is assumed to increase both the relative price and quantities. This framework thus allows us to decompose category-specific price changes that are orthogonal to our estimated common supply and demand factors into category-specific supply- and demand-side contributions. Given the expenditure weights associated with each category, we then aggregate those contributions to obtain a breakdown of total idiosyncratic inflation into its respective supply and demand contributions.

The results of this exercise, corresponding to the decomposition of pandemic-era inflation, are shown in Figure 4.²⁴ These estimates indicate a significant disinflation in the idiosyncratic component of total PCE inflation at the onset of the COVID-19 pandemic. As shown by the black line, over the three months ending in April 2020, total idiosyncratic prices fell at an annual rate of about 4.5 percent. According to our decomposition, this drop in idiosyncratic prices was primarily driven by the idiosyncratic demand-driven goods disinflation (the dark red bars) and the idiosyncratic supply-driven services disinflation (the light blue bars).

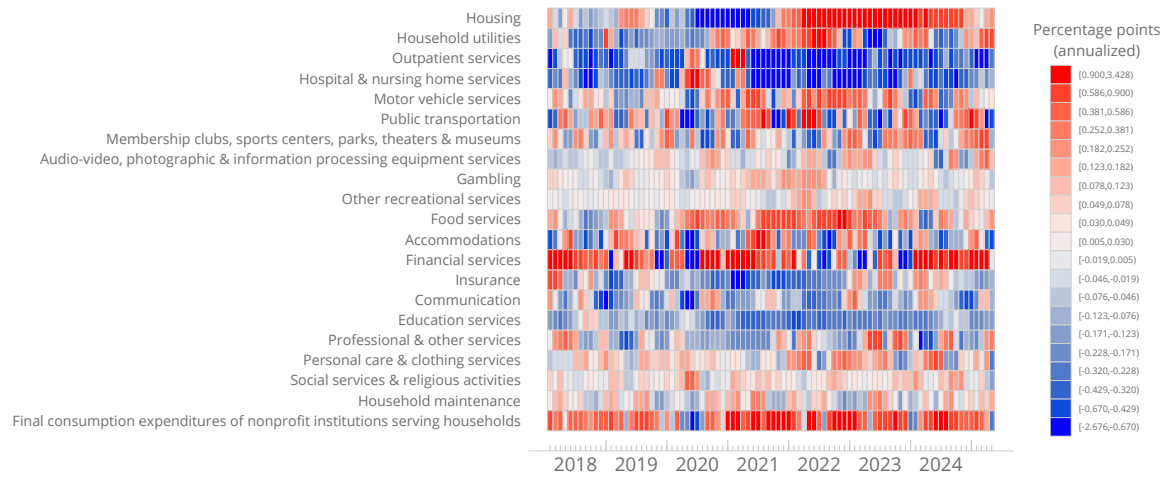
The rebound in the idiosyncratic demand-driven goods inflation during the summer and autumn of 2020 contributed notably to the burst in total idiosyncratic inflation during this period. While

²⁴ Analogous to Figure 2, Figure C-11 in Appendix C shows the decomposition of 12-month total idiosyncratic PCE inflation over the entire sample period.

FIGURE 5: Net Contributions of Idiosyncratic Price Changes



A. PCE goods categories



B. PCE services categories

NOTE: Monthly data from January 2018 through April 2025. The heatmap in Panel A shows the estimated net contributions to the three-month (annualized) total idiosyncratic PCE inflation (the black line in Figure 4) from the PCE goods categories, whereas the heatmap in Panel B shows the estimated net contributions from the PCE services categories.

SOURCE: Authors' calculations using data from the U.S. Bureau of Economic Analysis, the Federal Reserve Board, and the University of Michigan.

this inflationary impulse faded by the end of the year, idiosyncratic price pressures broadened appreciably in 2021, contributing to the renewed rise in idiosyncratic inflation and, by extension, to the acceleration in total PCE prices. The adverse supply developments that emerged in 2022 at the aggregate level are also evident at the idiosyncratic level—especially in the goods sector (the dark blue bars)—which bolstered total idiosyncratic inflation over this period.

Figure 5 looks “under the hood” of these idiosyncratic price fluctuations. Specifically, the heatmap in Panel A shows the estimated *net* contributions to the three-month (annualized) total idiosyncratic inflation from each of the 31 goods categories, whereas Panel B shows the corresponding contributions from each of the 21 services categories. A category-specific net contribution corresponds to the sum of the estimated demand- and supply-driven idiosyncratic three-month log-price changes in that category, weighted by the appropriate expenditure share.²⁵

Unsurprisingly, the category-specific net contributions to total idiosyncratic inflation are noisy, both in the cross-sectional and time-series dimensions. Nevertheless, some suggestive patterns emerge from this analysis. As shown in Panel A, our decomposition identifies large negative net contributions from the PCE goods categories **Garments**, **Motor Vehicle Fuels**, **Lubricants & Fluids**, **Recreational Items**, and **Fuel Oil & Other Oils** as chief culprits behind the drop in idiosyncratic demand-driven goods inflation early in the pandemic. The concomitant downward pressure from the idiosyncratic supply-driven prices in the services sector, on the other hand, is importantly due to **Public Transportation** and **Accommodations** categories, according to Panel B. These results are consistent with the significant and sudden reduction in travel and commuting during the early stages of the pandemic.

The 2021 run-up in idiosyncratic inflation owed substantially to its goods-demand component, as evidenced by lengthy “red streaks” in many goods categories during this period. Also notable is that, starting in mid-2021, net contributions of idiosyncratic housing inflation turned markedly positive, a trend that persisted well into 2024.²⁶ The pandemic significantly affected housing preferences, including a preference for larger homes and increased demand for second homes, factors that boosted the overall housing demand and home prices. While total idiosyncratic inflation started to recede in the second half of 2022, idiosyncratic housing inflation continued to increase, on net, for another two or so years, reflecting the lagged impact of these pandemic-related shifts.

4 External Validation

In this section, we present several exercises that provide external validation of our estimated supply and demand factors and their contributions to inflation. First, we compare our estimates of cyclical supply- and demand-driven inflation with commonly used measures of aggregate demand and supply conditions. Second, we assess the dynamic responses of supply- and demand-driven inflation to well-identified external supply and demand shocks.

²⁵The heatmaps in Figures C-12 and C-13 in Appendix C, show the corresponding estimates of demand- and supply-driven *gross* contributions in the goods and services sectors, respectively.

²⁶The **Housing** category accounts for about 15 percent of PCE, and the associated price index measures both rent for primary residences and the owners’ equivalent rent, which estimates what homeowners would pay if they were renting.

4.1 Comparison with Macroeconomic Indicators

On the supply side, we examine the co-movement between our estimate of cyclical supply-driven inflation and labor productivity, as measured by deviations in (real) output per hour in the U.S. nonfinancial corporate sector from its trend. On the demand side, we compare how our estimate of cyclical demand-driven inflation co-moves with labor market slack, as measured by deviations of the unemployment rate from its natural rate. Total supply-driven inflation corresponds to the sum of the contributions associated with the goods supply and services supply inflation factors (the blue areas in Figure 2), whereas total demand-driven inflation corresponds to the sum of the contributions associated with the goods and services demand inflation factors (the red areas in Figure 2).²⁷

The results of this exercise are reported in Figure 6. As shown in Panel A, periods of elevated supply-driven inflation correspond generally to periods of below-trend productivity growth. Not surprisingly, many of these episodes occur around recessions. However, the negative co-movement between the two series is also evident during economic expansions, a pattern consistent with a disinflationary impact of supply conditions when labor productivity runs persistently above trend.²⁸

Panel B shows the co-movement between demand-driven inflation and labor market slack. For the most part, our estimate of demand-driven inflation corresponds closely with the inverse of the unemployment gap, implying that labor market tightness is positively associated with demand-driven inflation.²⁹ All told, these simple exercises provide prima facie evidence that supports our interpretation of how the estimated inflation factors capture the aggregate supply- and demand-side price pressures.

4.2 Responsiveness to External Shocks

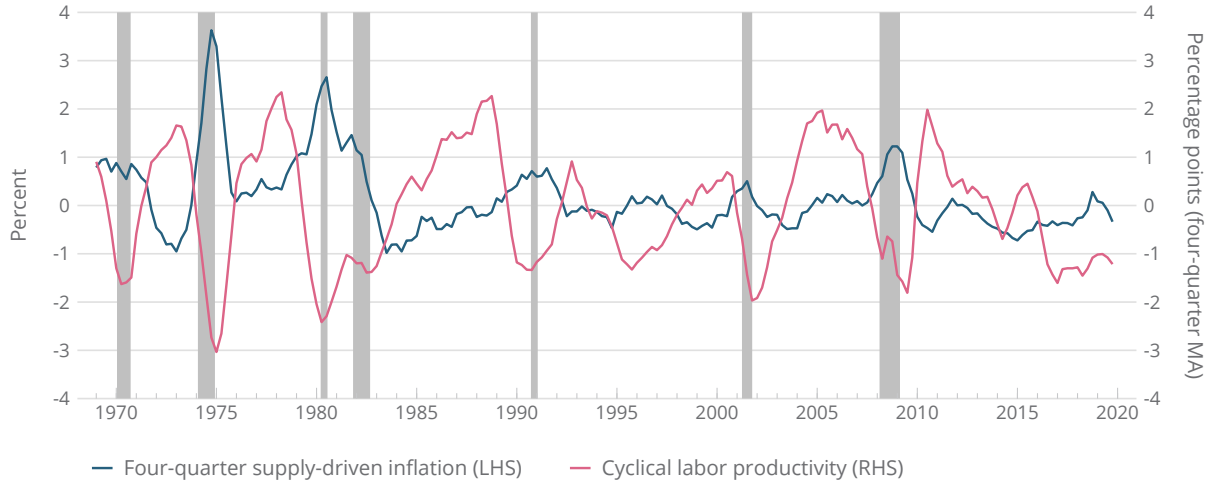
Our next set of external validation exercises considers the impact of well-identified external supply- and demand-side shocks on our estimates of demand- and supply-driven inflation. The maintained hypothesis underlying this exercise is that our estimated supply-driven inflation should respond strongly to supply-side shocks and be relatively insensitive to demand-side shocks. Conversely, our demand-driven inflation should be particularly sensitive to demand-side disturbances and be largely unaffected by supply-side disturbances.

²⁷Because labor productivity data are quarterly, we convert all monthly series (that is, supply- and demand-driven inflation and the unemployment rate) to a quarterly frequency. We estimate trend labor productivity using a [Hodrick and Prescott \(1997\)](#) filter with the “smoothing” parameter $\lambda = 10,000$, and we use the natural rate of unemployment estimated by the U.S. Congressional Budget Office to compute the unemployment gap, a standard measure of labor market slack. To avoid the distortionary effects of highly atypical pandemic-induced gyrations in macroeconomic series, we restrict the analysis to the 1968:Q2–2019:Q4 period.

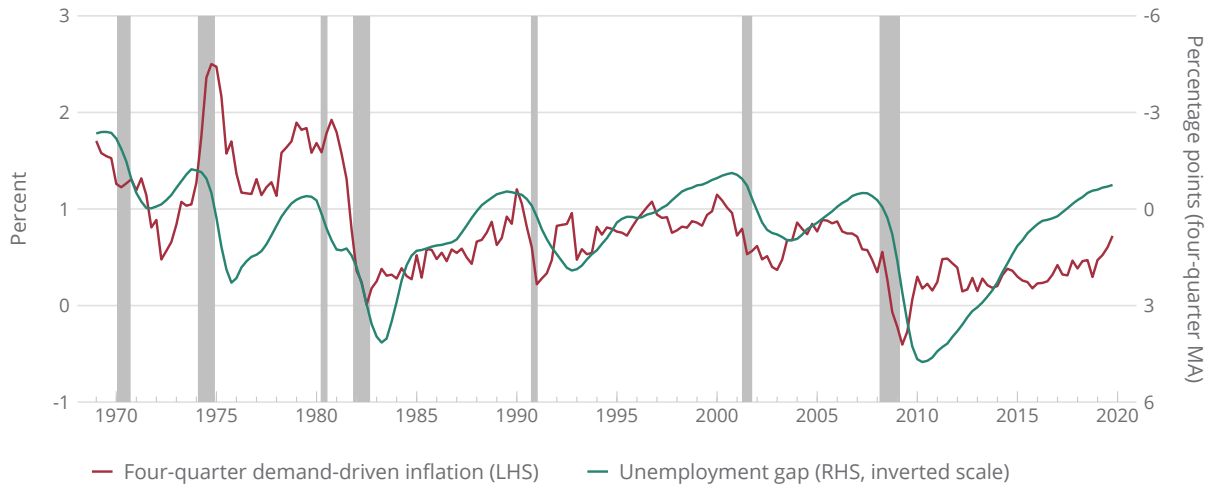
²⁸The correlation between the two series over the 1968:Q2–2019:Q4 period is -0.48 ($p < .001$). The corresponding correlations for the supply-driven goods inflation and supply-driven services inflation are -0.38 ($p < 0.001$) and -0.50 ($p < .001$), respectively.

²⁹The correlation between the two series over the full sample period is -0.47 ($p < .001$). The corresponding correlations for the demand-driven goods inflation and demand-driven services inflation are 0.36 ($p < 0.001$) and 0.47 ($p < .001$), respectively. We obtain very similar results when using the output gap in place of the unemployment gap to measure the degree of slack in the economy.

FIGURE 6: Cyclical Dynamics of Supply- and Demand-driven Inflation



A. Supply-driven inflation and labor productivity



B. Demand-driven inflation and labor market slack

NOTE: Quarterly data from 1969:Q1 through 2019:Q4. The lines in Panel A show the four-quarter cyclical supply-driven inflation and the four-quarter moving average of deviations of (real) output per hour in the U.S. nonfinancial corporate sector from its estimated trend. The lines in Panel B show the four-quarter cyclical demand-driven inflation and the four-quarter moving average of the unemployment gap. The shaded vertical bars depict recessions as determined by the National Bureau of Economic Research.

SOURCE: Authors' calculations using data from the Bureau of Economic Analysis, the Bureau of Labor Statistics, the Congressional Budget Office, the Federal Reserve Board, and the University of Michigan.

We formally test this hypothesis using the local projections methodology proposed by Jordà (2005). Specifically, letting $shock_t$ denote an identified external shock in month t , either from a

demand or supply side, we consider the following regression specification:

$$\pi_{t-1:t+h} = \alpha^{(h)} + \beta^{(h)} \times shock_t + \sum_{p=1}^{12} \mathbf{x}_{t-p}' \gamma_p^{(h)} + \varepsilon_{t+h}^{(h)}; \quad h = 0, 1, \dots, H, \quad (31)$$

where $\pi_{t-1:t+h}$ denotes the cumulative demand- or supply-driven inflation—for goods, services, and total—from month $t - 1$ to month $t + h$, and \mathbf{x}_{t-p} , $p = 1, 2, \dots, 12$, is a vector of control variables included to filter out the impact of macroeconomic conditions on our estimates of supply- and demand-driven inflation; these controls include the log of the total PCE price index, the civilian unemployment rate, the one-year and 10-year (nominal) Treasury yields, the excess bond premium of [Gilchrist and Zakrajšek \(2012\)](#), the log of the S&P 500 total return index, and the log of the overall commodity spot price index from the Commodity Research Bureau. We estimate specification (31) by OLS and use the heteroscedasticity-robust asymptotic covariance matrix to gauge the statistical significance of the local projections impulse responses—that is, the sequence of estimated coefficients $\hat{\beta}^{(h)}$, $h = 0, 1, \dots, H$.

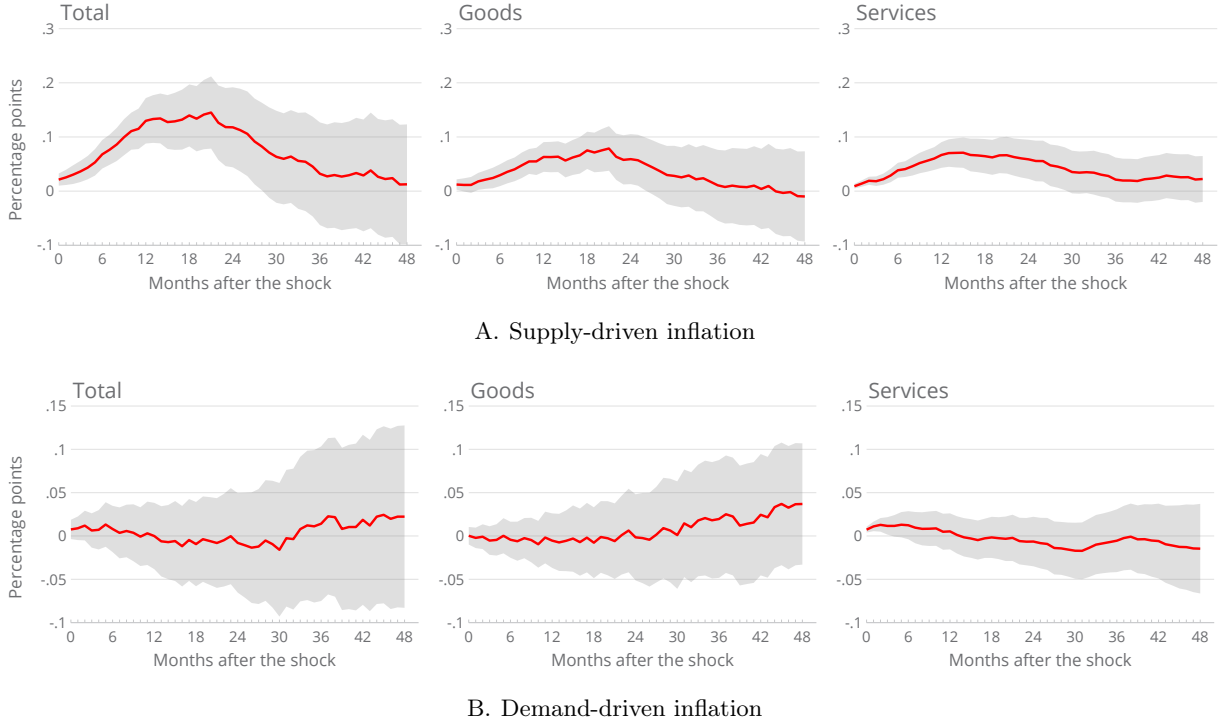
We begin the analysis with the oil supply news shocks of [Känzig \(2021\)](#), which are identified using movements in oil futures prices around Organization of the Petroleum Exporting Countries (OPEC) announcements. These shocks are scaled to represent an increase in the real price of oil of 10 percent upon impact. In the estimation, we use monthly shock series from January 1985 through December 2019. Our sample thus excludes the period of unstable inflation expectations and structural changes in the conduct of monetary policy during the 1970s and early 1980s, as well as the highly unusual macroeconomic dynamics during the COVID-19 pandemic.

Figure 7 plots the estimated responses, with Panel A focusing on the supply-driven inflation and Panel B on the demand-driven inflation. As shown in Panel A, an oil news shock that raises the real price of oil by 10 percent upon impact induces a persistent and significant increase—in both economic and statistical terms—in the supply-driven component of total PCE inflation over the subsequent two years. According to our estimates, the increase in total common supply-driven inflation (the left panel) accumulates to about 15 basis points about 20 months after the shock. This adverse supply shock affects the supply-driven goods inflation (the middle panel) and the supply-driven services inflation (the right panel) to the same extent, though the response of supply-driven services inflation is somewhat more persistent. By contrast, as shown in Panel B, negative oil news supply shocks have no discernible effect on our estimates of demand-driven inflation—the estimated responses are trivial in economic terms and statistically indistinguishable from zero.

To examine how demand-side disturbances affect the dynamics of supply- and demand-driven inflation, we turn to monetary policy shocks, as identified by [Nunes et al. \(2022\)](#) using high-frequency interest rate changes around FOMC announcements.³⁰ These shocks are scaled so that a contrac-

³⁰This approach follows a well-established literature that uses changes in interest rates or interest rate futures in narrow windows bracketing FOMC announcements to isolate monetary policy surprises (see [Kuttner, 2001](#); [Gürkaynak et al., 2005](#)). However, as [Jarociński and Karadi \(2020\)](#) and [Miranda-Agrippino and Ricco \(2021\)](#) point out, such surprises reflect a combination of “pure” monetary policy shocks—that is, the Federal Reserve’s unanticipated deviations from its usual stance—and “information” shocks capturing the Federal Reserve’s reactions to its private

FIGURE 7: The Impact of an Adverse Oil Supply News Shock



NOTE: Sample period: monthly data from January 1985 through December 2019. The lines in Panel A show the estimated responses of total, goods, and services cumulative supply-driven inflation over the specified horizon to an adverse oil supply news shock that increases the real price of oil by 10 percent upon impact (that is, in month 0); the lines in Panel B show the estimated responses of total, goods, and services cumulative demand-driven inflation over the specified horizon to the same shock. The shaded bands depict the associated 95 percent confidence intervals.

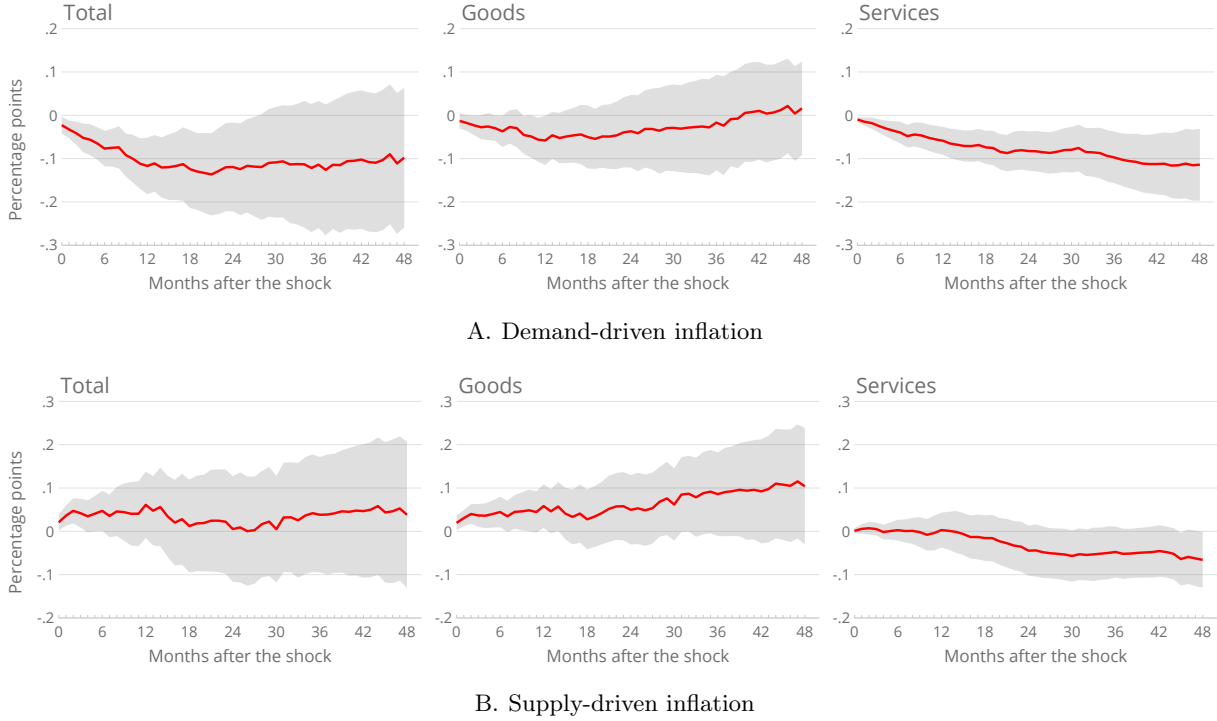
tionary (expansionary) monetary policy shock represents an increase (decrease) of 25 basis points in the one-year nominal Treasury yield upon impact; as in the case of oil supply news shocks, we estimate specification (31) using monthly data from January 1985 through December 2019.

Figure 8 presents the results of this exercise, with Panel A depicting responses of demand-driven inflation and Panel B depicting the corresponding responses of supply-driven inflation. As shown in Panel A, total common demand-driven inflation (the left panel) declines quickly and persistently in response to an unanticipated tightening of monetary policy: A policy-induced increase in the one-year Treasury yield of 25 basis points in month zero reduces the cumulative total demand-driven inflation by almost 15 basis points after 12 months.

Most of the disinflation in total common demand-driven inflation in response to a contractionary monetary policy shock is accounted for by a persistent decline in the services component of total demand-driven inflation (the right panel), which is estimated to decline over the entire response horizon. The response of demand-driven goods inflation (the middle panel), by contrast, is more

assessment of the economic outlook. Nunes et al. (2022) use information on changes in interest rate expectations around macroeconomic news data releases—in addition to changes around FOMC announcements—to obtain monetary policy shocks that are purged of the information effect.

FIGURE 8: The Impact of a Contractionary Monetary Policy Shock



NOTE: Sample period: monthly data from January 1985 through December 2019. The lines in Panel A show the estimated responses of total, goods, and services cumulative demand-driven inflation over the specified horizon to a contractionary monetary policy shock that increases the one-year nominal Treasury yield by 25 basis points upon impact (that is, in month 0); the lines in Panel B show the estimated responses of total, goods, and services cumulative supply-driven inflation over the specified horizon to the same shock. The shaded bands depict the associated 95 percent confidence intervals.

concentrated at near-term horizons. The greater sensitivity of demand-driven services inflation to monetary policy is consistent with the results of [Stock and Watson \(2020\)](#), who document that prices of services tend to be more sensitive to economic fluctuations—that is, they are “cyclically sensitive.”

As shown in Panel B, monetary policy has little effect on total common supply-driven inflation (the left panel). There is a modest, statistically significant uptick in total supply-driven inflation immediately following a contractionary monetary policy shock, driven entirely by a policy-induced rise in supply-driven goods inflation (the middle panel). These dynamics are consistent with the presence of the so-called cost channel of monetary policy, whereby policy-induced changes in interest rates directly affect firms’ production costs, particularly when firms rely heavily on external financing to cover their operational expenses (see [Barth and Ramey, 2001](#)). In other words, when interest rates rise in response to a switch to tight monetary policy, firms’ borrowing costs increase, leading to higher production costs and upward pressure on prices, a supply-side effect that can be especially pronounced for firms that operate in customer markets and are liquidity-constrained or have significant floating-rate debt obligations (see [Gilchrist et al., 2017](#); [Core et al., 2025](#)).

All told, these results confirm the interpretation of the estimated inflation factors: Our estimates of the cyclical common demand-driven inflation correlate closely with standard measures of economic slack and respond significantly—in both economic and statistical terms—to unanticipated changes in the stance of monetary policy, a significant source of fluctuations in aggregate demand. Our estimates of cyclical common supply-driven inflation, on the other hand, track labor productivity over time and are highly sensitive to adverse oil supply news shocks, events that increase uncertainty about future oil supplies and, in the process, drive up global crude oil prices.³¹

5 Forecasting Inflation

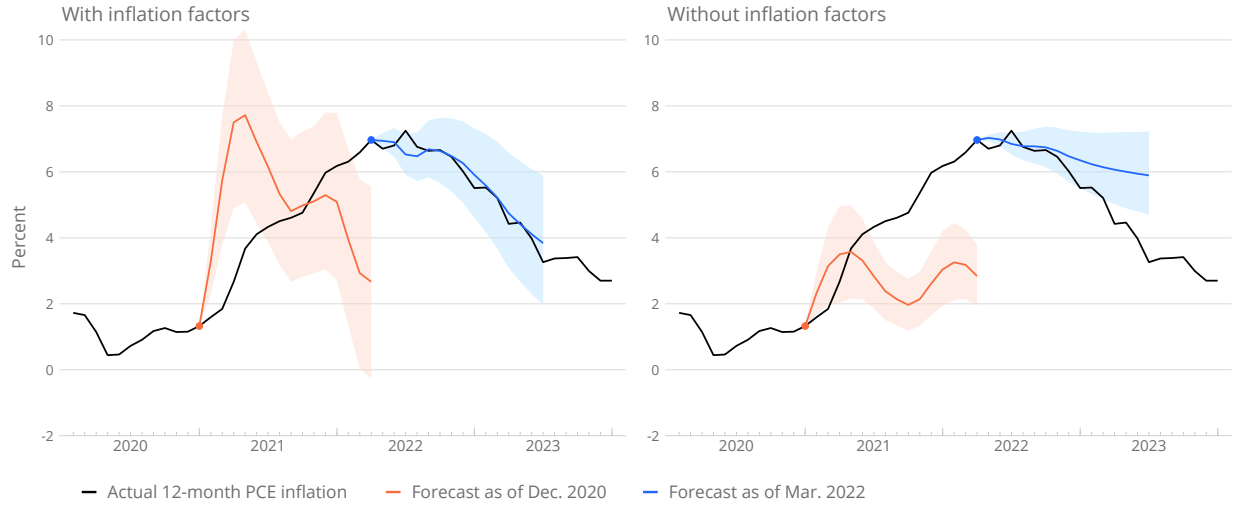
In this section, we demonstrate the usefulness of our factors for inflation forecasting. Specifically, we ask whether adding our inflation factors to a standard set of predictors helps improve the accuracy of inflation forecasts, a critical input into monetary policy decisionmaking. Recent work by [Chan \(2020\)](#) and [Bańbura et al. \(2025\)](#) shows that large Bayesian vector autoregressions (BVARs) provide a useful framework for forecasting inflation. Motivated by this literature, our baseline inflation forecasting framework relies on a BVAR(12) model consisting of (1) the 12-month log-difference of total PCE price index, (2) the civilian unemployment rate, (3) the 12-month log-difference of unit labor cost, (4) the 12-month log-difference of the energy price index in the CPI report, and (5) the two-year (nominal) Treasury yield. This set of variables encompasses lagged inflation dynamics, key indicators of labor market conditions, movements in energy prices, and the stance of monetary policy—predictors featured in canonical inflation forecasting models.

To evaluate the information content of our inflation factors for the near- and medium-term evolution of PCE inflation, we augment this baseline specification with the estimated supply- and demand-side inflation factors shown in [Figure 1](#). For each of these two BVAR(12) models, we consider two forecasts of 12-month total PCE inflation: one made using available information as of December 2020, right before inflation started to surge, and another using information as of March 2022, as inflation leveled off. To simulate a real-time forecasting environment, we re-estimate the inflation factors with disaggregated PCE price and quantity data available as of December 2020 and as of March 2022.

[Figure 9](#) presents the results of this exercise. As the red line in the left panel shows, including our estimated inflation factors in the baseline BVAR model would provide, in December 2020, a much more worrisome signal about near-term inflation developments compared with the forecast based on only standard predictors (the red line in the right panel). While the latter suggests a transitory spike in inflation, with inflation running above the Federal Reserve’s 2 percent target for only about six months, the former forecast features a much more rapid and potentially long-lasting inflation surge. In addition, the uncertainty around the inflation outlook beyond the near term increases substantially in the model with inflation factors, hinting at the highly unusual inflation dynamics that were to come.

³¹For completeness, [Figures C-14 and C-15](#) in [Appendix C](#) show the estimated impulse responses of supply- and demand-driven *idiosyncratic* inflation to oil supply news and monetary policy shocks, respectively.

FIGURE 9: Pandemic-era Real-time Inflation Forecasts



NOTE: Monthly data from January 2020 through December 2023. The black line in each panel shows the actual 12-month total PCE inflation. The red lines show the pseudo real-time forecasts of total PCE inflation as of December 2020, whereas the blue lines show the pseudo real-time forecasts of total PCE inflation as of March 2022; the shaded bands depict the associated [P10, P90] credible intervals. The forecasts in the left panel are based on the baseline BVAR(12) model augmented with the four inflation factors, while forecasts in the right panel are based on the baseline BVAR(12) model that excludes the four factors.

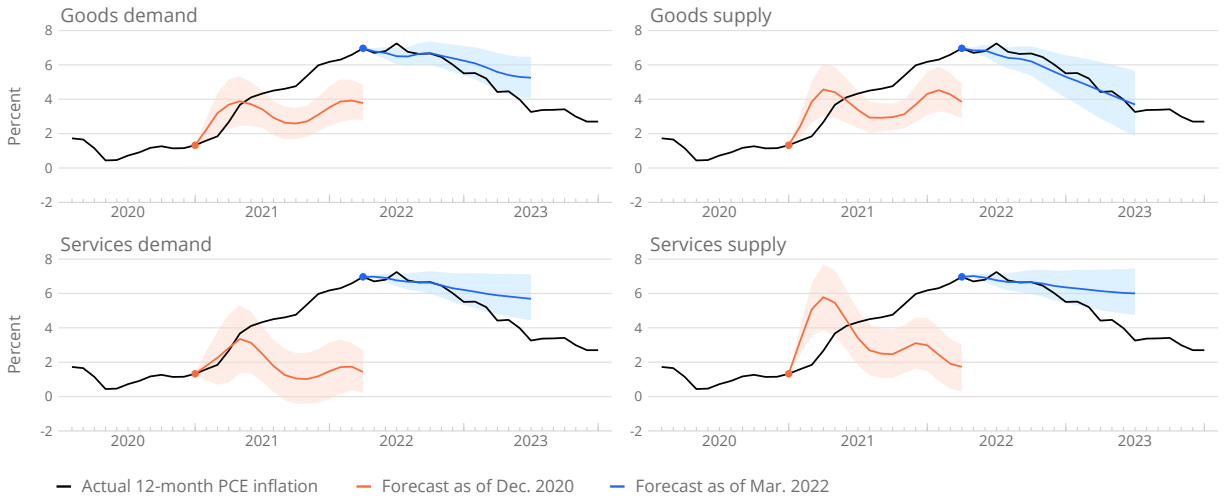
SOURCE: Authors' calculations using data from the Bureau of Economic Analysis, the Bureau of Labor Statistics, the Federal Reserve Board, the Federal Reserve Economic Data (FRED), and the University of Michigan.

Turning to the disinflation that began in mid-2022, the blue line in the right panel shows that the model without inflation factors would, as of March 2022, have failed to anticipate the swift decline in inflation over the subsequent year or so. By contrast, the projection that incorporates our inflation factors (the blue line in the left panel) captures remarkably well the disinflation over that period, the pace of which surprised many economists and policymakers. This suggests that incorporating our estimated inflation factors into workhorse models would have provided policymakers with a potentially more accurate understanding of the highly unusual pandemic-era inflationary dynamics, during both the initial surge and the subsequent disinflation.

To investigate which of the four factors would have contributed most to the improvement in forecast accuracy during the early 2020 inflation surge and the mid-2022 period of disinflation, we re-estimate the baseline BVAR model augmented with one factor at a time and then generate the associated inflation forecast. We repeat this exercise independently for each inflation factor; the results are shown in Figure 10. According to these results, in December 2020, the two common supply factors contained the greatest information content for the upcoming inflation surge. In particular, the common services supply factor (the red line in the bottom right panel) signaled at that point an especially sharp and sudden acceleration in total PCE prices over the first half of 2021.

In March 2022, all four projections capture the start of the gradual disinflation process reasonably

FIGURE 10: Inflation Factors and Pandemic-era Real-time Inflation Forecasts



NOTE: Monthly data from January 2020 through December 2023. The black line in each of the four panels shows the actual 12-month total PCE inflation. The red lines show the pseudo real-time forecasts of total PCE inflation as of December 2020, whereas the blue lines show the pseudo real-time forecasts of total PCE inflation as of March 2022; the shaded bands depict the associated [P10, P90] credible intervals. The forecasts in each panel are based on the baseline BVAR(12) model augmented with the specified inflation factor.

SOURCE: Authors' calculations using data from the Bureau of Economic Analysis, the Bureau of Labor Statistics, the Federal Reserve Board, the FRED, and the University of Michigan.

well. Notably, among the four factors, only the BVAR augmented with the common goods supply factor (the blue line in the upper-right panel) generates a decline in inflation that closely matches the actual evolution of total PCE inflation over the entire forecast horizon. Note that adding only one factor to the benchmark BVAR also implicitly provides the model with collective information about the remaining factors because the inflation factors are jointly estimated. All told, this exercise suggests that the different inflation factors can contribute to sharpening near- and medium-term inflation forecasts in distinct ways at different points in time.

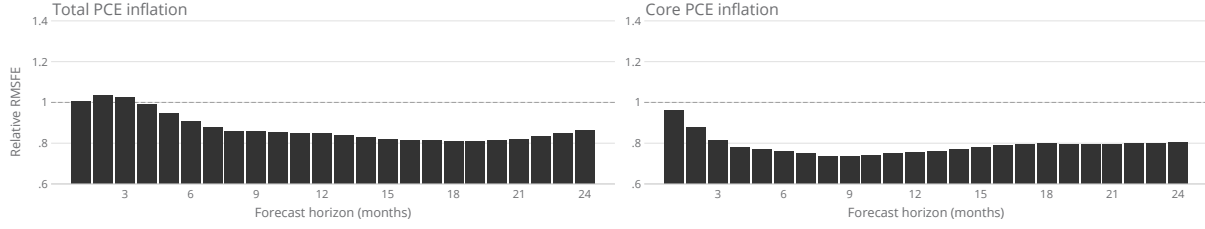
Lastly, we extend this forecast evaluation exercise beyond the pandemic era, focusing on the period from January 2010 to February 2020. In addition to forecasting 12-month total PCE inflation, we use the same forecasting framework to generate out-of-sample predictions of 12-month core PCE inflation, a key gauge of the underlying inflationary pressures.³² The pseudo real-time forecasts are computed recursively, with a maximum forecast horizon of 24 months ahead.³³

Figure 11 shows the relative root-mean-square forecast errors (RMSFEs) at horizons one month to 24 months ahead, where ratios smaller than one indicate that the model that contains information about inflation factors produces a lower RMSFE compared with the model that omits such information. As shown in Panel A, the inclusion of our inflation factors leads to notably more accurate

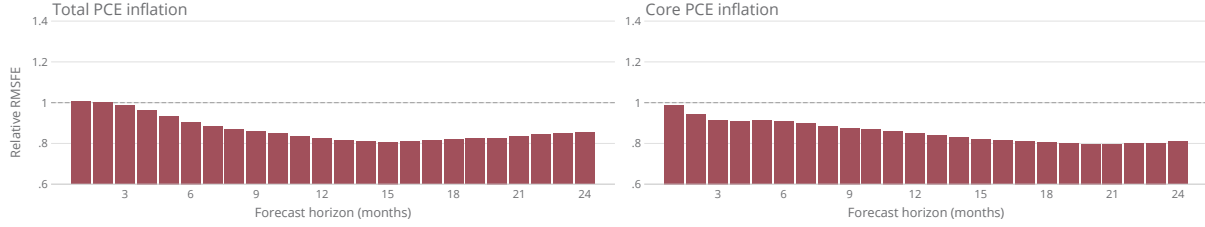
³²In this case, we replace the 12-month log-difference of total PCE prices in our BVAR specifications with the 12-month log-difference of core PCE prices, keeping the rest of the system the same.

³³As shown in Figures C-16 and C-17 in Appendix C, the pseudo real-time estimates of our inflation factors do not differ materially from the full-sample estimates shown in Figure 1.

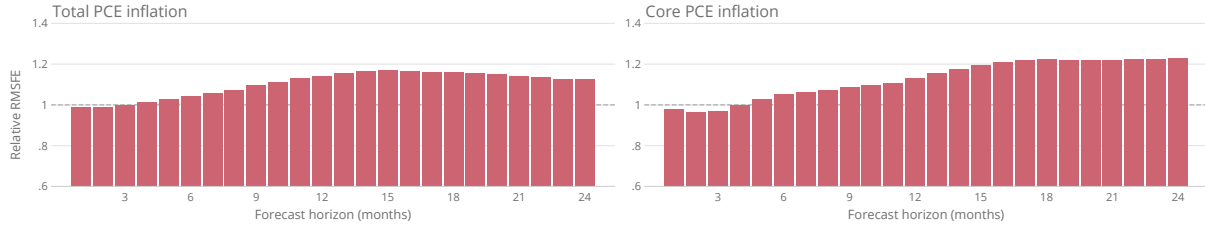
FIGURE 11: Out-of-sample Forecast Evaluation



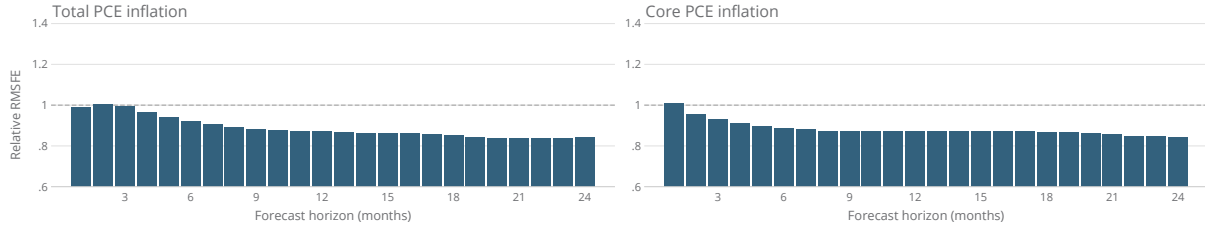
A. Baseline BVAR augmented with all four common factors



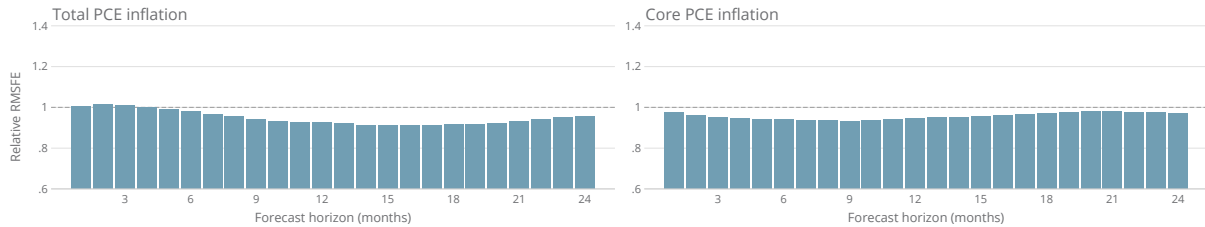
B. Baseline BVAR augmented with the common goods demand factor



C. Baseline BVAR augmented with the common services demand factor



D. Baseline BVAR augmented with the common goods supply factor



E. Baseline BVAR augmented with the common services supply factor

NOTE: Forecast evaluation period: January 2010 through February 2020. The figure's panels show the relative root-mean-square forecast errors (RMSFEs) for different BVAR specifications and forecast horizons. In the left panels, the forecast variable is the 12-month total PCE inflation, and in the right panels, the forecast variable is the 12-month core PCE inflation. The relative RMSFE at each horizon is calculated as the RMSFE from the BVAR model that includes the specified inflation factor(s) (see Figure 1) divided by the RMSFE from the model that excludes inflation factor(s).

medium-term forecasts of both total (the left panel) and core (the right panel) PCE inflation: Starting at about the six-month-ahead horizon, a BVAR augmented with our inflation factors generates out-of-sample forecasts for the 12-month total and core PCE inflation that are about 20 percent more accurate than the forecasts that do not include our factors.

The results from evaluating the predictive ability of each individual inflation factor indicate that the goods-related factors, when used independently (Panels B and D), generate the largest improvements in the accuracy of the predictions, followed by the common services supply factor (Panel E). By contrast, the common services demand factor (Panel C) does not yield forecast improvements when included in isolation in our BVAR forecasting model.

6 Conclusion

The unexpected surge in global inflation in 2021, driven by the COVID-19 pandemic, caught many economic observers off guard. The pandemic led to significant shifts in consumer behavior, with a marked initial increase in demand for goods over services followed by severe supply-side disruptions. These disruptions included labor shortages, global production chain interruptions, and heightened geopolitical tensions, all of which contributed to significant inflationary pressures that were compounded by the massive fiscal and monetary stimulus unleashed in response to the pandemic-induced economic shock.

In retrospect, the Federal Reserve’s initial characterization of that inflation episode as “transitory” proved too optimistic. At the same time, the unprecedented nature of the pandemic-induced economic shock made accurate forecasting exceptionally difficult in the United States and elsewhere. More generally, the recent inflation episode underscores the need for more accurate inflation forecasts, not only because better forecasts enable central banks to calibrate the magnitude and timing of interest rate changes or asset purchases more effectively, but also because they help monetary authorities maintain their credibility, which is vital for managing inflation expectations and maintaining public trust.

To help address the shortcomings of existing inflation forecasting frameworks, this paper introduces a sign-restricted dynamic factor model designed to decompose real-time inflation into its underlying common supply and common demand components—as well as their idiosyncratic counterparts—by leveraging the co-movement of prices and quantities across various PCE categories. Importantly, our SiR-DFM distinguishes between supply and demand drivers within the goods and services sectors and incorporates features such as time-varying volatility, outliers, and long-term inflation expectations. The model’s ability to decompose total PCE inflation into six components—common demand for goods, common demand for services, common supply of goods, common supply of services, inflation expectations, and idiosyncratic or category-specific demand and supply contributions—significantly enhances our understanding of pandemic-era inflation dynamics.

Validation exercises demonstrate the effectiveness of the SiR-DFM in accurately identifying key inflation drivers. Including our estimated supply and demand inflation factors in a standard inflation

forecasting framework leads to a notable improvement in the accuracy of medium-term inflation forecasts. All told, this improved understanding of inflation dynamics can inform monetary policy decisions in real time, helping to ensure macroeconomic stability in the face of complex and evolving economic conditions.

References

- AMANOR-BOADU, V. (2022): “Empirical Evidence for the “Great Resignation”,” *Monthly Labor Review*, November. U.S. Bureau of Labor Statistics. Available at <https://doi.org/10.21916/mlr.2022.29>.
- AMITI, M., S. HEISE, F. KARAHAN, AND A. ŞAHİN (2023): “Inflation Strikes Back: The Role of Import Competition and the Labor Market,” in *NBER Macroeconomics Annual*, ed. by M. Eichenbaum, E. Hurst, and V. A. Ramey, Chicago: University of Chicago Press, vol. 38, 71–131.
- ANTOLÍN-DÍAZ, J. AND J. RUBIO-RAMÍREZ (2018): “Narrative Sign Restrictions for SVARs,” *American Economic Review*, 108, 2802–2829.
- ARIAS, J., J. RUBIO-RAMÍREZ, AND D. WAGGONER (2018): “Inference Based on Structural Vector Autoregressions Identified with Sign and Zero Restrictions: Theory and Applications,” *Econometrica*, 86, 685–720.
- BAI, J. AND P. WANG (2015): “Identification and Bayesian Estimation of Dynamic Factor Models,” *Journal of Business and Economic Statistics*, 33, 221–240.
- BALL, L. M. AND S. MAZUMDER (2011): “Inflation Dynamics and the Great Recession,” *Brookings Papers on Economic Activity*, 42, 337–405.
- BAÑBURA, M., D. LEIVA-LEÓN, AND J.-O. MENZ (2025): “Do Inflation Expectations Improve Model-based Inflation Forecasts?” Forthcoming in the *Journal of Money, Credit and Banking*.
- BARTH, M. J. AND V. A. RAMEY (2001): “The Cost Channel of Monetary Transmission,” in *NBER Macroeconomics Annual*, ed. by B. S. Bernanke and K. Rogoff, Cambridge: The MIT Press, vol. 16, 199–249.
- BERNANKE, B. S. (2007): “Inflation Expectations and Inflation Forecasting,” <https://www.federalreserve.gov/newsevents/speech/bernanke20070710a.htm>, Speech at the Monetary Economics Workshop of the National Bureau of Economic Research Summer Institute, Cambridge, MA, July 10, 2007.
- (2024): “Forecasting for Monetary Policy Making and Communication at the Bank of England: A Review,” Report by the Independent Evaluation Office of the Bank of England, April 12, 2024.
- BERNANKE, B. S. AND O. J. BLANCHARD (2023): “What Caused the U.S. Pandemic-era Inflation?” Forthcoming in the *American Economic Journal: Macroeconomics*.
- BLANCHARD, O. J. AND D. QUAH (1989): “The Dynamic Effects of Aggregate Demand and Supply Disturbances,” *American Economic Review*, 79, 655–673.

- BORIO, C., P. DISYATAT, D. XIA, AND E. ZAKRAJŠEK (2021): “Monetary Policy, Relative Prices and Inflation Control: Flexibility Born Out of Success,” *BIS Quarterly Review*, September, 15–29.
- BORIO, C., M. J. LOMBARDI, J. YETMAN, AND E. ZAKRAJŠEK (2023): “The Two-regime View of Inflation,” BIS Papers No. 133. Available at <https://www.bis.org/publ/bppdf/bispap133.pdf>.
- BRAYTON, F. AND P. A. TINSLEY (1996): “A Guide to FRB/US: A Macroeconomic Model of the United States,” Finance and Economics Discussion Series Paper No. 96-42, Board of Governors of the Federal Reserve System (U.S.).
- CANOVA, F. (2007): *Methods for Applied Macroeconomic Research*, Princeton: Princeton University Press.
- CARTER, C. K. AND R. KOHN (1995): “On Gibbs Sampling for State Space Models,” *Biometrika*, 81, 541–553.
- CHAHAD, M., A.-C. HOFMANN-DRAHONSKY, B. MEUNIER, A. PAGE, AND M. TIRPÁK (2022): “What Explains Recent Errors in the Inflation Projections of Eurosystem and ECB Staff?” Published as part of the ECB Economic Bulletin, Issue 3/2022.
- (2023): “An Updated Assessment of Short-term Inflation Projections by Eurosystem and ECB Staff,” Published as part of the ECB Economic Bulletin, Issue 1/2023.
- CHAN, J. C. (2020): “Large Bayesian Vector Autoregressions,” in *Macroeconomic Forecasting in the Era of Big Data*, ed. by P. Fuleky, Springer International Publishing, chap. 4, 95–125.
- CHAN, J. C., T. E. CLARK, AND G. KOOP (2018): “A New Model of Inflation, Trend Inflation, and Long-run Inflation Expectations,” *Journal of Money, Credit, and Banking*, 50, 5–54.
- CLARIDA, R. H., B. DUYGAN-BUMP, AND C. SCOTTI (2021): “The COVID-19 Crisis and the Federal Reserve’s Policy Response,” in *Monetary Policy and Central Banking in the Covid Era*, ed. by B. English, K. Forbes, and A. Ubide, London: Centre for Economic Policy Research Press, 147–169.
- COIBION, O. AND Y. GORODNICHENKO (2015): “Is The Phillips Curve Alive and Well After All? Inflation Expectations and the Missing Disinflation,” *American Economic Journal: Macroeconomics*, 7, 197–232.
- CORE, F., F. DE MARCO, T. EISERT, AND G. SCHEPENS (2025): “Inflation and Floating-Rate Loans: Evidence from the Euro-Area,” ECB Working Paper No. 2025/3064. Available at <http://dx.doi.org/10.2139/ssrn.5332352>.
- DI GIOVANNI, J., Ş. KALEMLI-ÖZCAN, A. SILVA, AND M. A. YILDRIM (2023): “Pandemic-era Inflation Drivers and Global Spillovers,” NBER Working Paper No. 31887 (Revised February 2025).
- EICKMEIER, S. AND B. HOFMANN (2025): “What Drives Inflation? Disentangling Demand and Supply Factors,” Forthcoming in the *International Journal of Central Banking*.
- FERRANTE, F., S. GRAVES, AND M. IACOVIELLO (2023): “The Inflationary Effects of Sectoral Reallocation,” *Journal of Monetary Economics*, 140, S64–S81.
- FRY, R. A. AND A. R. PAGAN (2011): “Sign Restrictions in Structural Vector Autoregressions: A Critical Review,” *Journal of Economic Literature*, 49, 938–960.

- GIANNONE, D. AND G. PRIMICERI (2024): “The Drivers of Post-pandemic Inflation,” NBER Working Paper No. 32859.
- GILCHRIST, S., R. SCHOENLE, J. SIM, AND E. ZAKRAJŠEK (2017): “Inflation Dynamics during the Financial Crisis,” *American Economic Review*, 107, 785–823.
- GILCHRIST, S. AND E. ZAKRAJŠEK (2012): “Credit Spreads and Business Cycle Fluctuations,” *American Economic Review*, 102, 1692–1720.
- GUERRIERI, V., G. LORENZONI, L. STRAUB, AND I. WERNING (2022): “Macroeconomic Implications of COVID-19: Can Negative Supply Shocks Cause Demand Shortages?” *American Economic Review*, 112, 1437–1474.
- GÜRKAYNAK, R. S., B. SACK, AND E. T. SWANSON (2005): “Do Actions Speak Louder than Words? The Response of Asset Prices to Monetary Policy Actions and Statements,” *International Journal of Central Banking*, 1, 55–93.
- HAJDINI, I. (2023): “Mis-specified Forecasts and Myopia in an Estimated New Keynesian Model,” Federal Reserve Bank of Cleveland Working Paper No. 23-03R. Available at <http://dx.doi.org/10.2139/ssrn.4036817>.
- HERNÁNDEZ DE COS, P., K. FORBES, AND T. TOMBE (2024): “External Comments on the Review of the Bank of Canada’s Exceptional Policy Actions during the Pandemic,” Available at <https://www.bankofcanada.ca/wp-content/uploads/2025/01/external-panel-report.pdf>.
- HODRICK, R. J. AND E. C. PRESCOTT (1997): “Postwar U.S. Business Cycles: An Empirical Investigation,” *Journal of Money, Credit, and Banking*, 29, 1–16.
- IRELAND, P. N. (2007): “Changes in the Federal Reserve’s Inflation Target: Causes and Consequences,” *Journal of Money, Credit, and Banking*, 39, 1851–1882.
- JAROCIŃSKI, M. AND P. KARADI (2020): “Deconstructing Monetary Policy Surprises – The Role of Information Shocks,” *American Economic Journal: Macroeconomics*, 12, 1–43.
- JORDÀ, Ò. (2005): “Estimation and Inference of Impulse Responses by Local Projections,” *American Economic Review*, 95, 161–182.
- KÄNZIG, D. R. (2021): “The Macroeconomic Effects of Oil Supply News: Evidence from OPEC Announcements,” *American Economic Review*, 111, 1092–1125.
- KIM, C.-J. AND C. R. NELSON (1999): *State-Space Models with Regime Switching: Classical and Gibbs-Sampling Approaches with Applications*, Cambridge: The MIT Press.
- KIM, S., N. SHEPHARD, AND S. CHIB (1998): “Stochastic Volatility: Likelihood and Comparison with ARCH Models,” *Review of Economic Studies*, 65, 361–393.
- KUTTNER, K. N. (2001): “Monetary Policy Surprises and Interest Rates: Evidence from the Fed Funds Futures Market,” *Journal of Monetary Economics*, 47, 523–544.
- LUO, S. AND D. VILLAR (2023): “Propagation of Shocks in an Input–Output Economy: Evidence from Disaggregated Prices,” *Journal of Monetary Economics*, 137, 26–46.

- MATTHES, C. AND F. SCHWARTZMAN (2025): “The Consumption Origins of Business Cycles: Lessons from Sectoral Dynamics,” Forthcoming in the *American Economic Journal: Macroeconomics*.
- MIRANDA-AGRIPPINO, S. AND G. RICCO (2021): “The Transmission of Monetary Policy Shocks,” *American Economic Journal: Macroeconomics*, 13, 74–107.
- MONTES, J., C. SMITH, AND J. DAJON (2022): “The Great Retirement Boom: The Pandemic-era Surge in Retirements and Implications for Future Labor Force Participation,” Finance and Economics Discussion Series 2022-081, Board of Governors of the Federal Reserve System (U.S.). Available at <https://doi.org/10.17016/FEDS.2022.081>.
- NUNES, R., A. K. OZDAGLI, AND J. TANG (2022): “Interest Rate Surprises: A Tale of Two Shocks,” Federal Reserve Bank of Boston Working Paper No. 22-2. Available at <https://www.bostonfed.org/publications/research-department-working-paper/2022/interest-rate-surprises-a-tale-of-two-shocks.aspx>.
- RUGE-MURCIA, F. AND A. L. WOLMAN (2022): “Relative Price Shocks and Inflation,” Federal Reserve Bank of Richmond Working Paper No. 22-07R (revised March 2024). Available at <https://doi.org/10.21144/wp22-07>.
- SHAPIRO, A. H. (2024): “Decomposing Supply- and Demand-Driven Inflation,” Forthcoming in the *Journal of Money, Credit and Banking*.
- SHEREMIROV, V. (2022): “Are the Demand and Supply Channels of Inflation Persistent? Evidence from a Novel Decomposition of PCE Inflation,” Federal Reserve Bank of Boston *Current Policy Perspectives* No. 94983.
- STOCK, J. H. AND M. W. WATSON (2016): “Core Inflation and Trend Inflation,” *Review of Economics and Statistics*, 98, 770–784.
- (2020): “Slack and Cyclically Sensitive Inflation,” *Journal of Money, Credit, and Banking*, 52, 393–428.
- WOLMAN, A. L. AND F. DING (2005): “Inflation and Changing Expenditure Shares,” *Federal Reserve Bank of Richmond Economic Review*, 91, 1–20.
- YOUNG, M., J. SOZA-PARRA, AND G. CIRCELLA (2022): “The Increase in Online Shopping during COVID-19: Who is Responsible, Will It Last, and What Does It Mean for Cities?” *Regional Science Policy & Practice*, 14, 162–179.

Supplementary Material

— For Online Publication Only —

This section contains three Appendixes (A, B, and C). Appendix A describes the algorithm used to estimate our SiR-DFM; Appendix B details some key facts about the data used in the analysis; and Appendix C presents the supplementary results referenced in the main text.

A Estimation Algorithm

As noted in the main text, our estimation algorithm relies on Bayesian methods and uses the Gibbs sampler to simulate the posterior distribution of both parameters and latent variables that characterize the model. The sequence of steps in our estimation algorithm is described as follows.

Let the log-differences (from month $t - 1$ to month t) of quantities and prices associated with the goods-related categories in the PCE report be collected in a (column) vector

$$\mathbf{Y}_t^{(g)} = [\Delta q_{1,t} \dots \Delta q_{N_g,t} \Delta p_{1,t} \dots \Delta p_{N_g,t}]'.$$

The analogous information about quantities and prices associated with the services-related categories is gathered in a (column) vector

$$\mathbf{Y}_t^{(v)} = [\Delta q_{1,t} \dots \Delta q_{N_v,t} \Delta p_{1,t} \dots \Delta p_{N_v,t}]'.$$

Then, all the observed model variables can be expressed in a single (column) vector³⁴

$$\mathbf{Y}_t = [\mathbf{Y}_t^{(g)'} \mathbf{Y}_t^{(v)'}]'$$

The goods- and services-related latent common factors are collected in (column) vectors

$$\mathbf{F}_t^{(g)} = [s_t^{(g)} d_t^{(g)}]' \quad \text{and} \quad \mathbf{F}_t^{(v)} = [s_t^{(v)} d_t^{(v)}]',$$

respectively, and stacked in the vector

$$\mathbf{F}_t = [\mathbf{F}_t^{(g)'} \mathbf{F}_t^{(v)'}]'$$

The log-volatility processes of the innovations associated with the goods-related idiosyncratic terms are collected in a (column) vector

$$\mathbf{h}_t^{(g)} = [h_{\zeta_1^{(g)},t} \dots h_{\zeta_{N_g}^{(g)},t} h_{\omega_1^{(g)},t} \dots h_{\omega_{N_g}^{(g)},t}]',$$

whereas those pertaining to the services-related idiosyncratic terms are collected in a (column) vector

$$\mathbf{h}_t^{(v)} = [h_{\zeta_1^{(v)},t} \dots h_{\zeta_{N_v}^{(v)},t} h_{\omega_1^{(v)},t} \dots h_{\omega_{N_v}^{(v)},t}]'.$$

As earlier, we stack all the log-volatility process in a (column) vector

$$\mathbf{h}_t = [\mathbf{h}_t^{(g)'} \mathbf{h}_t^{(v)'}]'$$

³⁴All monthly log-differences in the vector \mathbf{Y}_t are scaled by their respective in-sample standard deviations.

Given a sample period $t = 0, 1, \dots, T$, let the vectors of observed variables, latent factors, and log-volatility terms be defined as

$$\begin{aligned}\tilde{\mathbf{Y}}_T &= [\mathbf{Y}'_1 \mathbf{Y}'_2 \dots \mathbf{Y}'_T]'; \\ \tilde{\mathbf{F}}_T &= [\mathbf{F}'_1 \mathbf{F}'_2 \dots \mathbf{F}'_T]'; \\ \tilde{\mathbf{h}}_T &= [\mathbf{h}'_1 \mathbf{h}'_2 \dots \mathbf{h}'_T]'. \end{aligned}$$

Furthermore, we define the vectors of autoregressive coefficients, factor loadings, and parameters governing the dynamics of idiosyncratic processes as

$$\begin{aligned}\Phi &= [\Phi'_{s,0} \text{vec}(\Phi_{s,1})' \text{vec}(\Phi_{s,2})' \Phi'_{d,0} \text{vec}(\Phi_{d,1})' \text{vec}(\Phi_{d,2})']'; \\ \lambda &= [\lambda_1^s \dots \lambda_{N_g}^s \lambda_1^d \dots \lambda_{N_g}^d \theta_1^s \dots \theta_{N_g}^s \theta_1^d \dots \theta_{N_g}^d \gamma_1^s \dots \gamma_{N_v}^s \gamma_1^d \dots \gamma_{N_v}^d \delta_1^s \dots \delta_{N_v}^s \delta_1^d \dots \delta_{N_v}^d]'; \\ \rho &= [\rho_1^s \dots \rho_{N_g}^s \psi_1^s \dots \psi_{N_g}^s \rho_1^v \dots \rho_{N_v}^v \psi_1^v \dots \psi_{N_v}^v]'; \\ \sigma &= [\sigma_{\zeta_1^{(g)}}^2 \dots \sigma_{\zeta_{N_g}^{(g)}}^2 \sigma_{\omega_1^{(g)}}^2 \dots \sigma_{\omega_{N_g}^{(g)}}^2 \sigma_{\zeta_1^{(v)}}^2 \dots \sigma_{\zeta_{N_v}^{(v)}}^2 \sigma_{\omega_1^{(v)}}^2 \dots \sigma_{\omega_{N_v}^{(v)}}^2]'; \\ \chi &= [\chi_{\zeta_1^{(g)}} \dots \chi_{\zeta_{N_g}^{(g)}} \chi_{\omega_1^{(g)}} \dots \chi_{\omega_{N_g}^{(g)}} \chi_{\zeta_1^{(v)}} \dots \chi_{\zeta_{N_v}^{(v)}} \chi_{\omega_1^{(v)}} \dots \chi_{\omega_{N_v}^{(v)}}]'. \end{aligned}$$

Within each iteration of the Gibbs sampler, our estimation algorithm consists of the following steps:

Step 1: Sample $\tilde{\mathbf{F}}_T$ from $\Pr(\tilde{\mathbf{F}}_T | \Phi, \lambda, \rho, \sigma, \chi, \tilde{\mathbf{h}}_T, \tilde{\mathbf{Y}}_T)$. To address the large number of latent idiosyncratic terms involved in the factor model, we employ an alternative representation of each price and quantity equation. Specifically, we multiply each price and quantity equation by the corresponding lag operator function as defined in equations (21) through (24) in the main text, which yields:

$$\Delta q_{j,t}^* = \lambda_j^s \rho_j^g s_t^{(g)}(L) + \lambda_j^d \rho_j^g d_t^{(g)}(L) + \zeta_{j,t}^{(g)}, \quad j = 1, 2, \dots, N_g; \quad (\text{A-1})$$

$$\Delta p_{j,t}^* = \theta_j^s \psi_j^g s_t^{(g)}(L) + \theta_j^d \psi_j^g d_t^{(g)}(L) + \omega_{j,t}^{(g)}, \quad j = 1, 2, \dots, N_g; \quad (\text{A-2})$$

$$\Delta q_{k,t}^* = \gamma_k^s \rho_k^v s_t^{(v)}(L) + \gamma_k^d \rho_k^v d_t^{(v)}(L) + \zeta_{k,t}^{(v)}, \quad k = 1, 2, \dots, N_v; \quad (\text{A-3})$$

$$\Delta p_{k,t}^* = \delta_k^s \psi_k^v s_t^{(v)}(L) + \delta_k^d \psi_k^v d_t^{(v)}(L) + \omega_{k,t}^{(v)}, \quad k = 1, 2, \dots, N_v, \quad (\text{A-4})$$

where

$$\begin{aligned}\Delta q_{j,t}^* &= \rho_j^g \Delta q_{j,t}(L), \quad j = 1, 2, \dots, N_g; \\ \Delta p_{j,t}^* &= \psi_j^g \Delta p_{j,t}(L), \quad j = 1, 2, \dots, N_g; \\ \Delta q_{k,t}^* &= \rho_k^v \Delta q_{k,t}(L), \quad k = 1, 2, \dots, N_v; \\ \Delta p_{k,t}^* &= \psi_k^v \Delta p_{k,t}(L), \quad k = 1, 2, \dots, N_v. \end{aligned}$$

Defining

$$\mathbf{Y}_t^{(g*)} = [\Delta q_{1,t}^* \dots \Delta q_{N_g,t}^* \Delta p_{1,t}^* \dots \Delta p_{N_g,t}^*]'$$

and

$$\mathbf{Y}_t^{(v*)} = [\Delta q_{1,t}^* \dots \Delta q_{N_v,t}^* \Delta p_{1,t}^* \dots \Delta p_{N_v,t}^*]'$$

for the goods- and services-related categories, respectively, and setting the lag order $n = 2$, the model defined by equations (11) through (14) in the main text can be cast in a state-space representation,

where the system of measurement equations is given by

$$\begin{bmatrix} \mathbf{Y}_t^{(g*)} \\ \mathbf{Y}_t^{(v*)} \end{bmatrix} = \begin{bmatrix} \mathbf{\Lambda} & [0] & \mathbf{\Lambda} & [0] & \mathbf{\Lambda} & [0] \\ [0] & \mathbf{\Gamma} & [0] & \mathbf{\Gamma} & [0] & \mathbf{\Gamma} \end{bmatrix} \begin{bmatrix} \mathbf{F}_t^{(g)} \\ \mathbf{F}_t^{(v)} \\ \mathbf{F}_{t-1}^{(g)} \\ \mathbf{F}_{t-1}^{(v)} \\ \mathbf{F}_{t-2}^{(g)} \\ \mathbf{F}_{t-2}^{(v)} \end{bmatrix} + \begin{bmatrix} \mathbf{U}_t^{(g)} \\ \mathbf{U}_t^{(v)} \end{bmatrix},$$

and where $[0]$ denotes a zero matrix of size that makes the state-space representation conformable. In this representation, the innovations of the idiosyncratic terms are collected in vectors

$$\mathbf{U}_t^{(g)} = [\zeta_{1,t}^{(g)} \dots \zeta_{N_g,t}^{(g)} \omega_{1,t}^{(g)} \dots \omega_{N_g,t}^{(g)}]' \quad \text{and} \quad \mathbf{U}_t^{(v)} = [\zeta_{1,t}^{(v)} \dots \zeta_{N_v,t}^{(v)} \omega_{1,t}^{(v)} \dots \omega_{N_v,t}^{(v)}]';$$

and the sub-matrices of factor loadings are given by

$$\mathbf{\Lambda} = \begin{bmatrix} \lambda_1^s \rho_1^g & \lambda_1^d \rho_1^g \\ \lambda_2^s \rho_2^g & \lambda_2^d \rho_2^g \\ \vdots & \vdots \\ \lambda_{N_g}^s \rho_{N_g}^g & \lambda_{N_g}^d \rho_{N_g}^g \\ \theta_1^s \psi_1^g & \theta_1^d \psi_1^g \\ \theta_2^s \psi_2^g & \theta_2^d \psi_2^g \\ \vdots & \vdots \\ \theta_{N_g}^s \psi_{N_g}^g & \theta_{N_g}^d \psi_{N_g}^g \end{bmatrix} \quad \text{and} \quad \mathbf{\Gamma} = \begin{bmatrix} \gamma_1^s \rho_1^v & \gamma_1^d \rho_1^v \\ \gamma_2^s \rho_2^v & \gamma_2^d \rho_2^v \\ \vdots & \vdots \\ \gamma_{N_v}^s \rho_{N_v}^v & \gamma_{N_v}^d \rho_{N_v}^v \\ \delta_1^s \psi_1^v & \delta_1^d \psi_1^v \\ \delta_2^s \psi_2^v & \delta_2^d \psi_2^v \\ \vdots & \vdots \\ \delta_{N_v}^s \psi_{N_v}^v & \delta_{N_v}^d \psi_{N_v}^v \end{bmatrix}.$$

The state vector summarizes information about common factors. In particular, the system of transition equations of the state-space representation is given by

$$\begin{bmatrix} \mathbf{F}_t^{(g)} \\ \mathbf{F}_t^{(v)} \\ \mathbf{F}_{t-1}^{(g)} \\ \mathbf{F}_{t-1}^{(v)} \\ \mathbf{F}_{t-2}^{(g)} \\ \mathbf{F}_{t-2}^{(v)} \end{bmatrix} = \begin{bmatrix} \boldsymbol{\mu}_t^{(g)} \\ \boldsymbol{\mu}_t^{(v)} \\ \mathbf{0} \\ \mathbf{0} \\ \mathbf{0} \\ \mathbf{0} \end{bmatrix} + \begin{bmatrix} \boldsymbol{\Psi}_1^{(g,g)} & \boldsymbol{\Psi}_1^{(g,v)} & \boldsymbol{\Psi}_2^{(g,g)} & \boldsymbol{\Psi}_2^{(g,v)} & [0] & [0] \\ \boldsymbol{\Psi}_1^{(v,g)} & \boldsymbol{\Psi}_1^{(v,v)} & \boldsymbol{\Psi}_2^{(v,g)} & \boldsymbol{\Psi}_2^{(v,v)} & [0] & [0] \\ \mathbf{I} & [0] & [0] & [0] & [0] & [0] \\ [0] & \mathbf{I} & [0] & [0] & [0] & [0] \\ [0] & [0] & \mathbf{I} & [0] & [0] & [0] \\ [0] & [0] & [0] & \mathbf{I} & [0] & [0] \end{bmatrix} \begin{bmatrix} \mathbf{F}_{t-1}^{(g)} \\ \mathbf{F}_{t-1}^{(v)} \\ \mathbf{F}_{t-2}^{(g)} \\ \mathbf{F}_{t-2}^{(v)} \\ \mathbf{F}_{t-3}^{(g)} \\ \mathbf{F}_{t-3}^{(v)} \end{bmatrix} + \begin{bmatrix} \mathbf{e}_t^{(g)} \\ \mathbf{e}_t^{(v)} \\ \mathbf{0} \\ \mathbf{0} \\ \mathbf{0} \\ \mathbf{0} \end{bmatrix},$$

where

$$\mathbf{e}_t^{(g)} = [\epsilon_t^{(g)} \nu_t^{(g)}]' \quad \text{and} \quad \mathbf{e}_t^{(v)} = [\epsilon_t^{(v)} \nu_t^{(v)}]'$$

The parameters of the system are given by the intercept vectors

$$\boldsymbol{\mu}_t^{(g)} = \begin{bmatrix} \boldsymbol{\Phi}_{s,0}^{[1,1]} + \beta_s^{(g)} \pi_{t-1}^E \\ \boldsymbol{\Phi}_{d,0}^{[1,1]} + \beta_d^{(g)} \pi_{t-1}^E \end{bmatrix} \quad \text{and} \quad \boldsymbol{\mu}_t^{(v)} = \begin{bmatrix} \boldsymbol{\Phi}_{s,0}^{[2,1]} + \beta_s^{(v)} \pi_{t-1}^E \\ \boldsymbol{\Phi}_{d,0}^{[2,1]} + \beta_d^{(v)} \pi_{t-1}^E \end{bmatrix};$$

and the coefficient matrices

$$\boldsymbol{\Psi}_\iota^{(g,g)} = \begin{bmatrix} \boldsymbol{\Phi}_{s,\iota}^{[1,1]} & 0 \\ 0 & \boldsymbol{\Phi}_{d,\iota}^{[1,1]} \end{bmatrix}; \quad \boldsymbol{\Psi}_\iota^{(g,v)} = \begin{bmatrix} \boldsymbol{\Phi}_{s,\iota}^{[1,2]} & 0 \\ 0 & \boldsymbol{\Phi}_{d,\iota}^{[1,2]} \end{bmatrix}, \quad \text{for } \iota = 1, 2;$$

$$\boldsymbol{\Psi}_\iota^{(v,g)} = \begin{bmatrix} \boldsymbol{\Phi}_{s,\iota}^{[2,1]} & 0 \\ 0 & \boldsymbol{\Phi}_{d,\iota}^{[2,1]} \end{bmatrix}; \quad \boldsymbol{\Psi}_\iota^{(v,v)} = \begin{bmatrix} \boldsymbol{\Phi}_{s,\iota}^{[2,2]} & 0 \\ 0 & \boldsymbol{\Phi}_{d,\iota}^{[2,2]} \end{bmatrix}, \quad \text{for } \iota = 1, 2,$$

where $\boldsymbol{\Phi}_{s,\iota}^{[a,b]}$ corresponds to the a -th row and the b -th column of the specified matrix. We rely on the algorithm of [Carter and Kohn \(1995\)](#) to generate inference about the state vector.

Step 2: Sample Φ from $\Pr(\Phi | \tilde{\mathbf{F}}_T, \tilde{\mathbf{Y}}_T)$. The prior for the parameters of the VAR-X(m) process governing the evolution of the vector of latent supply factors $[s_t^{(g)} s_t^{(v)}]'$ and the VAR-X(m) process governing the evolution of the vector of latent demand factors $[d_t^{(g)} d_t^{(v)}]'$ is $\mathcal{N}(\mathbf{0}, \Xi)$, where the elements of the covariance matrix Ξ are set following the type of shrinkage used in the Minnesota prior. Specifically, the elements of Ξ are determined by the hyper-parameters $\kappa_1, \kappa_2, \kappa_3, \kappa_4$, and κ_5 , according to

$$\left(\frac{\kappa_1}{m\kappa_3}\right)^2 \text{ if } i_\Phi = j_\Phi \quad \text{and} \quad \left(\frac{\kappa_1\kappa_2}{m\kappa_3}\right)^2 \text{ if } i_\Phi \neq j_\Phi,$$

where i_Φ refers to the dependent variable in the VAR-X equation and j_Φ refers to the explanatory variable in the same equation. For the intercept terms and for the parameters associated with inflation expectations (that is, the exogenous variable), the elements of Ξ are given by

$$(\kappa_4)^2 \quad \text{and} \quad (\kappa_5)^2,$$

respectively. The prior hyper-parameters are set to $\kappa_1 = 0.1, \kappa_2 = 0.1, \kappa_3 = 0.1, \kappa_4 = 0.1$, and $\kappa_5 = 0.05$. As noted in the main text, we set the order of the VAR-X process $m = 2$ in all cases. Given our conjugate prior, we follow [Canova \(2007\)](#) and generate draws of the VAR-X parameters based on the corresponding multivariate normal posterior density.

Step 3: Sample λ from $\Pr(\lambda | \rho, \sigma, \chi, \tilde{\mathbf{h}}_T, \tilde{\mathbf{F}}_T, \tilde{\mathbf{Y}}_T)$. Draws of the factor loadings are generated independently for each $j = 1, 2, \dots, N_g$ and $k = 1, 2, \dots, N_v$, based on the regression specifications (A-1) through (A-4). In doing so, we use a normal prior distribution $\mathcal{N}(\underline{\lambda}, \underline{\Sigma}_\lambda)$, where the hyper-parameters are defined according to the sign restrictions used to identify the latent supply and demand factors, as defined in equations (15) through (18) in the main text. In particular, the vector of prior means is given by

$$\underline{\lambda} = \begin{cases} [1 \ 1]' & \text{for } [\lambda_j^s \ \lambda_j^d]', \quad j = 1, 2, \dots, N_g; \\ [-1 \ 1]' & \text{for } [\theta_j^s \ \theta_j^d]', \quad j = 1, 2, \dots, N_g; \\ [1 \ 1]' & \text{for } [\gamma_k^s \ \gamma_k^d]', \quad k = 1, 2, \dots, N_v; \\ [-1 \ 1]' & \text{for } [\delta_k^s \ \delta_k^d]', \quad k = 1, 2, \dots, N_v, \end{cases}$$

where the sign restrictions are verified at every iteration—that is, if a draw complies with the corresponding restrictions, it is retained; otherwise, it is discarded, and a new draw is made. To ensure a reasonable acceptance rate, the prior covariance matrix is set to $\underline{\Sigma}_\lambda = \mathbf{I} \times 0.005$. Draws of the factor loadings are then generated based on the corresponding posterior density.

Step 4: Sample ρ from $\Pr(\rho | \lambda, \sigma, \chi, \tilde{\mathbf{h}}_T, \tilde{\mathbf{F}}_T, \tilde{\mathbf{Y}}_T)$. Conditional on the common factors and factor loadings, the idiosyncratic terms can be recovered from equations (11) through (14) in the main text. Draws of the autoregressive coefficients associated with the idiosyncratic terms are generated independently for each $j = 1, 2, \dots, N_g$ and $k = 1, 2, \dots, N_v$. We use a normal prior distribution $\mathcal{N}(\underline{\rho}, \underline{\Sigma}_\rho)$, with $\underline{\rho} = [0 \ 0]'$ and $\underline{\Sigma}_\rho = \mathbf{I}$, and generate draws from the corresponding posterior distribution. For each idiosyncratic term, we only retain draws of the autoregressive coefficients that satisfy the stationarity condition.

Step 5: Sample σ from $\Pr(\sigma | \tilde{\mathbf{h}}_T, \tilde{\mathbf{Y}}_T)$. To sample the variance of innovations driving the log-volatility processes of the idiosyncratic terms, we use an inverse-Gamma prior distribution, denoted by $InvGamma(\underline{\eta}, \underline{v})$, with $\underline{\eta} = 3$ and $\underline{v} = 2$. We generate draws from the posterior distribution

$$\sigma_i^2 \sim InvGamma(\bar{\eta}, \bar{v}), \quad i \in \{\zeta_j^{(g)}, \omega_j^{(g)}, \zeta_k^{(v)}, \omega_k^{(k)}\},$$

where

$$\bar{\eta} = \underline{\eta} + T \quad \text{and} \quad \bar{v} = \underline{v} + \sum_{t=2}^T (h_{i,t} - h_{i,t-1})^2.$$

This procedure is applied independently for each $i \in \{\zeta_j^{(g)}, \omega_j^{(g)}, \zeta_k^{(v)}, \omega_k^{(k)}\}$ and for each $j = 1, 2, \dots, N_g$ and $k = 1, 2, \dots, N_v$.

Step 6: Sample χ from $\Pr(\chi | \lambda, \rho, \tilde{\mathbf{h}}_T, \tilde{\mathbf{F}}_T, \tilde{\mathbf{Y}}_T)$. Conditional on the common factors, factor loadings, autoregressive coefficients, and log-volatilities of idiosyncratic terms, the innovations of the idiosyncratic terms can be recovered from equations (21) through (24) in the main text. These innovations are then used to generate the outliers, denoted by $o_{i,t}$, according to equation (27) in the main text. Conditional on the outliers, draws of the probability of occurrence of an outlier, denoted by χ_i , are generated independently for all $i \in \{\zeta_j^{(g)}, \omega_j^{(g)}, \zeta_k^{(v)}, \omega_k^{(k)}\}$ and for $j = 1, \dots, N_g$ and $k = 1, \dots, N_v$. Following [Stock and Watson \(2016\)](#), we use a Beta distribution as conjugate prior with hyper-parameters $\underline{\chi}_a = 2.5$ and $\underline{\chi}_b = 117.5$. Therefore, draws of the probabilities of outlier occurrence are generated from the posterior density

$$\chi_i \sim \text{Beta}(\underline{\chi}_a + \tau, \underline{\chi}_b + T - \tau), \quad i \in \{\zeta_j^{(g)}, \omega_j^{(g)}, \zeta_k^{(v)}, \omega_k^{(k)}\},$$

where $\tau = \sum_{t=1}^T \mathbb{I}(o_{i,t} > 1)$, and $\mathbb{I}(\cdot)$ denotes a 0/1-indicator function that equals one if its argument is true and zero otherwise.

Step 7: Sample $\tilde{\mathbf{h}}_T$ from $\Pr(\tilde{\mathbf{h}}_T | \lambda, \rho, \sigma, \chi, \tilde{\mathbf{F}}_T, \tilde{\mathbf{Y}}_T)$. To generate draws of the log-volatility process associated with the idiosyncratic innovations, we use the so-called auxiliary mixture sampler independently for all $i \in \{\zeta_j^{(g)}, \omega_j^{(g)}, \zeta_k^{(v)}, \omega_k^{(k)}\}$, $j = 1, 2, \dots, N_g$, and $k = 1, 2, \dots, N_v$. Specifically, each idiosyncratic innovation and its corresponding log-volatility process are related through a state-space representation, where the measurement equation is given by

$$z_{i,t}^* = h_{i,t} + v_t^*, \tag{A-5}$$

with

$$z_{i,t}^* = \ln \left(\frac{z_{i,t}^2}{o_{i,t}^2} + c \right);$$

and

$$v_t^* = \ln(v_t^2) \text{ with } v_t \sim \mathcal{N}(0, 1).$$

The transition equation of the state-space representation is given by equation (26) in the main text.³⁵ We employ a seven-component Gaussian mixture to approximate the density function of v_t^* and sample the mixture component indicator, as proposed by [Kim et al. \(1998\)](#). Next, the [Carter and Kohn \(1995\)](#) algorithm can be readily applied to obtain draws of $h_{i,t}$, based on the state-space representation defined by the preceding equation (A-5) and equation (26) in the main text.

Steps 1 through 7 are repeated for $M = 10,000$ iterations, where the first $M_0 = 2,000$ iterations are discarded to avoid the potential influence of initial conditions. The set of $M^* = M - M_0 = 8,000$ draws is then used to compute the posterior densities associated with both the parameters and latent variables of the model.

³⁵The idiosyncratic innovation $z_{i,t}$ is defined by equation (25) in the main text. To avoid numerical problems when $z_{i,t}$ is close to zero, a small constant $c = 10^{-4}$ is included.

B Data Description

This section details some key aspects of the data used in the analysis.

- We use monthly, seasonally adjusted data on prices and quantities for 51 PCE categories from January 1968 through April 2025 in the estimation. This so-called Level 4 disaggregation includes a total of 53 PCE categories, but as is typical, our analysis excludes the two Level 4 categories with occasionally negative expenditure weights—that is, **Net Expenditures Abroad by US Residents** and **Net Foreign Travel**. Table B-1 lists the 51 PCE categories used in the analysis, along with their re-normalized average expenditure weights.
- Figure B-1 shows the two measures of expected inflation used in the estimation, with the yellow line depicting our preferred measure of inflation expectations and the purple line depicting an alternative measure used in the model-selection exercise summarized in Table 1 in the main text. Starting in April 1990, the yellow line corresponds to the median expected PCE inflation over the next five to 10 years, as reported in the monthly University of Michigan’s Survey of Consumers. For the earlier period, we use long-term expected inflation from the Federal Reserve Board’s FRB/US database (see Brayton and Tinsley, 1996); this series is available at a quarterly frequency, and we interpolate it to a monthly frequency by assuming that the quarterly value is the same for all three months of the quarter. Starting in January 1978, the purple line corresponds to the median expected year-ahead inflation, as reported in the monthly University of Michigan’s Survey of Consumers. For the earlier period, we use the average expected year-ahead inflation, which is available at a quarterly frequency, and we interpolate it to a monthly frequency by assuming that the quarterly value is the same for all three months of the quarter.

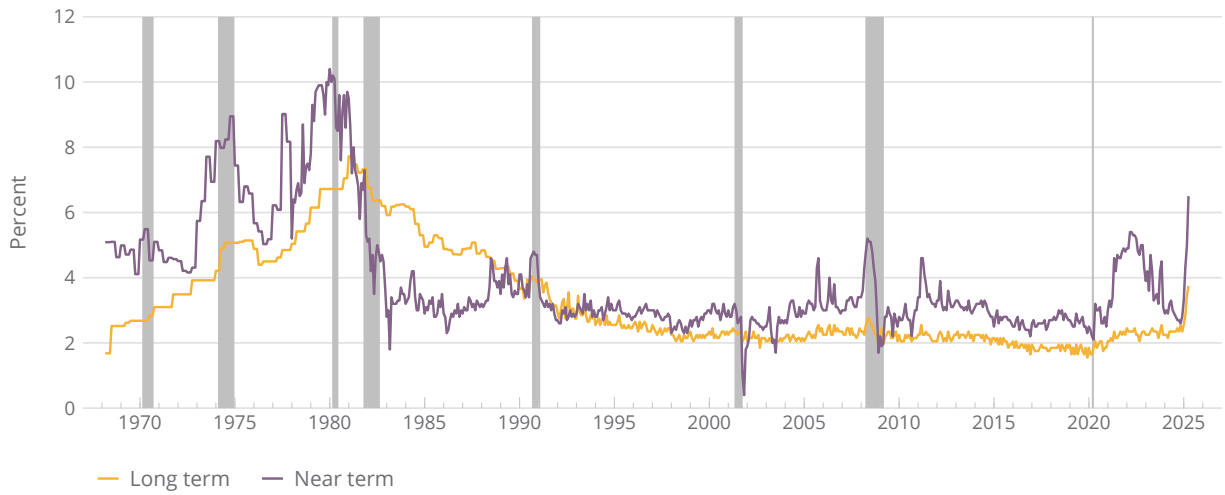
TABLE B-1: PCE Categories Used in the Estimation

#	Description	Weight ^a
5	New motor vehicles (55)	3.10
12	Net purchases of used motor vehicles (56)	1.12
20	Motor vehicle parts & accessories (58)	0.75
24	Furniture & furnishings (parts of 31 & 32)	1.83
29	Household appliances (part of 33)	0.65
32	Glassware, tableware & household utensils (34)	0.46
35	Tools & equipment for house & garden (35)	0.26
39	Video, audio, photographic & information processing equipment & media (75, 76, & part of 93)	1.63
52	Sporting equipment, supplies, guns & ammunition (part of 80)	0.53
53	Sports & recreational vehicles (79)	0.53
60	Recreational books (part of 90)	0.26
61	Musical instruments (part of 80)	0.06
63	Jewelry & watches (part of 119)	0.69
66	Therapeutic appliances & equipment (42)	0.41
69	Educational books (96)	0.10
70	Luggage & similar personal items (part of 119)	0.27
71	Telephone & related communication equipment	0.09
74	Food & nonalcoholic beverages purchased for off-premises consumption (4)	8.78
99	Alcoholic beverages purchased for off-premises consumption (5)	1.33
103	Food produced & consumed on farms (6)	0.03
105	Garments	3.72
109	Other clothing materials & footwear (13 & 17)	0.88
114	Motor vehicle fuels, lubricants & fluids (59)	3.00
117	Fuel oil & other fuels (29)	0.39
121	Pharmaceutical & other medical products (40 & 41)	2.14
126	Recreational items (parts of 80, 92, & 93)	1.33
131	Household supplies (parts of 32 & 36)	1.34
137	Personal care products (part of 118)	1.03
141	Tobacco (127)	1.07
142	Magazines, newspapers & stationery (part of 90)	0.79
153	Housing	14.92
165	Household utilities	3.04
173	Outpatient services	6.02
182	Hospital & nursing home services	7.20
191	Motor vehicle services	2.14
199	Public transportation	1.10
210	Membership clubs, sports centers, parks, theaters & museums (82)	1.31
218	Audio-video, photographic & information processing equipment services (parts of 77 & 93)	0.88
226	Gambling (91)	0.76
230	Other recreational services (81, 94, & part of 92)	0.32
235	Food services	5.75
249	Accommodations (104)	0.77
253	Financial services	3.92
270	Insurance	2.78
281	Communication	1.91
290	Education services	1.73
298	Professional & other services (121)	1.56
307	Personal care & clothing services (14 & parts of 17 & 118)	1.16
315	Social services & religious activities (120)	1.12
327	Household maintenance (parts of 31, 33, & 36)	0.72
342	Final consumption expenditures of nonprofit institutions serving households (NPISHs) (132)	2.28

NOTE: The entries in the table list the 51 consumption categories from the U.S. Bureau of Economic Analysis' Personal Income and Outlays report that are used in the estimation; categories **Net Expenditures Abroad by U.S. Residents** and **Net Foreign Travel** are not used in the estimation because of their occasionally negative expenditure weights.

^a Average (re-normalized) expenditure weight (in percent) over the April 1968 to April 2025 period.

FIGURE B-1: Inflation Expectations



NOTE: Monthly data from March 1968 through April 2025. The yellow line shows the measure of long-term inflation expectations used in the analysis. For comparison, the purple line shows the measure of near-term inflation expectations used in the model-selection exercises reported in Table 1 in the main text.

SOURCE: Authors' calculations using data from the Federal Reserve Board and the University of Michigan.

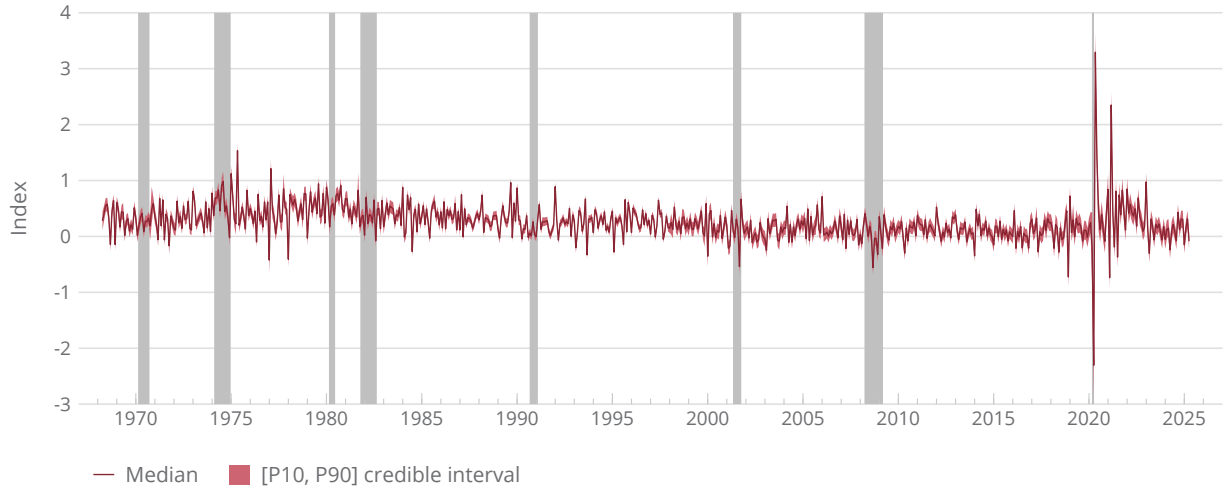
C Additional Results

This section contains additional results referenced in the main text.

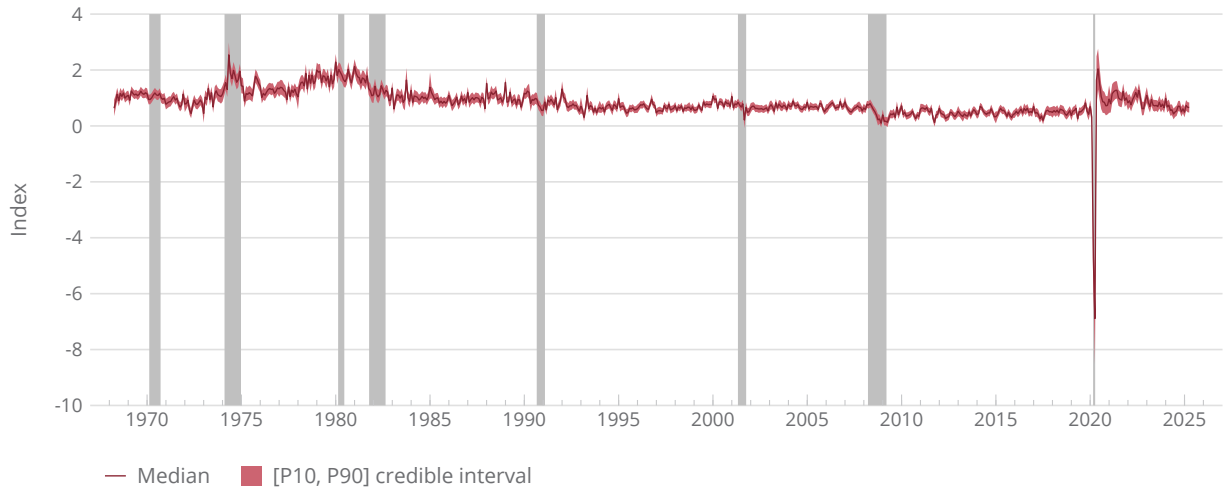
- Figures C-1 and C-2 depict the estimates of the monthly common demand factors ($d_t^{(g)}$ and $d_t^{(v)}$) and the estimates of the monthly common supply factors ($s_t^{(g)}$ and $s_t^{(v)}$), respectively, along with their corresponding measures of uncertainty.
- Figures C-3 through C-6 depict the estimated factor loadings on the common goods demand ($d_t^{(g)}$), common goods supply ($s_t^{(g)}$), common services demand ($d_t^{(v)}$), and common services supply ($s_t^{(v)}$) factors, respectively. These factor loadings determine the sensitivity of category-specific standardized log-price and log-quantity changes from month $t - 1$ to month t to a change in the specified common factor in month t .
- Figures C-7 and C-8 depict the estimated time-varying (log) variances and the estimated occurrence and size of the outliers of innovations associated with the category-specific VAR(2) process governing the evolution of idiosyncratic monthly log-price changes ($\eta_{j,t}^{(g)}$ and $\eta_{k,t}^{(v)}$) and idiosyncratic monthly log-quantity changes ($\zeta_{j,t}^{(g)}$ and $\zeta_{k,t}^{(v)}$), respectively. See equations (21) through (24) and the associated discussion in the main text for details.
- Figure C-9 depicts the estimated sensitivities of the common demand and supply factors to long-term expected inflation (the yellow line in Figure B-1). According to equations (19) and (20) in the main text, the coefficient vectors $\beta_d = [\beta_d^{(g)} \ \beta_d^{(v)}]'$ and $\beta_s = [\beta_s^{(g)} \ \beta_s^{(v)}]'$ determine the sensitivity of the common demand and supply factors $d_t^{(g)}$, $d_t^{(v)}$, $s_t^{(g)}$, and $s_t^{(v)}$ to π_{t-1}^E , expectations of inflation over the next five to 10 years based on information available as of month $t - 1$.
- Figure C-10 depicts the estimated sensitivities of category-specific log-price changes to long-term expected inflation (the yellow line in Figure B-1), implied by the estimated coefficients $\beta_d^{(g)}$, $\beta_d^{(v)}$, $\beta_s^{(g)}$, and $\beta_s^{(v)}$, and the estimated factor loadings θ_j^d and θ_j^s , $j = 1, 2, \dots, N_g$, and factor loadings δ_k^d and δ_k^s , $k = 1, 2, \dots, N_v$. As discussed in the main text, these coefficients determine the sensitivity of category-specific standardized log-price changes from month $t - 1$ to month t to π_{t-1}^E , expectations of inflation over the next five to 10 years based on information available as of month $t - 1$.
- Figure C-11 depicts the historical decomposition of the 12-month total idiosyncratic PCE inflation referenced in the main text.
- The heatmaps in Figure C-12 depict the 20 estimated category-specific contributions from the PCE goods sector to the three-month (annualized) total idiosyncratic PCE inflation shown by the black line in Figure 4 in the main text. Specifically, Panel A depicts the estimated demand-driven contributions, whereas Panel B depicts the estimated supply-driven contributions.
- The heatmaps in Figure C-13 depict the 31 estimated category-specific contributions from the PCE services sector to the three-month (annualized) total idiosyncratic PCE inflation shown by the black line in Figure 4 in the main text. Specifically, Panel A depicts the estimated demand-driven contributions, whereas Panel B depicts the estimated supply-driven contributions.
- Panel A of Figure C-14 depicts the estimated responses of supply-driven idiosyncratic inflation to an adverse oil supply news shock, whereas Panel B depicts the estimated responses of demand-driven idiosyncratic inflation to the same shock.

- Panel A of Figure C-15 depicts the estimated responses of demand-driven idiosyncratic inflation to a contractionary monetary policy shock, whereas Panel B depicts the estimated responses of supply-driven idiosyncratic inflation to the same shock.
- Figure C-16 depicts the pseudo real-time estimates of the common goods demand factor $d_t^{(g)}$ (Panel A) and the common services demand factor $d_t^{(v)}$ (Panel B). Figure C-17 depicts the pseudo real-time estimates of the common goods supply factor $s_t^{(g)}$ (Panel A) and the common services supply factor $s_t^{(v)}$ (Panel B). These pseudo real-time estimates of the four inflation factors are used in the out-of-sample forecast-evaluation exercises shown in Figure 11 in the main text.

FIGURE C-1: Common Demand Factors



A. Common goods demand factor

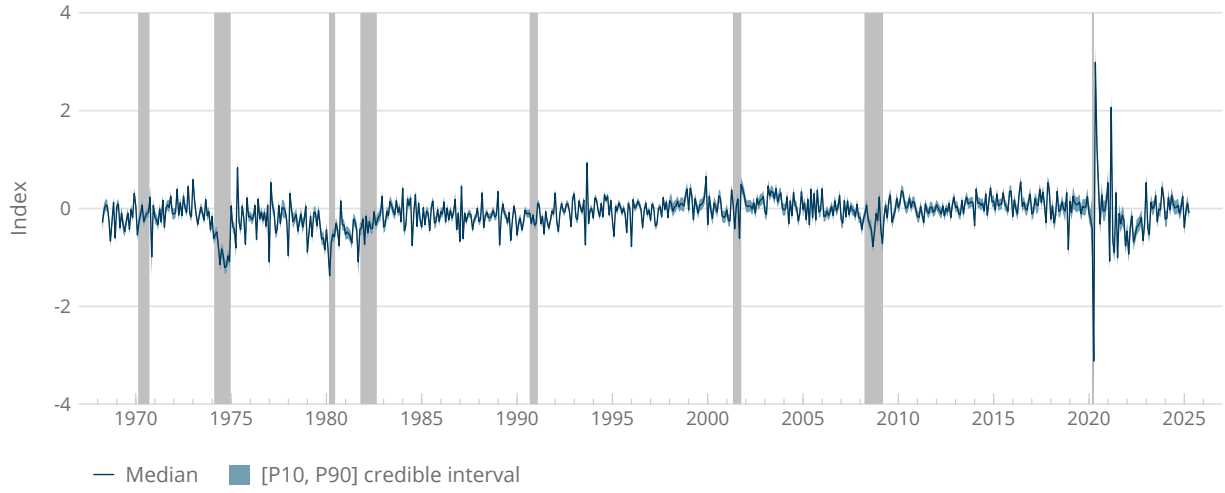


B. Common services demand factor

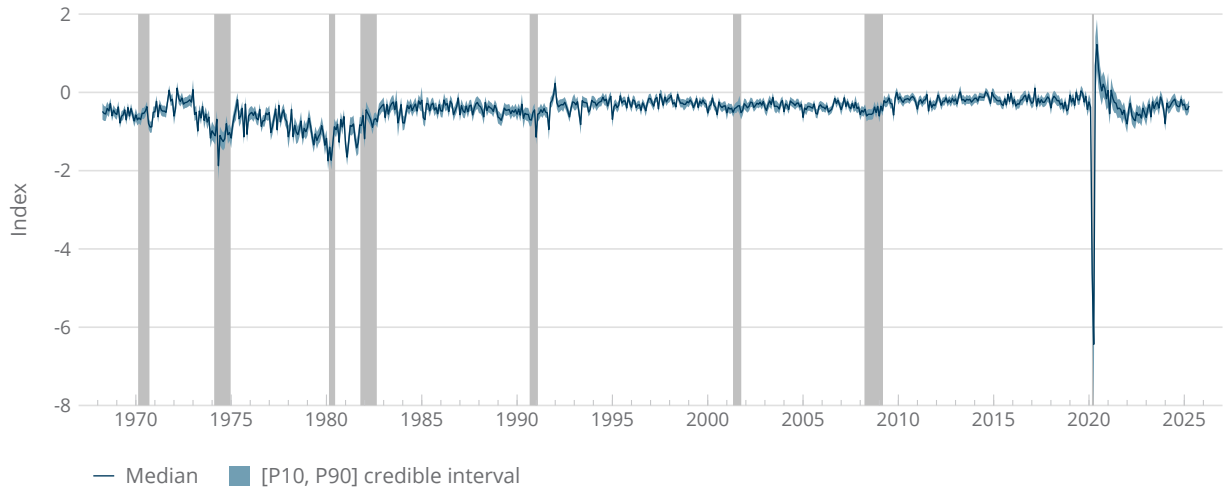
NOTE: Monthly data from April 1968 through April 2025. The line in Panel A shows the median of the posterior distribution of the common goods demand factor ($d_t^{(g)}$), whereas the line in Panel B shows the median of the posterior distribution of the common services demand factor ($d_t^{(v)}$). The shaded bands depict the corresponding [P10, P90] credible intervals. The shaded vertical bars depict recessions as determined by the National Bureau of Economic Research.

SOURCE: Authors' calculations using data from the U.S. Bureau of Economic Analysis, the Federal Reserve Board, and the University of Michigan.

FIGURE C-2: Common Supply Factors



A. Common goods supply factor

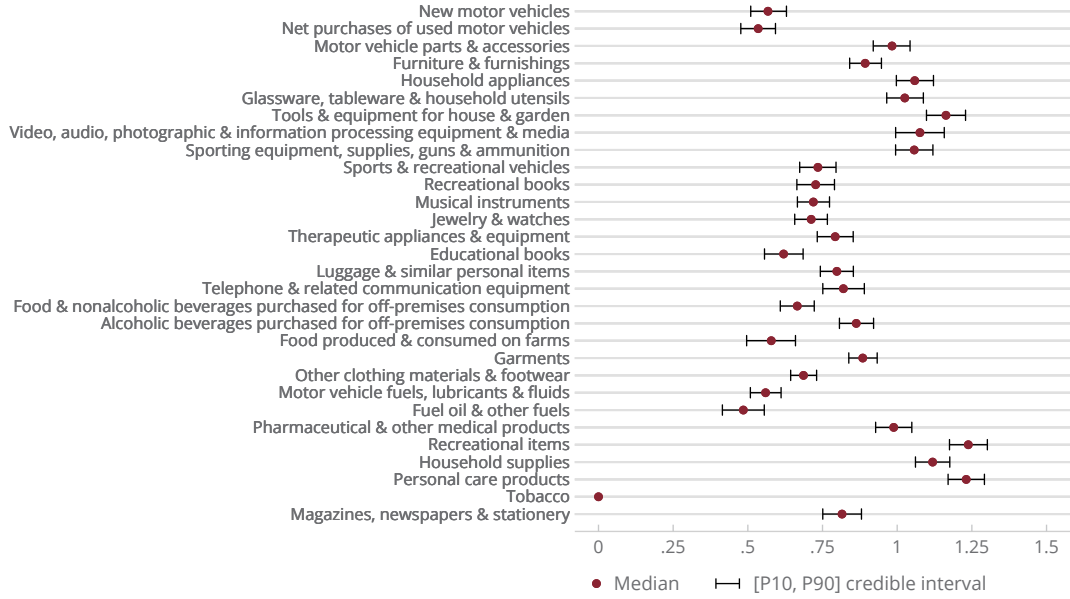


B. Common services supply factor

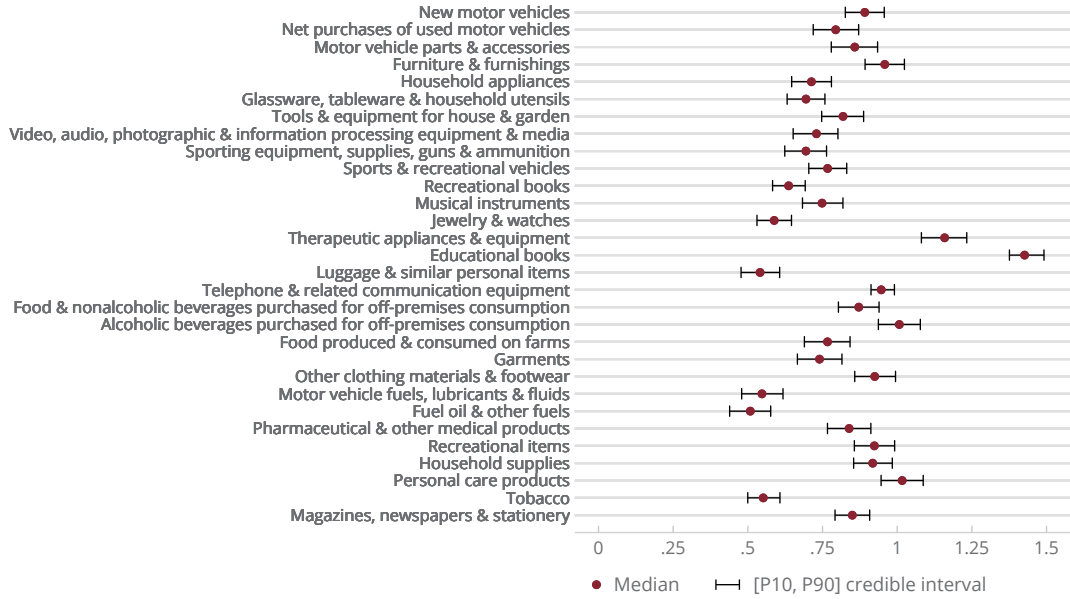
NOTE: Monthly data from April 1968 through April 2025. The line in Panel A shows the median of the posterior distribution of the common goods supply factor ($s_t^{(g)}$), whereas the line in Panel B shows the median of the posterior distribution of the common services supply factor ($s_t^{(v)}$). The shaded bands depict the corresponding [P10, P90] credible intervals. The shaded vertical bars depict recessions as determined by the National Bureau of Economic Research.

SOURCE: Authors' calculations using data from the U.S. Bureau of Economic Analysis, the Federal Reserve Board, and the University of Michigan.

FIGURE C-3: Loadings on the Common Goods Demand Factor



A. PCE goods categories – quantity changes

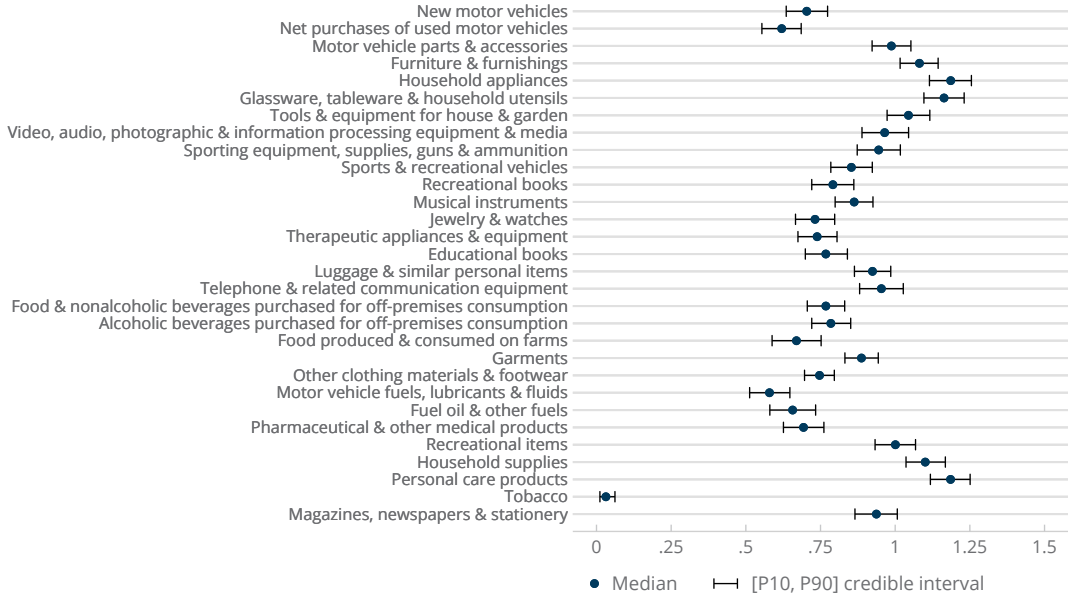


B. PCE goods categories – price changes

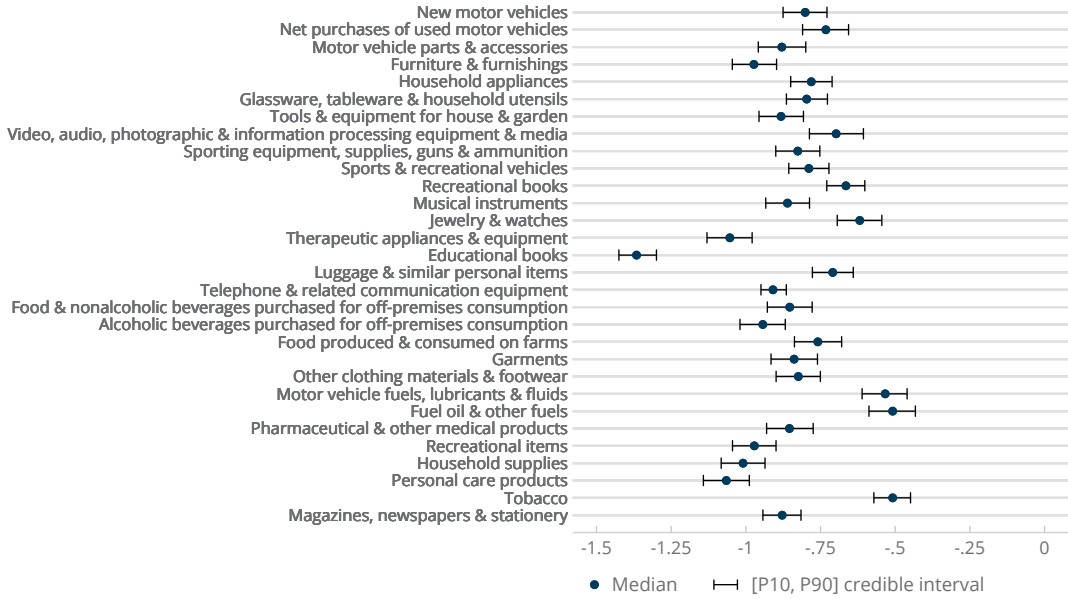
NOTE: The figure shows the estimated category-specific factor loadings on the common goods demand factor $d_t^{(g)}$ (see Panel A of Figure C-1) for monthly log-quantity changes ($\Delta q_{j,t}$) in the goods sector (Panel A) and for the corresponding monthly log-price changes ($\Delta p_{j,t}$) in the same sector (Panel B). Specifically, the red dots in Panel A show the posterior medians of the factor loadings λ_j^d , $j = 1, 2, \dots, N_g$, in equation (11) in the main text, whereas the red dots in Panel B show the posterior medians of the factor loadings θ_j^d , $j = 1, 2, \dots, N_g$, in equation (12) in the main text; the black whiskers depict the associated [P10, P90] credible intervals. The factor loading for Tobacco in Panel A is set to zero for identification purposes (see the main text for details).

SOURCE: Authors' calculations using data from the U.S. Bureau of Economic Analysis, the Federal Reserve Board, and the University of Michigan.

FIGURE C-4: Loadings on the Common Goods Supply Factor



A. PCE goods categories – quantity changes

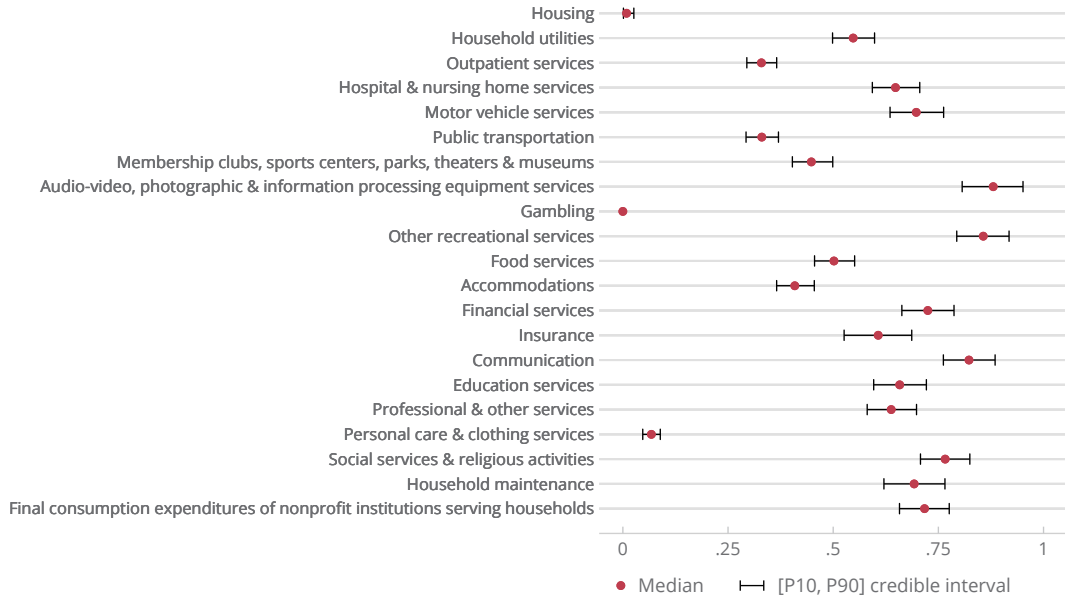


B. PCE goods categories – price changes

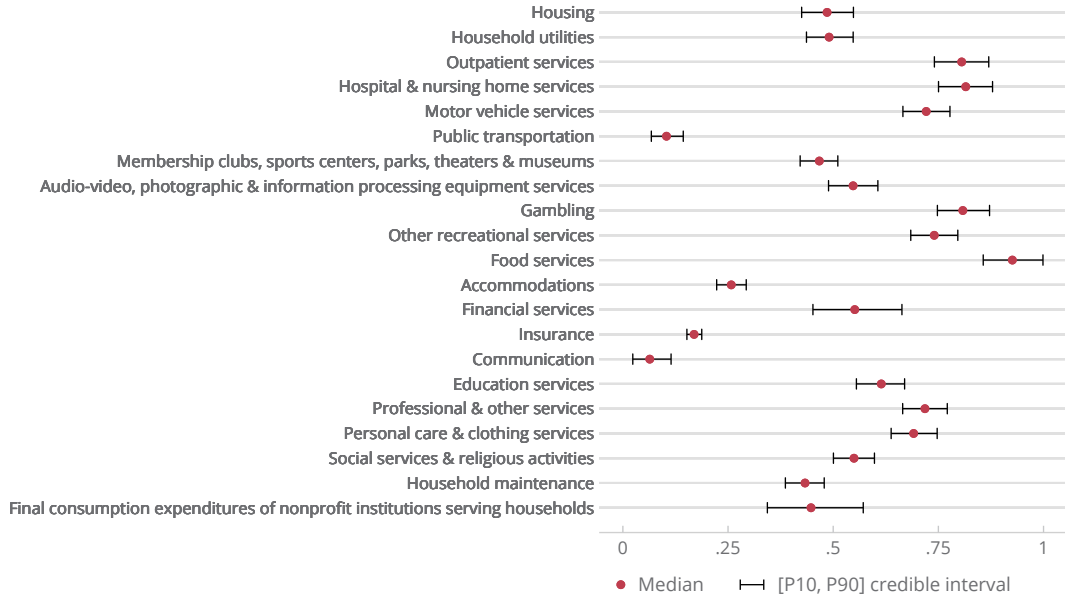
NOTE: The figure shows the estimated category-specific factor loadings on the common goods supply factor $s_t^{(g)}$ (see Panel A of Figure C-2) for the monthly log-quantity changes ($\Delta q_{j,t}$) in the goods sector (Panel A) and for the corresponding monthly log-price changes ($\Delta p_{j,t}$) in the same sector (Panel B). Specifically, the red dots in Panel A show the posterior medians of the factor loadings λ_j^s , $j = 1, 2, \dots, N_g$, in equation (11) in the main text, whereas the red dots in Panel B show the posterior medians of the factor loadings θ_j^s , $j = 1, 2, \dots, N_g$, in equation (12) in the main text; the black whiskers depict the associated [P10, P90] credible intervals.

SOURCE: Authors' calculations using data from the U.S. Bureau of Economic Analysis, the Federal Reserve Board, and the University of Michigan.

FIGURE C-5: Loadings on the Common Services Demand Factor



A. PCE services categories – quantity changes

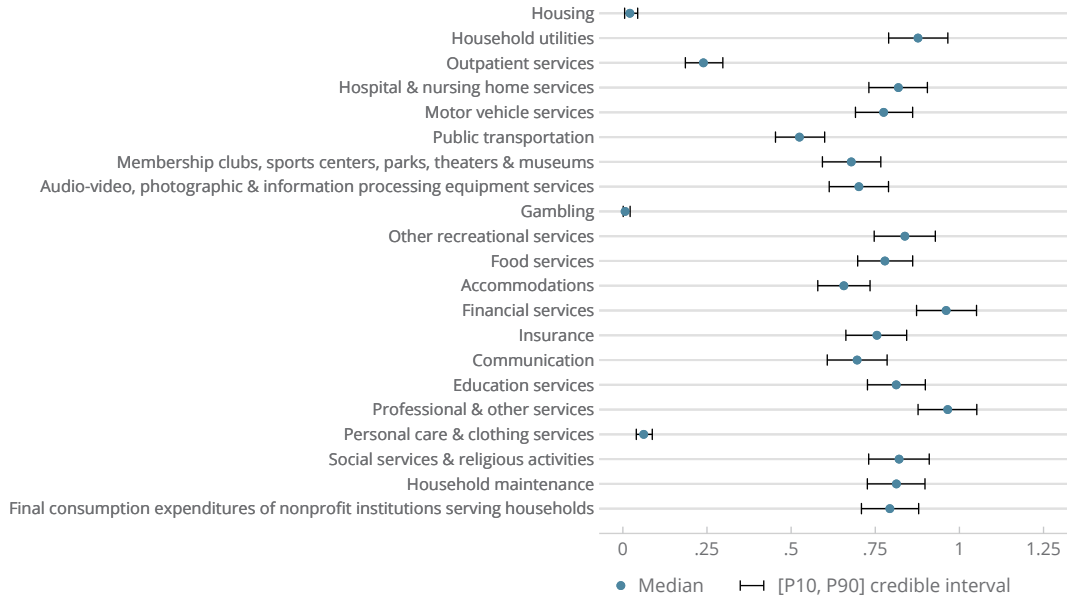


B. PCE services categories – price changes

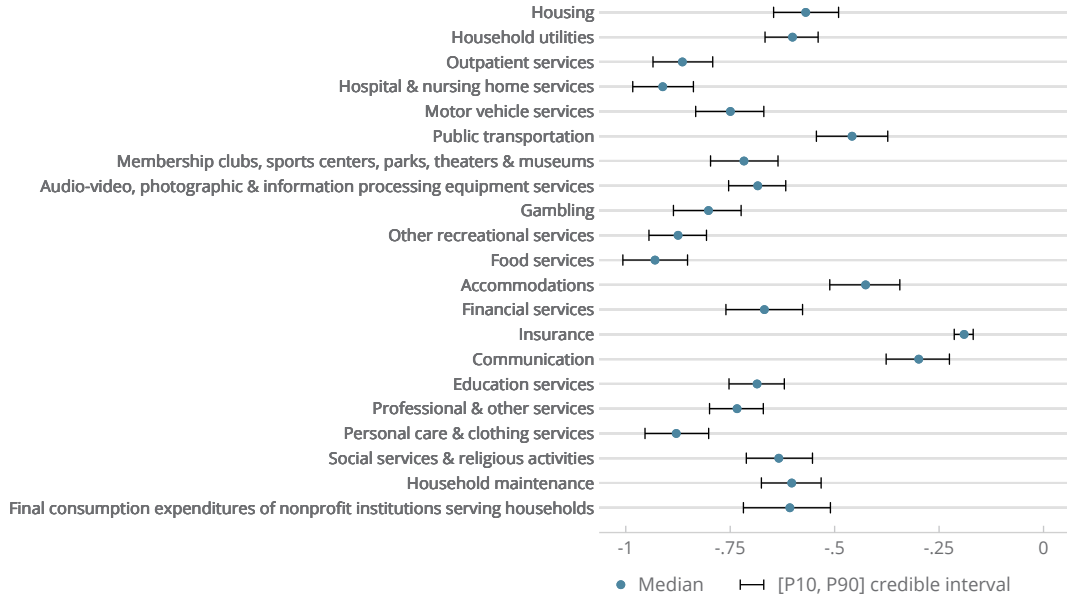
NOTE: The figure shows the estimated category-specific factor loadings on the common services demand factor $d_t^{(v)}$ (see Panel B of Figure C-1) for monthly log-quantity changes ($\Delta q_{k,t}$) in the services sector (Panel A) and for the corresponding monthly log-price changes ($\Delta p_{k,t}$) in the same sector (Panel B). Specifically, the red dots in Panel A show the posterior medians of the factor loadings γ_k^d , $k = 1, 2, \dots, N_v$, in equation (13) in the main text, whereas the red dots in Panel B show the posterior medians of the factor loadings δ_k^d , $k = 1, 2, \dots, N_v$, in equation (14) in the main text; the black whiskers depict the associated [P10, P90] credible intervals. The factor loading for **Gambling** in Panel A is set to zero for identification purposes (see the main text for details).

SOURCE: Authors' calculations using data from the U.S. Bureau of Economic Analysis, the Federal Reserve Board, and the University of Michigan.

FIGURE C-6: Loadings on the Common Services Supply Factor



A. PCE services categories – quantity changes

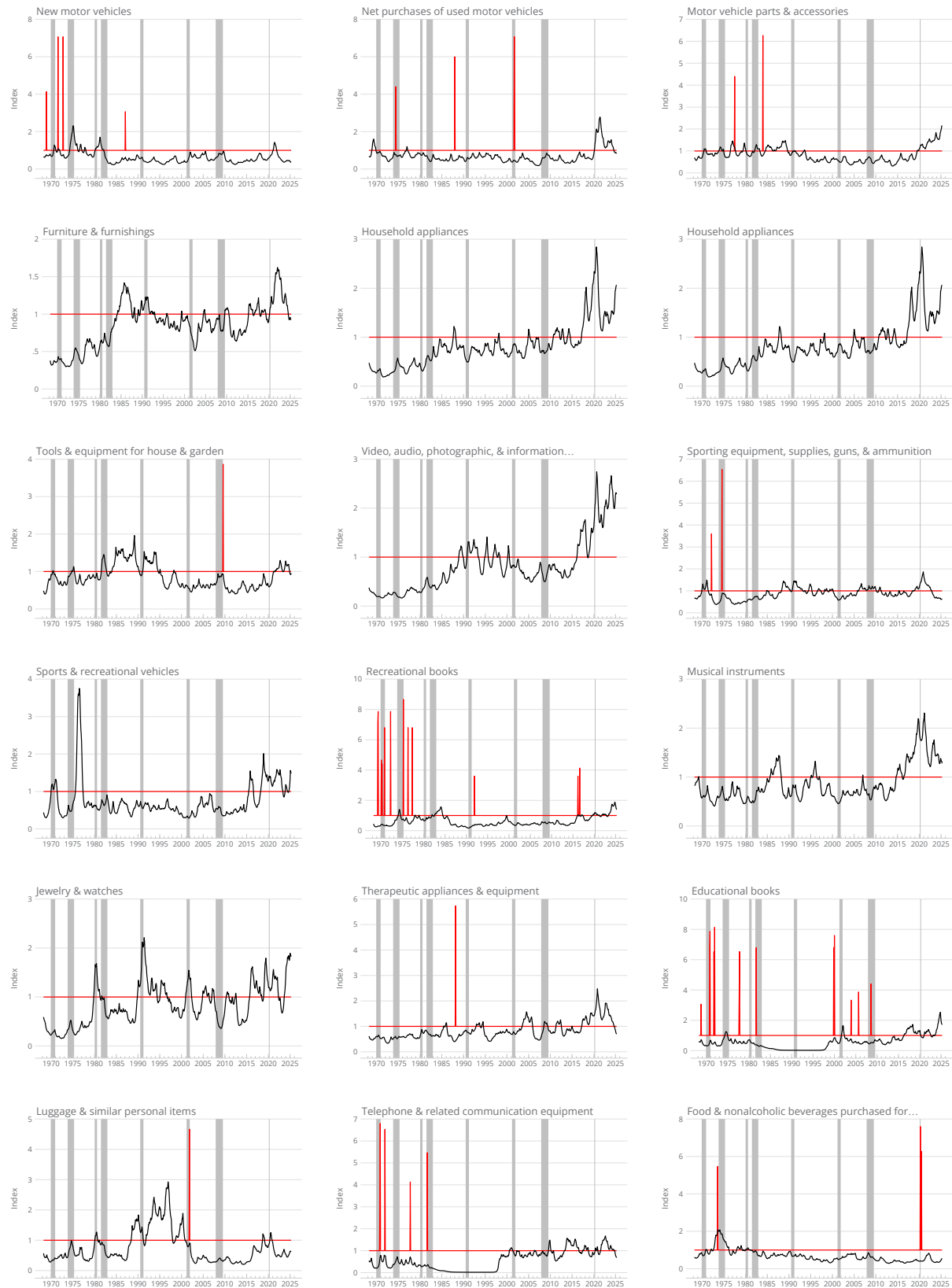


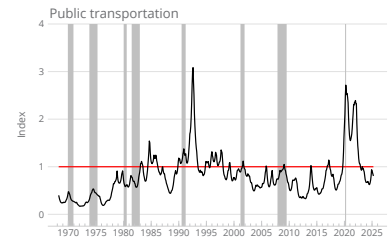
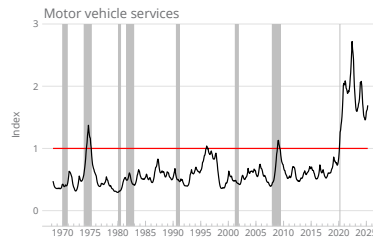
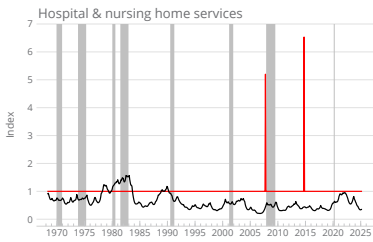
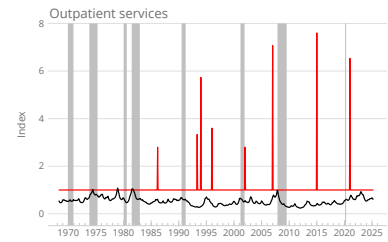
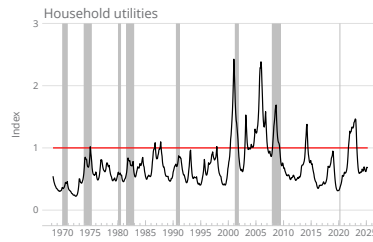
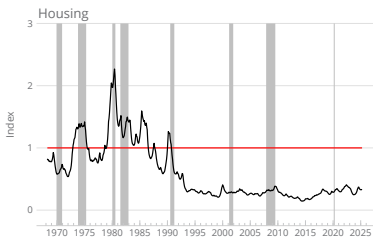
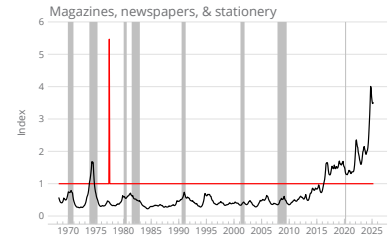
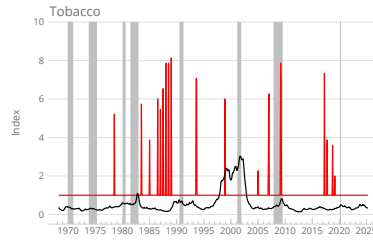
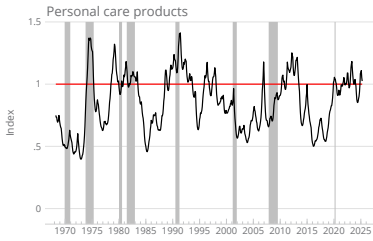
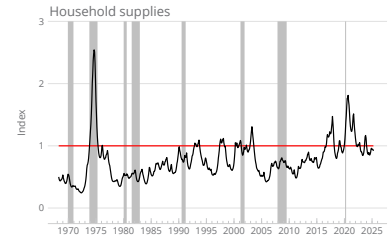
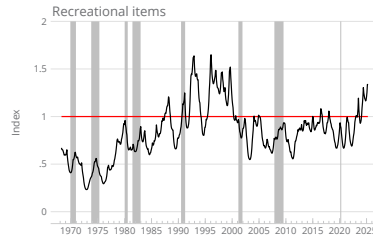
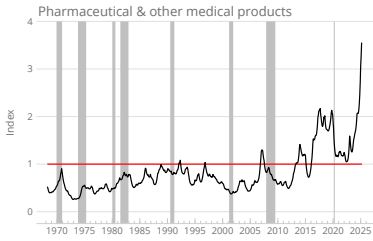
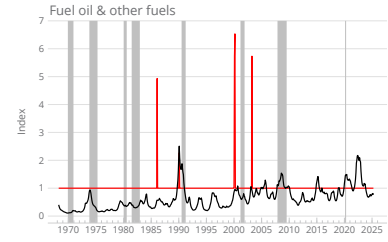
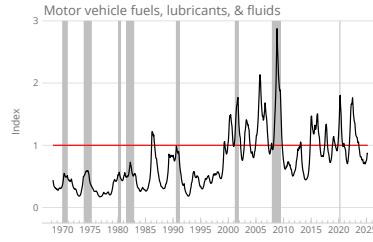
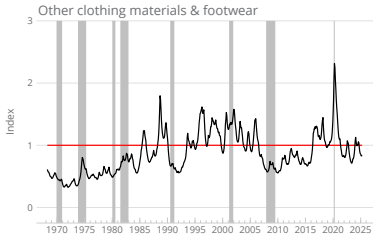
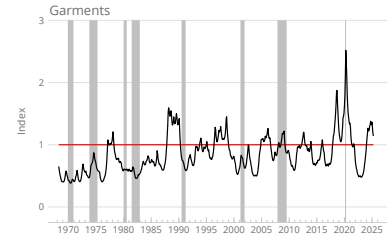
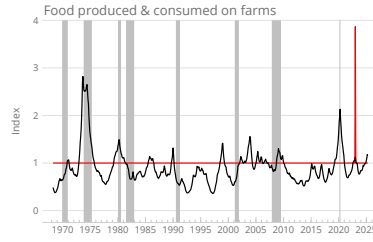
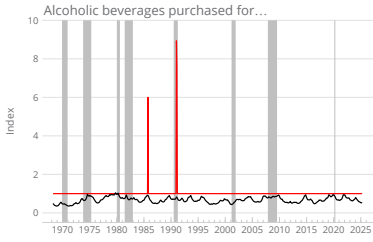
B. PCE services categories – price changes

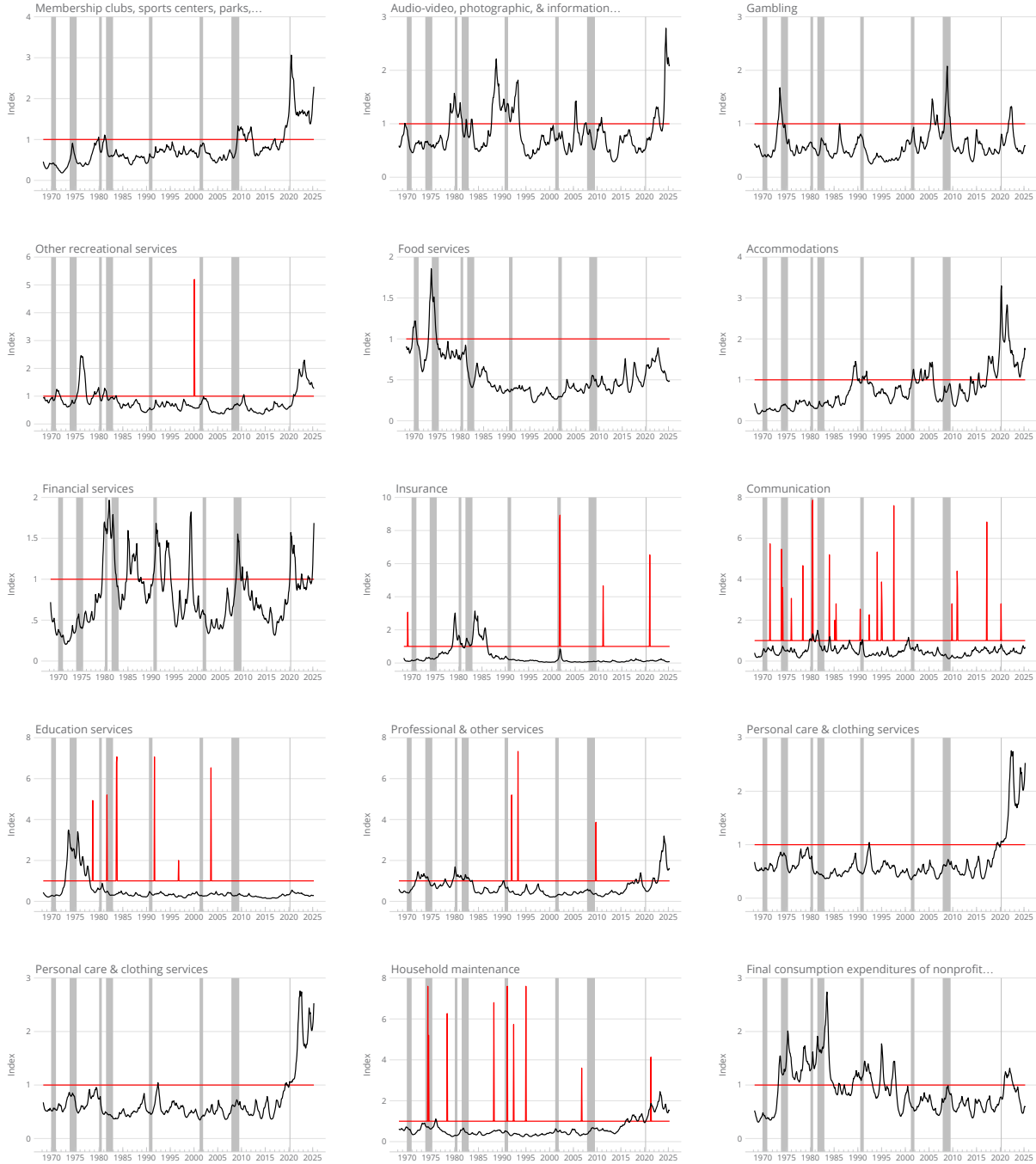
NOTE: The figure shows the estimated category-specific factor loadings on the common services supply factor $s_t^{(v)}$ (see Panel B of Figure C-2) for monthly log-quantity changes ($\Delta q_{k,t}$) in the services sector (Panel A) and for the corresponding monthly log-price changes ($\Delta p_{k,t}$) in the same sector (Panel B). Specifically, the red dots in Panel A show the posterior medians of the factor loadings γ_k^s , $k = 1, 2, \dots, N_v$, in equation (13) in the main text, whereas the red dots in Panel B show the posterior medians of the factor loadings δ_k^s , $k = 1, 2, \dots, N_v$, in equation (14) in the main text; the black whiskers depict the associated [P10, P90] credible intervals.

SOURCE: Authors' calculations using data from the U.S. Bureau of Economic Analysis, the Federal Reserve Board, and the University of Michigan.

FIGURE C-7: Volatility of Idiosyncratic Price Innovations



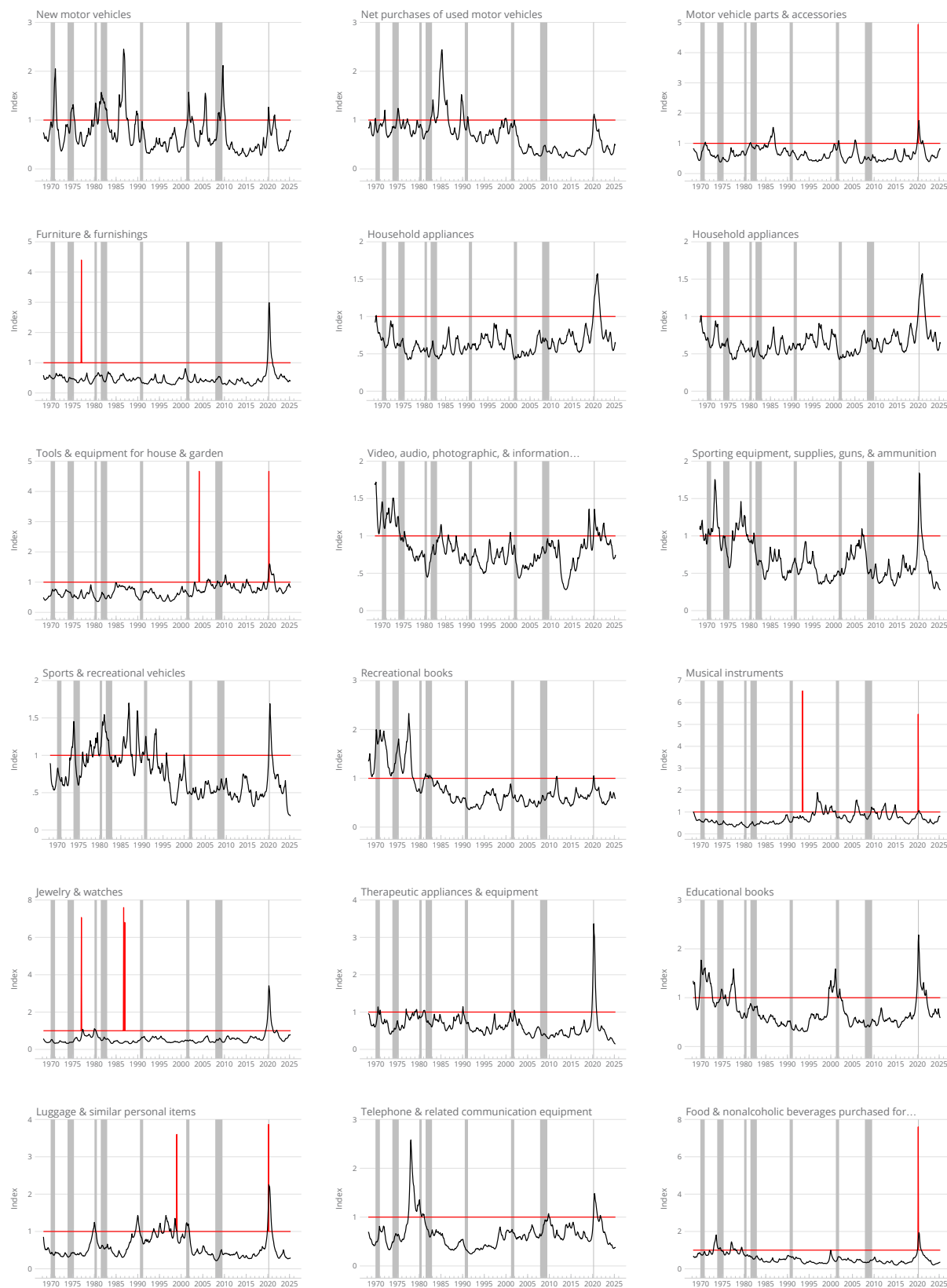


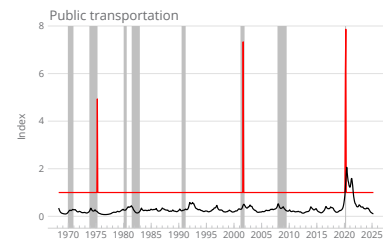
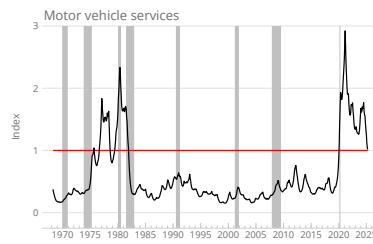
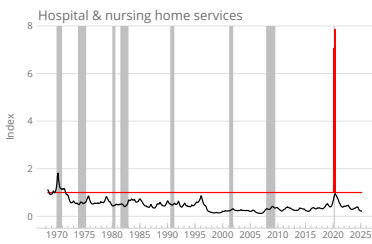
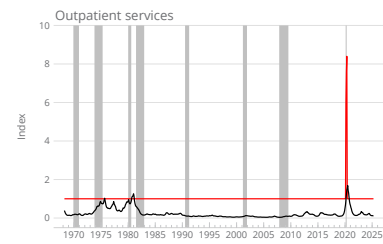
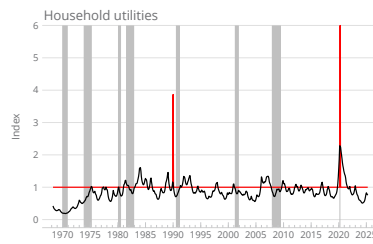
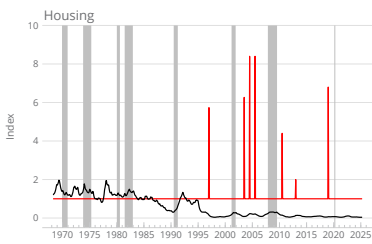
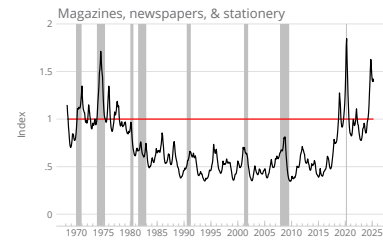
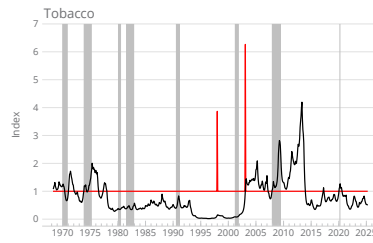
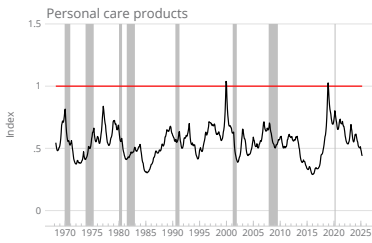
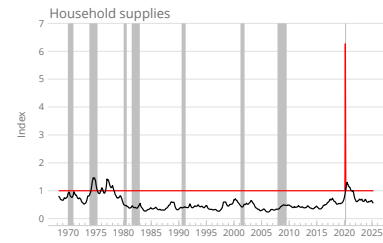
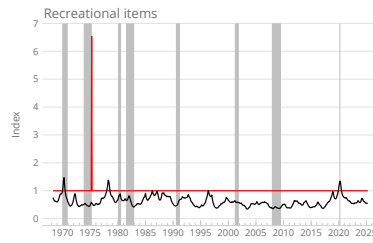
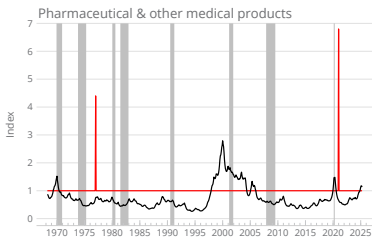
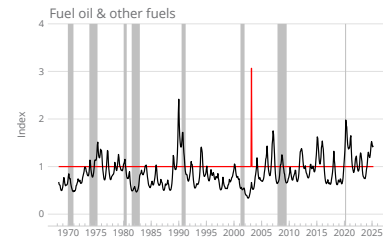
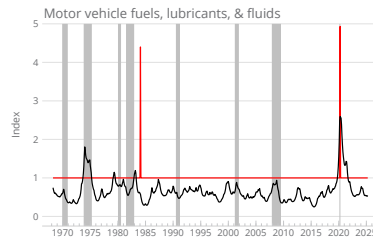
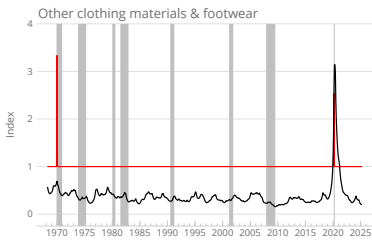
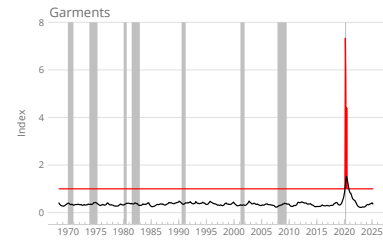
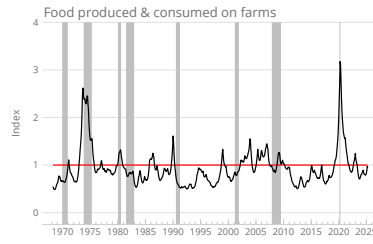
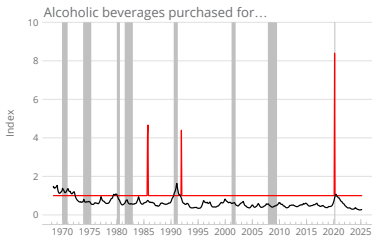


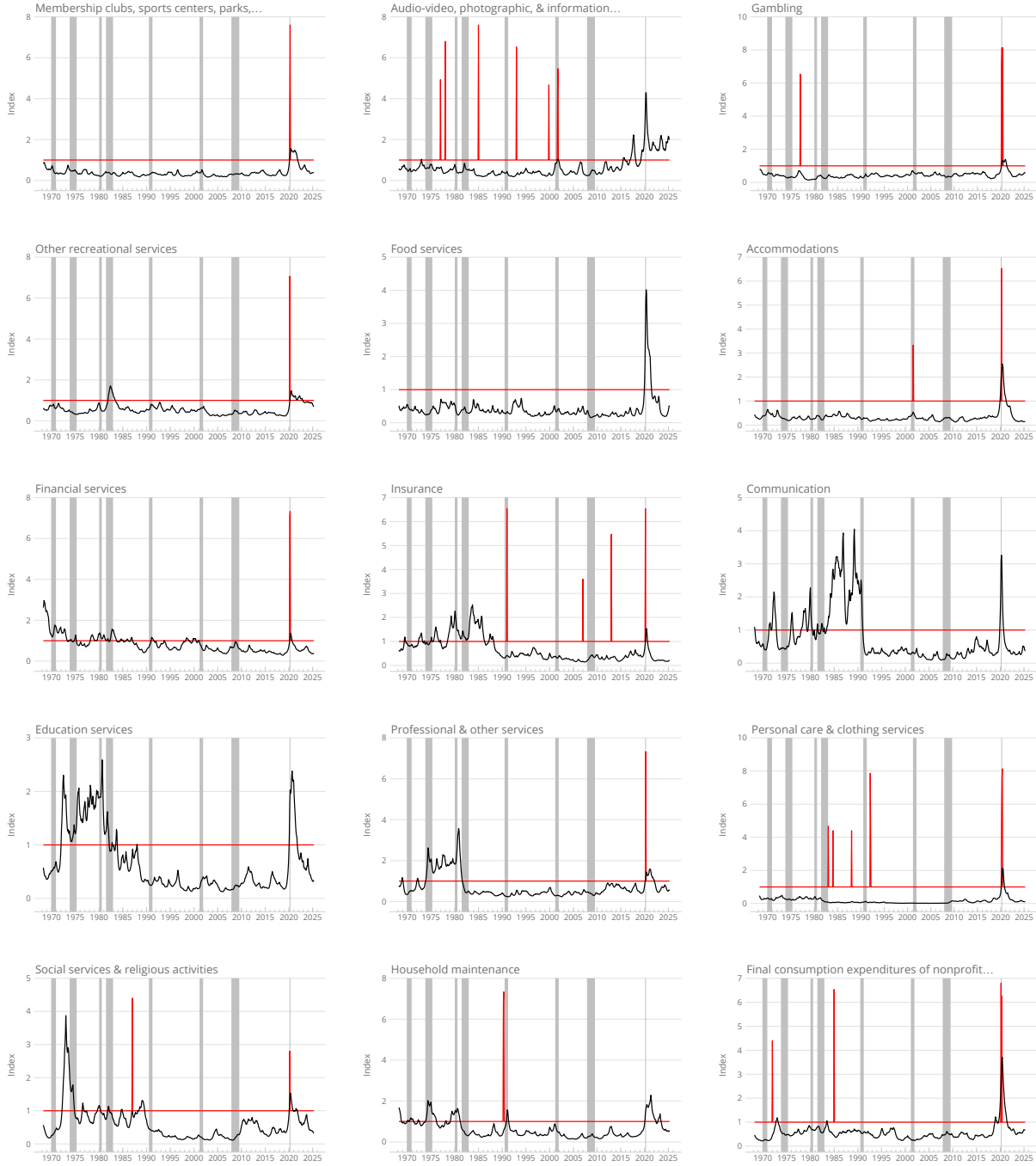
NOTE: Monthly data from April 1968 through April 2025. The black line in each panel shows the estimated time-varying (log) volatility of innovations $\zeta_{j,t}^{(g)}$, $j = 1, 2, \dots, N_g$, and $\zeta_{k,t}^{(v)}$, $k = 1, 2, \dots, N_v$, associated with the category-specific AR(2) process governing the evolution of idiosyncratic log-price changes $\eta_{j,t}^{(g)}$ and $\eta_{k,t}^{(v)}$; the red lines show the estimated occurrence and size of outliers for each process (see the main text for details). The shaded vertical bars depict recessions as determined by the National Bureau of Economic Research.

SOURCE: Authors' calculations using data from the U.S. Bureau of Economic Analysis, the Federal Reserve Board, and the University of Michigan.

FIGURE C-8: Volatility of Idiosyncratic Quantity Innovations



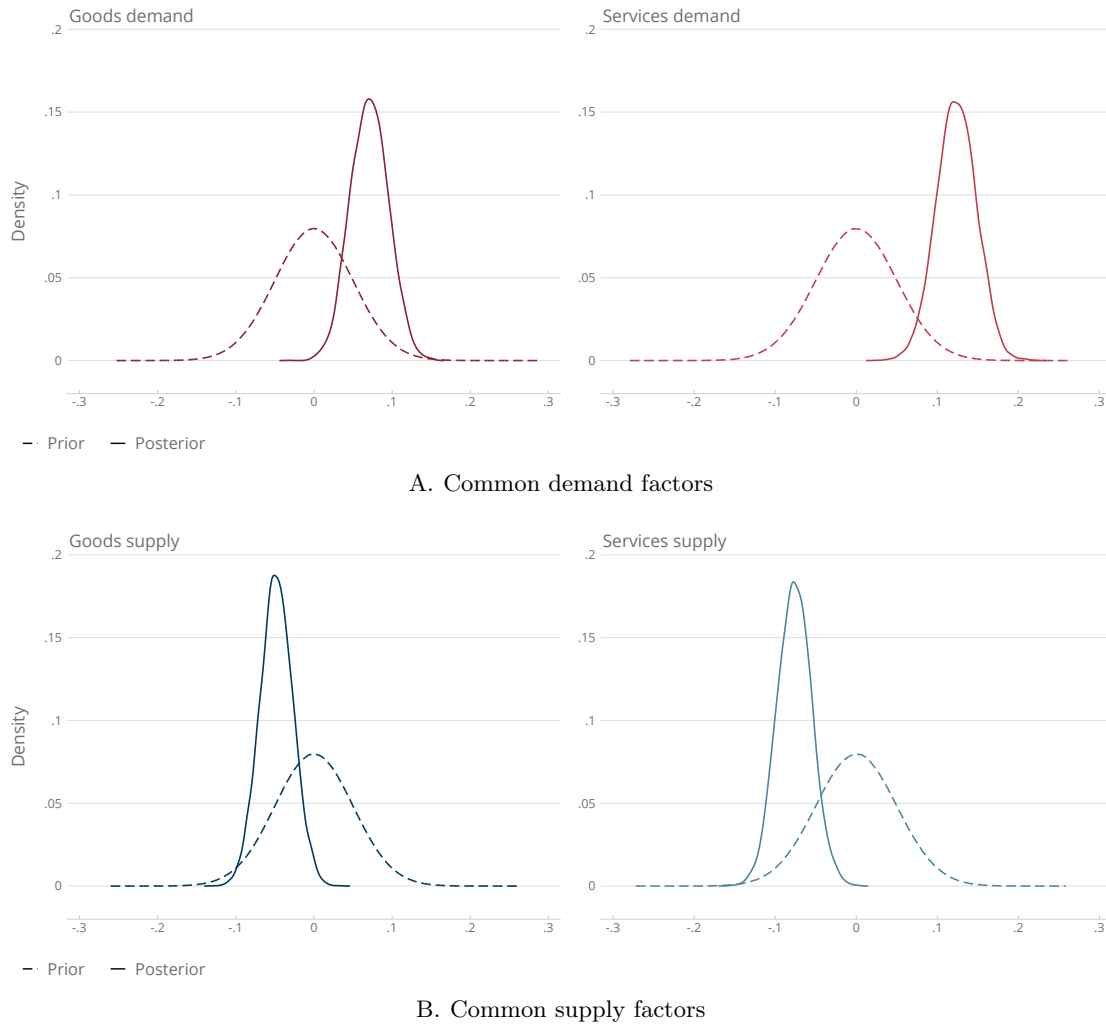




NOTE: Monthly data from April 1968 through April 2025. The black line in each panel shows the estimated time-varying (log) volatility of innovations $\omega_{j,t}^{(g)}$, $j = 1, 2, \dots, N_g$, and $\omega_{k,t}^{(v)}$, $k = 1, 2, \dots, N_v$, associated with the category-specific AR(2) process governing the evolution of idiosyncratic log-quantity changes $\zeta_{j,t}^{(g)}$ and $\zeta_{k,t}^{(v)}$; the red lines show the estimated occurrence and size of outliers for each process (see the main text for details). The shaded vertical bars depict recessions as determined by the National Bureau of Economic Research.

SOURCE: Authors' calculations using data from the U.S. Bureau of Economic Analysis, the Federal Reserve Board, and the University of Michigan.

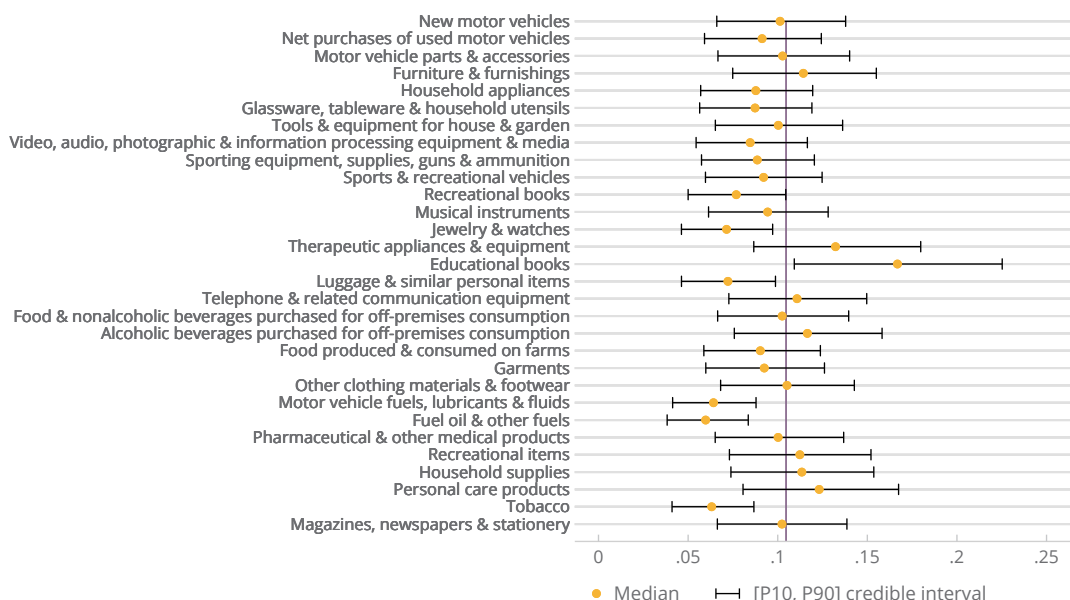
FIGURE C-9: Sensitivities of Common Factors to Inflation Expectations



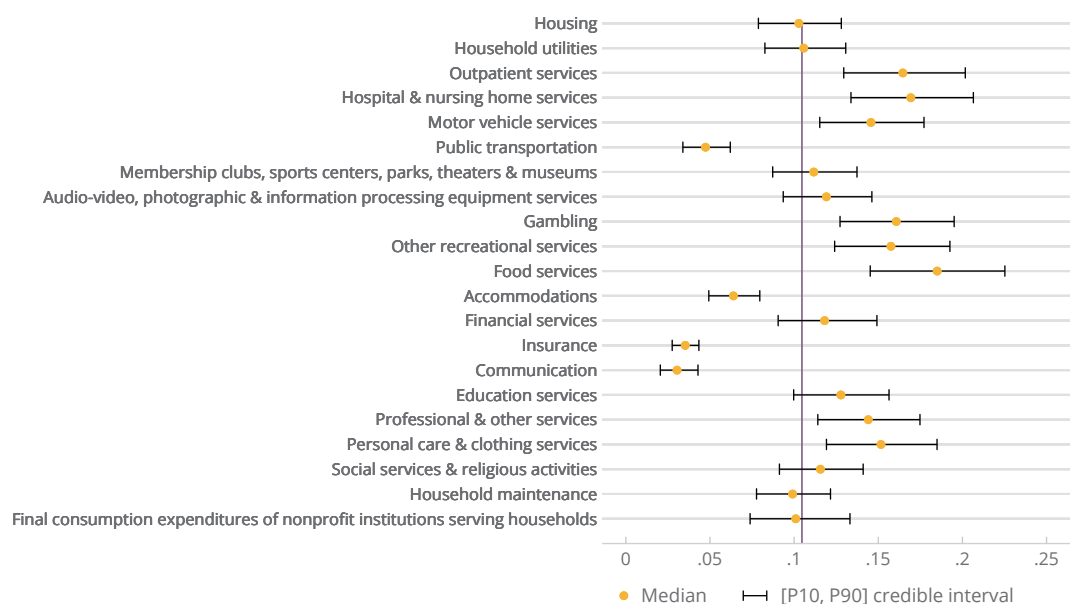
NOTE: The figure shows the estimated sensitivities of common demand factors (Panel A) and common supply factors (Panel B) to our preferred measure of long-term expected inflation (the yellow line in Figure B-1). Specifically, the solid lines in Panel A show the posterior densities of the coefficients $\beta_d^{(g)}$ (left) and $\beta_d^{(v)}$ (right), whereas the solid lines in Panel B show the posterior densities of the coefficients $\beta_s^{(g)}$ (left) and $\beta_s^{(v)}$ (right). The corresponding dashed lines depict the priors used in the estimation (see Appendix A for details).

SOURCE: Authors' calculations using data from the U.S. Bureau of Economic Analysis, the Federal Reserve Board, and the University of Michigan.

FIGURE C-10: Sensitivity of Category-specific Price Changes to Inflation Expectations



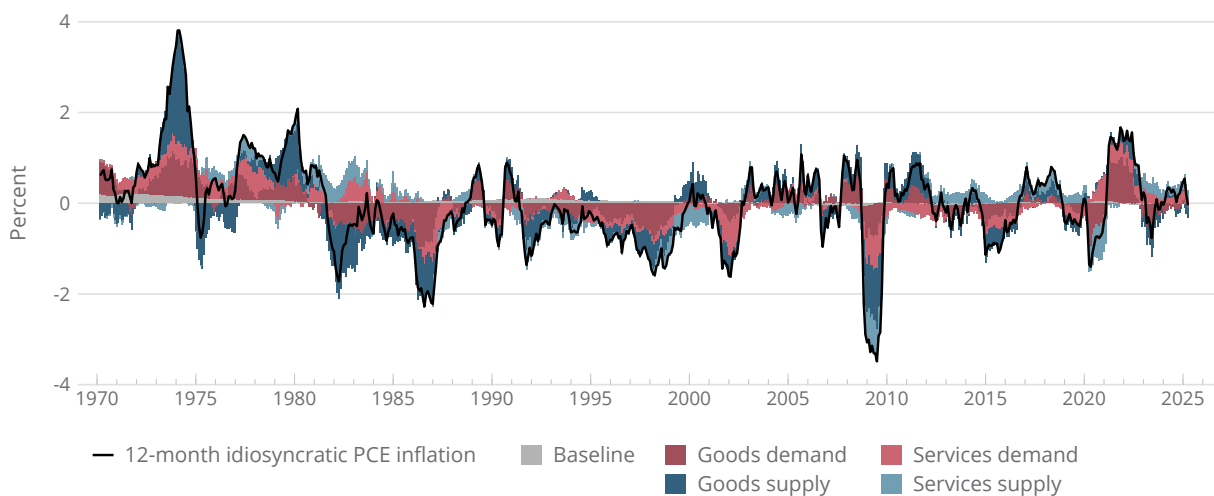
A. PCE goods categories



B. PCE services categories

NOTE: The figure shows the sensitivities of category-specific monthly log-price changes in the goods sector (Panel A) and category-specific monthly log-price changes in the services sector (Panel B) to our preferred measure of long-term expected inflation (the yellow line in Figure B-1). Specifically, the yellow dots in Panel A show the posterior medians of the coefficients $\alpha_j^{(g)} = \theta_j^d \beta_d^{(g)} + \theta_j^s \beta_s^{(g)}$, $j = 1, 2, \dots, N_g$, whereas the yellow dots in Panel B show the posterior medians of the coefficients $\alpha_k^{(v)} = \delta_k^d \beta_d^{(v)} + \delta_k^s \beta_s^{(v)}$, $k = 1, 2, \dots, N_v$; the black whiskers depict the associated [P10, P90] credible intervals. The vertical line in each panel corresponds to a weighted median of the posterior medians in each broad consumption category, using the average expenditure shares in Table B-1 as weights. SOURCE: Authors' calculations using data from the U.S. Bureau of Economic Analysis, the Federal Reserve Board, and the University of Michigan.

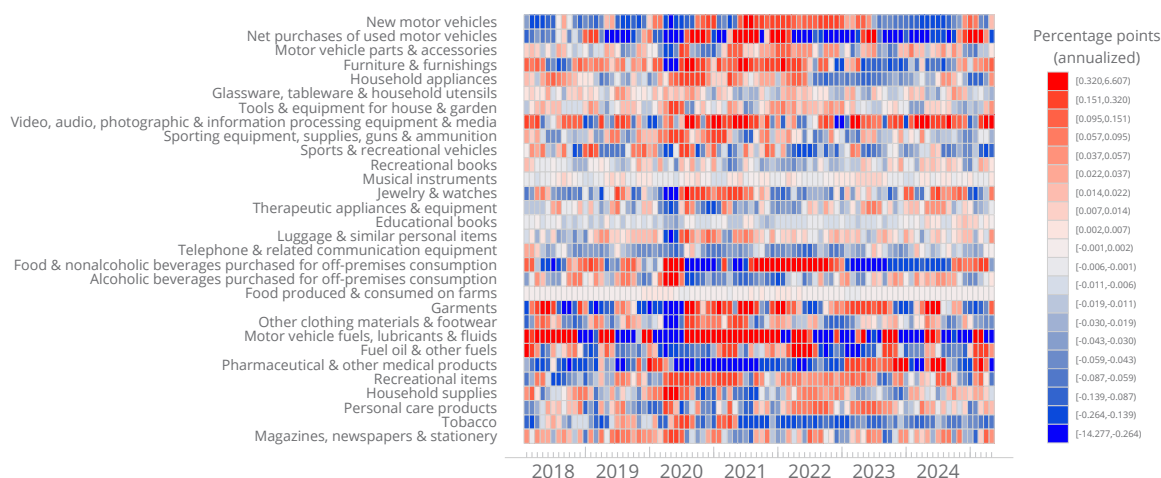
FIGURE C-11: Historical Decomposition of Idiosyncratic Inflation



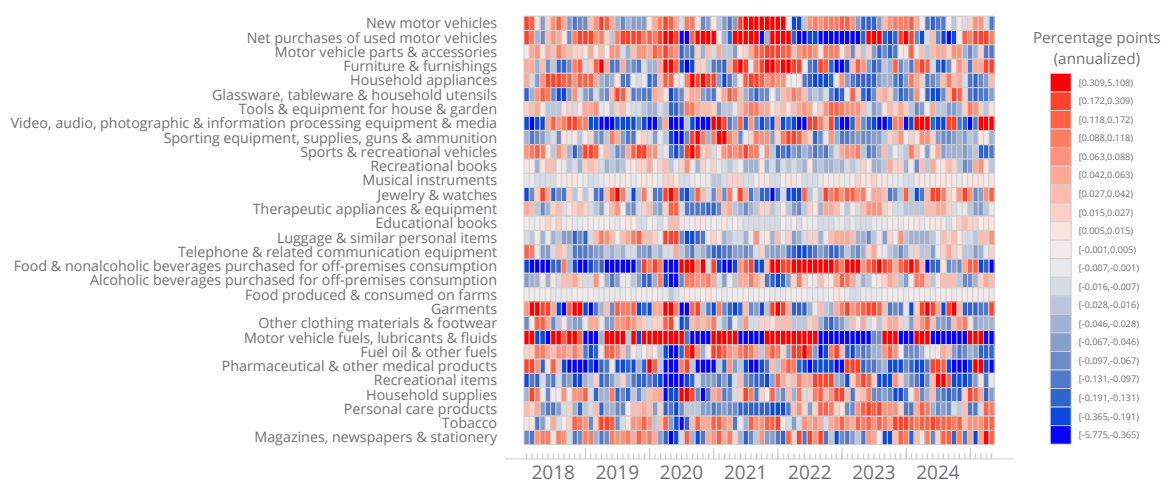
NOTE: Monthly data from March 1970 through April 2025. The black line shows the 12-month total idiosyncratic PCE inflation implied by our model (the gray area in Figure 2 in the main text), with the colored areas showing the estimated contributions of goods- and services-related idiosyncratic supply and demand shocks (see the main text for details).

SOURCE: Authors' calculations using data from the Bureau of Economic Analysis, the Federal Reserve Board, and the University of Michigan.

FIGURE C-12: Pandemic-era Idiosyncratic Price Changes in the Goods Sector



A. Demand-driven contributions to total idiosyncratic inflation

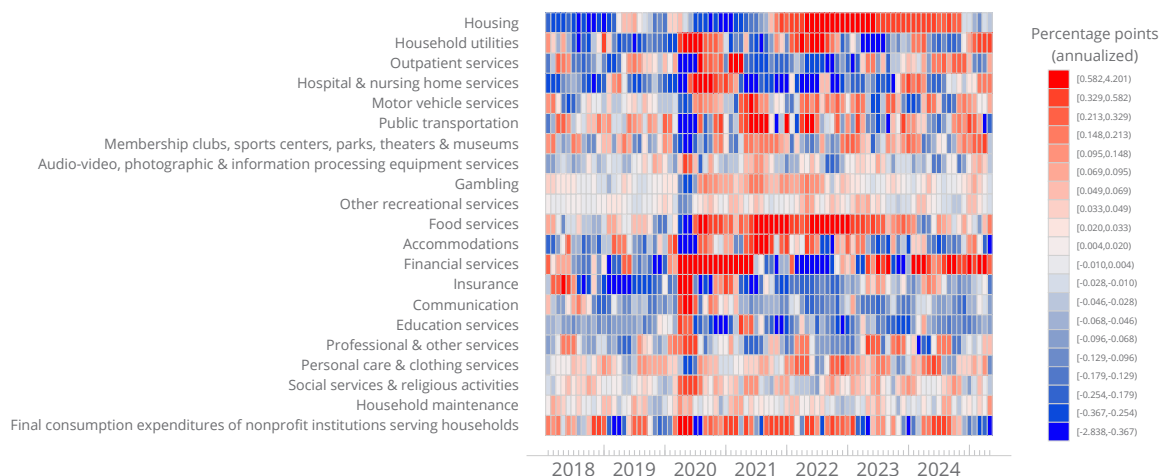


B. Supply-driven contributions to total idiosyncratic inflation

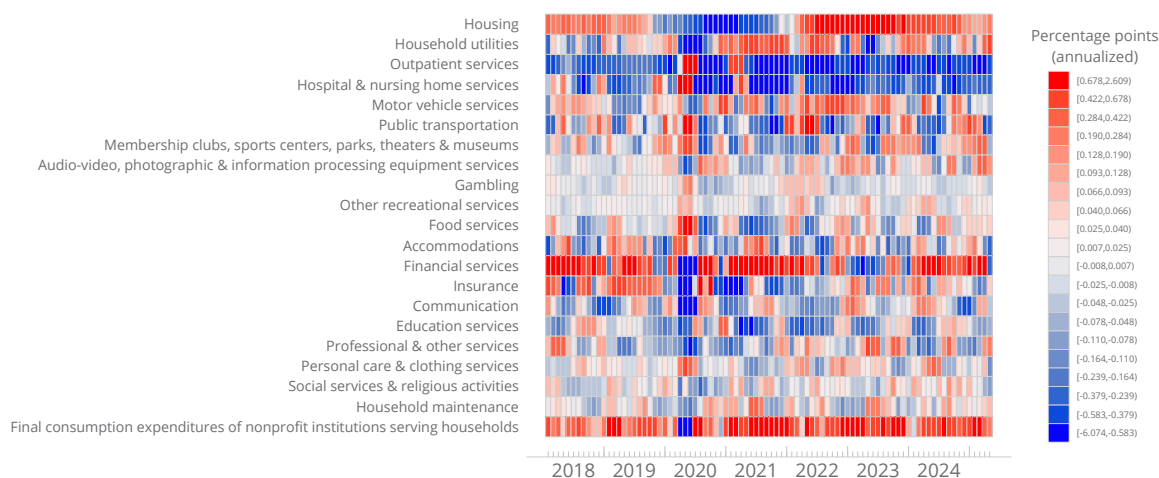
NOTE: Monthly data from January 2018 through April 2025. The heatmap in Panel A shows the estimated demand-driven gross contributions to the three-month (annualized) total idiosyncratic PCE inflation (the black line in Figure 4) from the PCE goods categories, whereas the heatmap in Panel B shows the estimated supply-driven gross contributions from the same categories (see the main text for details).

SOURCE: Authors' calculations using data from the U.S. Bureau of Economic Analysis, the Federal Reserve Board, and the University of Michigan.

FIGURE C-13: Pandemic-era Idiosyncratic Price Changes in the Services Sector



A. Demand-driven contributions to total idiosyncratic inflation

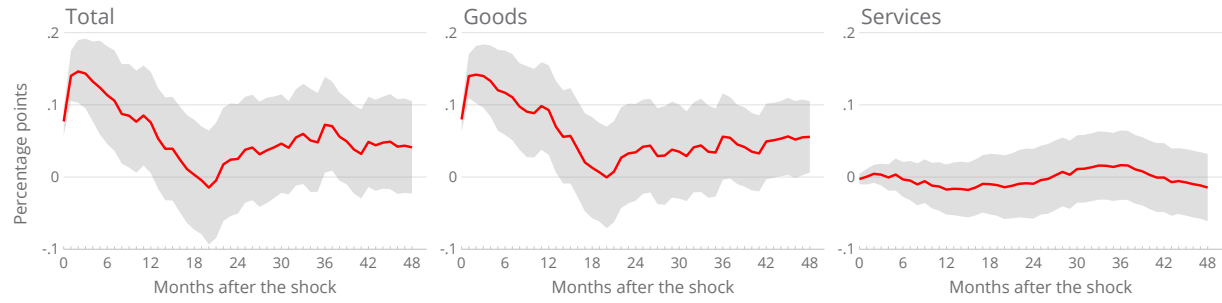


B. Supply-driven contributions to total idiosyncratic inflation

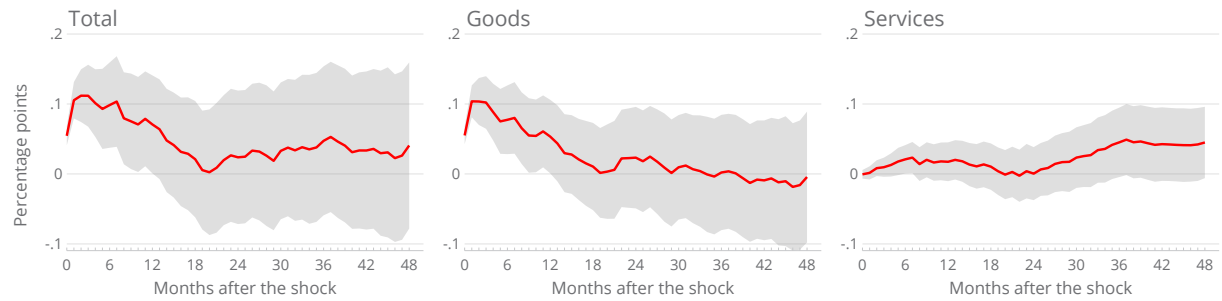
NOTE: Monthly data from January 2018 through April 2025. The heatmap in Panel A shows the estimated demand-driven gross contributions to the three-month (annualized) total idiosyncratic PCE inflation (the black line in Figure 4) from the PCE services categories, whereas the heatmap in Panel B shows the estimated supply-driven gross contributions from the same categories (see the main text for details).

SOURCE: Authors' calculations using data from the U.S. Bureau of Economic Analysis, the Federal Reserve Board, and the University of Michigan.

FIGURE C-14: The Impact of an Adverse Oil Supply News Shock



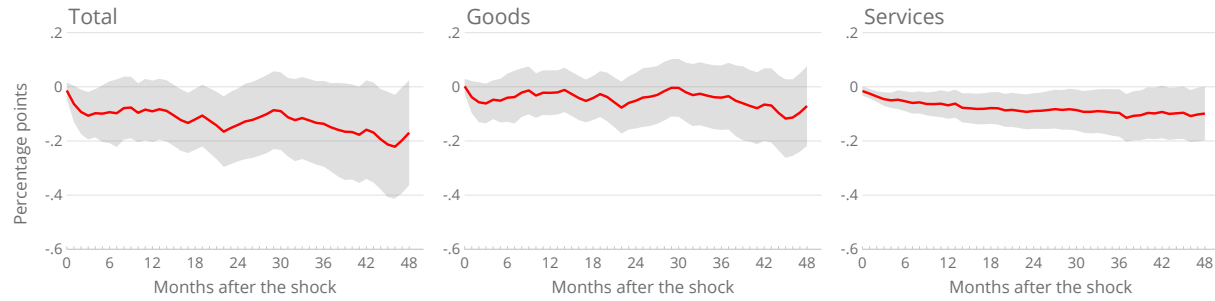
A. Supply-driven idiosyncratic inflation



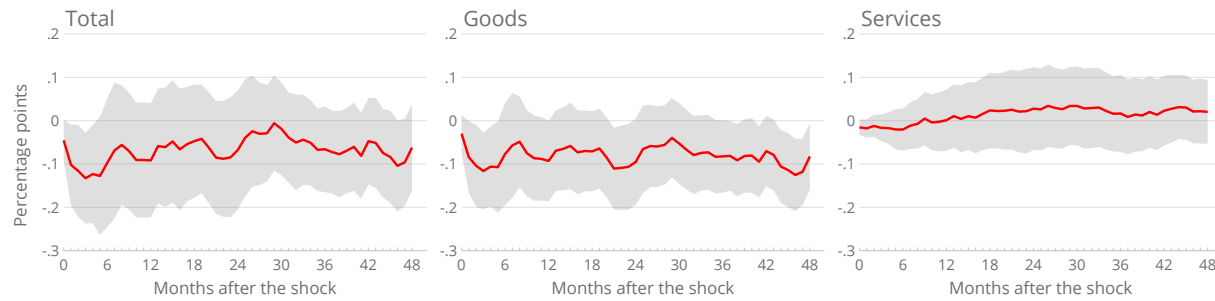
B. Demand-driven idiosyncratic inflation

NOTE: Sample period: monthly data from January 1985 through December 2019. The lines in Panel A show the estimated responses of total, goods, and services cumulative supply-driven idiosyncratic inflation over the specified horizon to an adverse oil supply news shock, which increases the real price of oil by 10 percent upon impact (that is, in month 0); the lines in Panel B show the estimated responses of total, goods, and services cumulative demand-driven idiosyncratic inflation over the specified horizon to the same shock. The shaded bands depict the associated 95 percent confidence intervals (see the main text for details).

FIGURE C-15: The Impact of a Contractionary Monetary Policy Shock



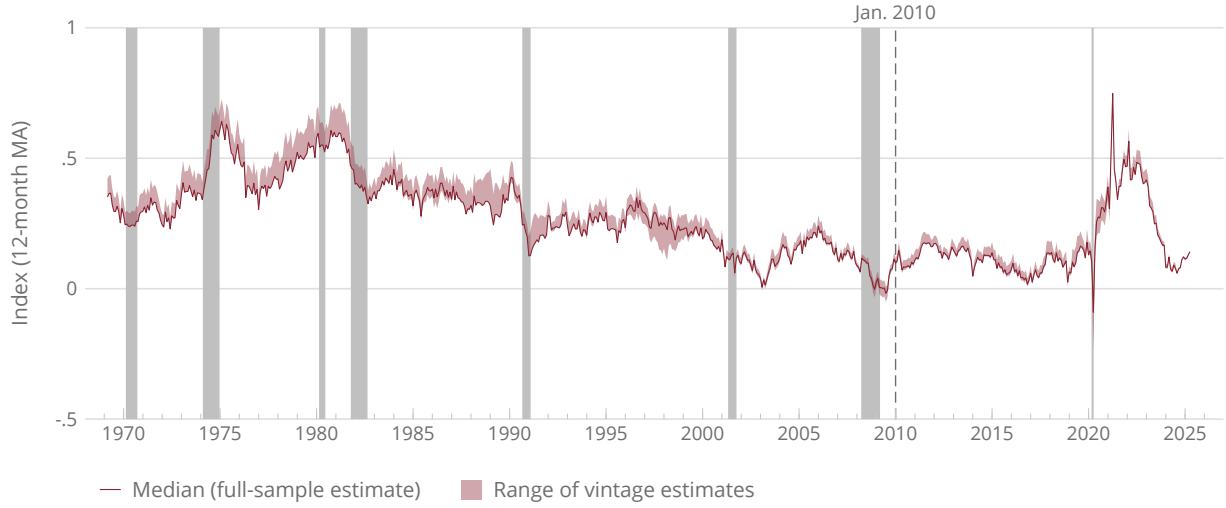
A. Demand-driven idiosyncratic inflation



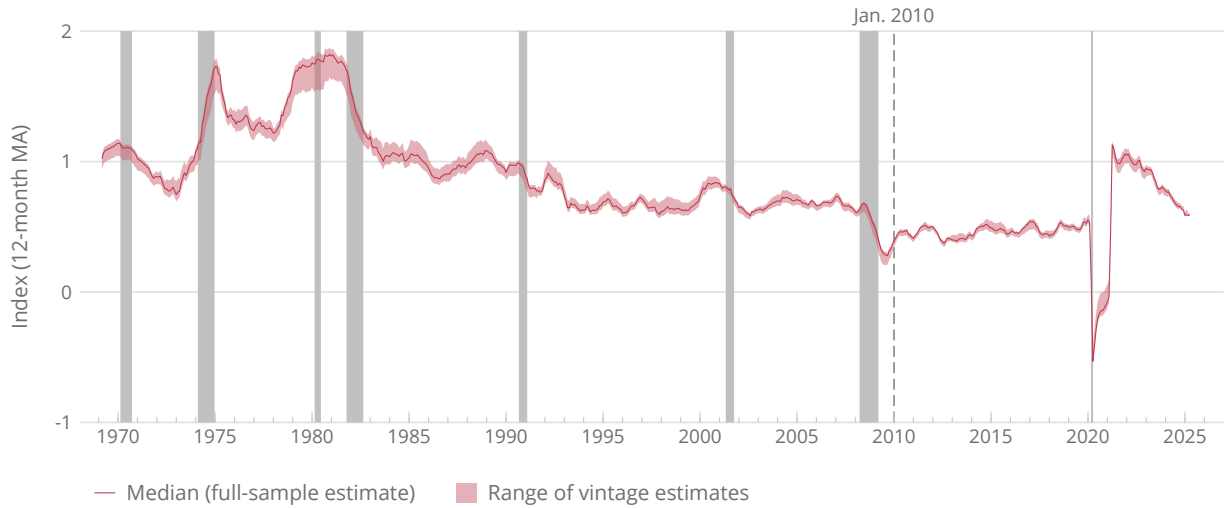
B. Supply-driven idiosyncratic inflation

NOTE: Sample period: monthly data from January 1985 to December 2019. The lines in Panel A show the estimated responses of total, goods, and services cumulative demand-driven idiosyncratic inflation over the specified horizon to a contractionary monetary policy shock, which increases the one-year nominal Treasury yield by 25 basis points upon impact (that is, in month 0); the lines in Panel B show the estimated responses of total, goods, and services cumulative supply-driven idiosyncratic inflation over the specified horizon to the same shock. The shaded bands depict the associated 95 percent confidence intervals (see the main text for details).

FIGURE C-16: Pseudo Real-time Estimates of Common Demand Factors



A. Common goods demand factor

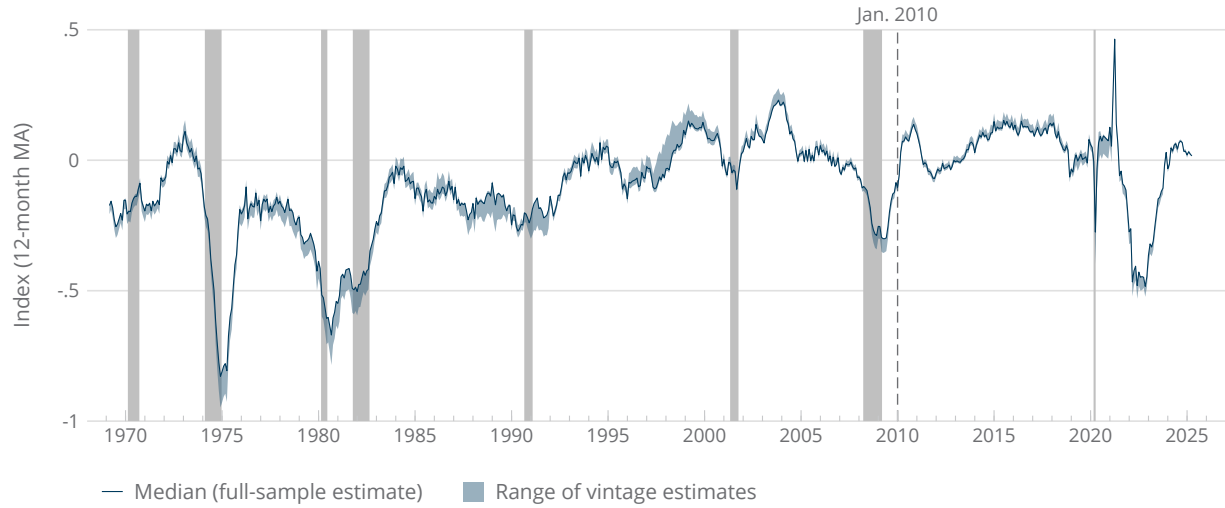


B. Common services demand factor

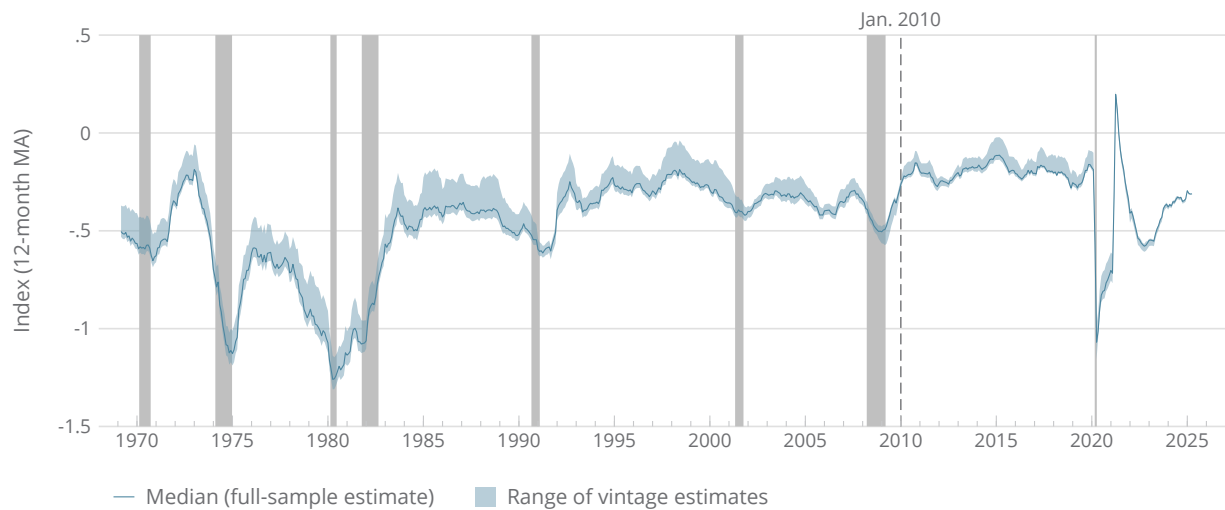
NOTE: Monthly data from March 1969 through April 2025. The line in Panel A depicts the 12-month moving average of the median of the posterior distribution of the common goods demand factor ($d_t^{(g)}$), whereas the line in Panel B depicts the 12-month moving average of the median of the posterior distribution of the common services demand factor ($d_t^{(v)}$), with both factors estimated over the full sample period (see Panel A of Figure 1 in the main text). The corresponding shaded bands represent the ranges of vintages of the posterior medians of $d_t^{(g)}$ and $d_t^{(v)}$ (smoothed using a 12-month moving-average filter), estimated starting in January 2010 and ending in March 2025. The shaded vertical bars depict recessions as determined by the National Bureau of Economic Research.

SOURCE: Authors' calculations using data from the U.S. Bureau of Economic Analysis, the Federal Reserve Board, and the University of Michigan.

FIGURE C-17: Pseudo Real-time Estimates of Common Supply Factors



A. Common goods supply factor



B. Common services supply factor

NOTE: Monthly data from March 1969 through April 2025. The line in Panel A depicts the 12-month moving average of the median of the posterior distribution of the common goods supply factor ($s_t^{(g)}$), whereas the line in Panel B depicts the 12-month moving average of the median of the posterior distribution of the common services supply factor ($s_t^{(v)}$), with both factors estimated over the full sample period (see Panel B of Figure 1 in the main text). The corresponding shaded bands represent the ranges of vintages of the posterior medians of $s_t^{(g)}$ and $s_t^{(v)}$ (smoothed using a 12-month moving-average filter), estimated starting in January 2010 and ending in March 2025. The shaded vertical bars depict recessions as determined by the National Bureau of Economic Research.

SOURCE: Authors' calculations using data from the U.S. Bureau of Economic Analysis, the Federal Reserve Board, and the University of Michigan.